EXPERIMENTAL INVESTIGATION ON FORMABILITY OF CRYOROLLED ALUMINIUM ALLOY SHEET

A Thesis submitted to Gujarat Technological University

For the Award of

Doctor of Philosophy

in

Mechanical Engineering

By

Parmar Manishkumar Navinchandra

Enrolment No. **199999919527**

Under supervision of

Dr. Anand B.Dhruv



GUJARAT TECHNOLOGICAL UNIVERSITY

AHMEDABAD

[August – 2025]

EXPERIMENTAL INVESTIGATION ON FORMABILITY OF CRYOROLLED ALUMINIUM ALLOY SHEET

A Thesis submitted to Gujarat Technological University

For the Award of

Doctor of Philosophy

in

Mechanical Engineering

By

Parmar Manishkumar Navinchandra

Enrolment No. **199999919527**

Under supervision of

Dr. Anand B.Dhruv



GUJARAT TECHNOLOGICAL UNIVERSITY

AHMEDABAD

[August – 2025]

I dedicated my thesis to my parents, my wife Shital
and my lovable son Tathya
who always picked me up on time
and encouraged me to go on every adventure,
especially this one

© [Parmar Manishkumar Navinchandra]

DECLARATION

I declare that the thesis entitled **"Experimental Investigation on Formability of Cryorolled Aluminium Alloy Sheet"** submitted by me for the degree of Doctor of Philosophy is the record of research work carried out by me during the period from 2019 to 2025 under the supervision of Dr. Anand B.Dhruv and this has not formed the basis for the award of any degree, diploma, associate ship, fellowship, titles in this or any other University or other institution of higher learning.

I further declare that the material obtained from other sources has been duly acknowledged in the thesis. I shall be solely responsible for any plagiarism or other irregularities, if noticed in the thesis.

Signature of the Research Scholar:..... Date: 01-08-2025

Name of Research Scholar: **Parmar Manishkumar Navinchandra**

Place: Ahmedabad

CERTIFICATE

I certify that the work incorporated in the thesis **"Experimental Investigation on Formability of Cryorolled Aluminium Alloy Sheet** by **Mr. Manishkumar Navinchandra Parmar** was carried out by the candidate under my supervision/guidance. To the best of my knowledge: (i) the candidate has not submitted the same research work to any other institution for any degree/diploma, Associateship, Fellowship or other similar titles (ii) the thesis submitted is a record of original research work done by the Research Scholar during the period of study under my supervision, and (iii) the thesis represents independent research work on the part of the Research Scholar.

Signature of Supervisor:..... Date: 01-08-2025

Name of Supervisor: **Dr.Anand B Dhruv**

Place: Government Engineering College, Patan.

Course-work Completion Certificate

This is to certify that **Mr. Manishkumar Navinchandra Parmar** enrollment no.**199999919527** is a PhD scholar enrolled for PhD program in the branch **Mechanical Engineering** of Gujarat Technological University, Ahmedabad.

(Please tick the relevant option(s))

☐ He/She has been exempted from the course-work (successfully completed during M.Phil Course)

☐ He/She has been exempted from Research Methodology Course only (successfully completed during M.Phil Course)

☑ He/She has successfully completed the PhD course work for the partial requirement for the award of PhD Degree. His/ Her performance in the course work is as follows-

Grade Obtained in Research Methodology (PHD2001)	Grade Obtained in Research and Publication Ethics (PHD2002)	Grade Obtained in Self-Study Course (PHD2003)
AB	**BB**	**AA**

Supervisor's Sign

(Dr. Anand B Dhruv)

Originality Report Certificate

It is certified that PhD Thesis titled **"EXPERIMENTAL INVESTIGATION ON FORMABILITY OF CRYOROLLED ALUMINIUM ALLOY SHEET"** by **Mr. Manishkumar Navinchandra Parmar** has been examined by us.

We undertake the following:

a. Thesis has significant new work / knowledge as compared already published or are under consideration to be published elsewhere. No sentence, equation, diagram, table, paragraph or section has been copied verbatim from previous work unless it is placed under quotation marks and duly referenced.

b. The work presented is original and own work of the author (i.e. there is no plagiarism). No ideas, processes, results or words of others have been presented as Author own work.

c. There is no fabrication of data or results which have been compiled / analyzed.

d. There is no falsification by manipulating research materials, equipment or processes, or changing or omitting data or results such that the research is not accurately represented in the research record.

e. The thesis has been checked using **"Turnitin Plagiarism checker"** (copy of originality report attached) and found within limits as per GTU Plagiarism Policy and instructions issued from time to time (i.e. permitted similarity index <10%).

Signature of the Research Scholar:..... Date: 01-08-2025

Name of Research Scholar: **Mr. Manishkumar Navinchandra Parmar**

Place: Ahmedabad

Signature of Supervisor:..... Date: 01-08-2025

Name of Supervisor: **Dr. Anand B.Dhruv**

Place: Government Engineering College, Patan.

ManishParmar

Thesis

Manish Thesis

PhD_Manish

Gujarat Technological University

Document Details

Submission ID
trn:oid:::1:3251607788

Submission Date
May 16, 2025, 11:17 AM GMT+5:30

Download Date
May 16, 2025, 12:58 PM GMT+5:30

File Name
Thesis_16-05-2025.pdf

File Size
8.4 MB

84 Pages

15,935 Words

85,324 Characters

7% Overall Similarity

The combined total of all matches, including overlapping sources, for each database.

Filtered from the Report

- Bibliography

Exclusions

- 339 Excluded Matches

Match Groups

68 Not Cited or Quoted 5%
Matches with neither in-text citation nor quotation marks

4 Missing Quotations 0%
Matches that are still very similar to source material

36 Missing Citation 3%
Matches that have quotation marks, but no in-text citation

2 Cited and Quoted 0%
Matches with in-text citation present, but no quotation marks

Top Sources

5% Internet sources
5% Publications
2% Submitted works (Student Papers)

Integrity Flags

0 Integrity Flags for Review

No suspicious text manipulations found.

Our system's algorithms look deeply at a document for any inconsistencies that would set it apart from a normal submission. If we notice something strange, we flag it for you to review.

A Flag is not necessarily an indicator of a problem. However, we'd recommend you focus your attention there for further review.

PhD THESIS Non-Exclusive License to GUJARAT TECHNOLOGICAL UNIVERSITY

In consideration of being a PhD Research Scholar at GTU and in the interests of the facilitation of research at GTU and elsewhere, I, **Mr. Manishkumar Navinchandra Parmar** having Enrollment No.**199999919527** hereby grant a non-exclusive, royalty free and perpetual license to GTU on the following terms:

a) GTU is permitted to archive, reproduce and distribute my thesis, in whole or in part, and/or my abstract, in whole or in part (referred to collectively as the "Work") anywhere in the world, for non-commercial purposes, in all forms of media;

b) GTU is permitted to authorize, sub-lease, sub-contract or procure any of the acts mentioned in paragraph (a);

c) GTU is authorized to submit the Work at any National / International Library, under the authority of their "Thesis Non-Exclusive License";

d) The Universal Copyright Notice (©) shall appear on all copies made under the authority of this license;

e) I undertake to submit my thesis, through my University, to any Library and Archives. Any abstract submitted with the thesis will be considered to form part of the thesis.

f) I represent that my thesis is my original work, does not infringe any rights of others, including privacy rights, and that I have the right to make the grant conferred by this non-exclusive license.

g) If third party copyrighted material was included in my thesis for which, under the terms of the Copyright Act, written permission from the copyright owners is required, I have obtained such permission from the copyright owners to do the acts mentioned in paragraph (a) above for the full term of copyright protection.

h) I retain copyright ownership and moral rights in my thesis, and may deal with the copyright in my thesis, in any way consistent with rights granted by me to my University in this non-exclusive license.

i) I further promise to inform any person to whom I may hereafter assign or license my copyright in my thesis of the rights granted by me to my University in this non-exclusive license.

j) I am aware of and agree to accept the conditions and regulations of PhD including all policy matters related to authorship and plagiarism.

Date : 01-08-2025
Place: Ahmedabad

Signature of the Research Scholar

Recommendation of the Supervisor: Recommended

Signature of Supervisor:

Name of Supervisor: **Dr. Anand B.Dhruv**

Date: 01-08-2025

Place: Government Engineering College, Patan.

Thesis Approval Form

The viva-voce of the Ph.D. Thesis submitted by **Mr. Manishkumar Navinchandra Parmar** (Enrollment No. **199999919527**) entitled "**Experimental Investigation on Formability of Cryorolled Aluminium Alloy Sheet**" was conducted on **Friday, 1st August 2025** at Gujarat Technological University.

(Please tick any one of the following options)

[✓] The performance of the candidate was satisfactory. We recommend that he be awarded the Ph.D. degree.

[✗] Any further modifications in research work recommended by the panel after three months from the date of first viva-voce upon request of the Supervisor or request of Independent Research Scholar after which viva-voce can be re-conducted by the same panel again.

[ ]

[✗] The performance of the candidate was unsatisfactory. We recommend that he/she should not be awarded a Ph.D. degree.

[ ]

Dr.Vijay Gautam 01/08/25

1) (External Examiner- Name and Signature)

Dr. Anand B Dhruv

Name and Signature of Supervisor with Seal

1/8/25

Dr.Ramesh S.

2) (External Examiner- Name and Signature)

ABSTRACT

The demand for lightweight metals and alloys such as Al alloys has increased significantly in automotive, aerospace, marine and other industries in the recent decades. But one of the main limitations of these alloys is lower strength and formability when compared to traditional low carbon steel sheets. Cryorolling is one of the important severe plastic deformation processes to produce ultrafine grained aluminum alloy sheets with high strength and hardness.

Aluminum alloy AA8011 which is generally used in various types of packaging industries as well as automotive and aerospace industries. The principal strengthening agents in AA8011 alloy are the Fe-Si constituent particles. These particles are capable of stabilizing a fine grain or subgrain structure, which can develop interesting combinations of strength and ductility. However, most of the investigations carried out on the AA8011 aluminum sheets are concerned with the recrystallization and precipitation behavior of the material.

In this study, an AA8011 alloy sheet of 3mm thickness in as received condition of H14 is used. A 3mm thick sheets of AA8011 alloy were cold rolled and cryorolled in multiple passes to a final thickness of 1mm. These 1mm thick sheets were annealed at 200°C for 45min then it is air cooled in atmosphere. In cold rolling it required 4 number of pass for the thickness reduction of 3mm to 1mm while in cold rolling it required 6 number of pass. The mechanical properties, Microstructure, surface roughness, Limiting Dome Height Test (LDH), forming limit diagram and drawability of cryorolled annealed and cold rolled annealed AA8011 alloy sheets have been investigated and a comparisons have been carried out. Cryorolling would yield a good combination of strength and ductility. Microstructural investigations showed that the cryorolled annealed samples possess bimodal grain structure with ultrafine grains which is responsible for better mechanical properties than cold rolled sheets. Surface roughness have been found decreased in cryorolling as compared to cold rolling. From the LDH experimental results forming limit diagrams have been developed. The limit strains of cryorolled sheets have been found to be slightly higher as compared to conventional cold rolled annealed sheets in all modes of deformation. In the next part, an attempts have been made for drawing operations with various punch size and blank size. A comparison of drawability and cup height for annealed cold rolled and cryorolled have been

carried out. This work clearly demonstrates that cryorolling of AA8011 alloy sheets followed by annealing shows bimodal grain structure with higher strength, hardness, better surface roughness, improved drawability and increase in cup height than conventional cold rolled sheets with increase in formability hence it can be used for various sheet metal forming applications.

Acknowledgement

First of all I thank and praise God the creator and almighty who showered his blessings upon me and lead me to the success of the Research work.

I, **Parmar Manishkumar Navinchandra**, hereby take this opportunity to thank all those valuable people who have provided immense support to assist me in completing my doctoral study. I would like to take an opportunity to express my sincere gratitude that have contributed to this research work and supported me during this journey.

I am extremely grateful to my honorable Supervisor **Dr. Anand B Dhruv**, for his continuous guidance, motivation, encouragement and support for throughout my research work. His guidance helped me in all the time of research and writing of this thesis, I could not have imagined having a better advisor and mentor for my research work.

Besides my advisor, I would like to appreciate to my Doctoral Progress Committee Members **Dr. Jitendra A Vadher**, Professor in Mechanical Department, Government Engineering College, Modasa and **Dr. Mahesh K Chudasama**, Associate Professor in Mechanical Department, Government Engineering College, Surat for their rigorous examinations and precious suggestion during my research. Their valuable suggestions and constructive criticisms from time to time enabled me to complete my work successfully.

I am thankful to Honorable Vice-Chancellor, Registrar, Controller of Examination, Dean Ph.D. section, and all staff members of the Ph.D. Section of Gujarat Technological University, Ahmedabad for their assistance and support. I am grateful to my Ph.D. thesis examiners for sparing their valuable time to evaluate the thesis.

Above all, I place on record my gratitude and reverence to my parents, family members and friends for their good will and prayers. Their constant support, guidance, love, care, blessings, all can be less in words and more in thoughts. I acknowledge to all of them, who directly or indirectly helped me in completing this journey of research work.

Table of Content

	Details	Page No.
	ABSTRACT.....	xi
	Acknowledgement.....	xiii
	Table of Content.....	xiv
	List of Abbreviation.....	xvii
	List of Symbol.....	xviii
	List of Figures.....	xix
	List of Tables.....	xxii
	Appendices.....	xxiii
CHAPTER 1	**INTRODUCTION**.....	1
	1.1. Sheet Metal Forming Processes.....	1
	1.2. Formability.....	3
	1.3. Factors Affecting Formability.....	6
	1.4. Importance of Aluminum Alloys.....	7
	1.5. Limitations of Aluminum Alloys for Sheet Metal Forming.....	7
	1.6. Applications of Aluminum Alloys.....	8
	1.7. Techniques for Enhancing Strength of Aluminum Alloys.....	9
	1.7.1 Cryogenic Rolling of Aluminum Alloys.....	9
	1.7.2 Hydroforming.....	10
	1.7.3.Drawing Processes.....	13
CHAPTER 2	**LITERATURE REVIEW**.....	18

2.1 Microstructural Changes during Cryorolling..... 18

2.2 Effect of Cryorolling on Mechanical Properties..... 21

2.3 Effect of Cryorolling on Formability..... 24

2.4 Methods to Enhance Formability..... 30

2.4.1 Warm Forming..... 30

2.4.2 Super plastic Forming..... 30

2.4.3 Viscous Pressure Forming..... 31

2.4.4 Hydroforming..... 31

2.4.5 Incremental Forming…… 31

2.5 Summary of Literature Review..... 31

2.6 Motivation and objectives of the Present Work..... 32

CHAPTER 3 MATERIAL PROCESSING AND CHARACTERIZATION..... 34

3.1 Material Selection..... 34

3.2 Methodology..... 35

3.3 Cold rolling and Cryorolling..... 36

3.4 Rolling Defects..... 40

3.5 Characterization of Microstructure and Mechanical Properties 40

3.5.1 Microstructure..... 40

3.5.2 Hardness..... 41

3.5.3 Surface Roughness Measurement..... 43

3.5.4 Tensile Test..... 44

3.5.5 Anisotropy..... 45

3.5.6 Limiting Dome Height Test..... 46

3.5.7 Forming Limit Diagram..... 53

3.5.8 Strain Measurement..... 54

3.5.9 Drawing Process..... 54

CHAPTER 4 **RESULT AND DISCUSSION**..... 61

4.1 Microstructure and Mechanical Properties of Rolled Sheets..... 61

4.1.1 Microstructure..... 61

4.1.2 Hardness..... 62

4.1.3 Surface Roughness Measurement..... 63

4.1.4 Tensile Test..... 65

4.2 Limiting Dome Height Test..... 72

4.3 Forming Limit Diagram..... 73

4.4 Strain Measurement..... 74

4.5 Drawing Process..... 76

4.6 Summary..... 79

CHAPTER 5 **CONCLUSION AND SUGGESTIONS FOR FUTURE WORK**.... 81

5.1 Conclusion..... 81

5.2 Scope of Future Work..... 83

References..... 84

List of Publications..... 94

Appendices..... 95

List of Abbreviation

Nomenclature

LDR	Limiting Drawing Ratio
LDH	Limiting Dome Height Test
FLD	Forming Limit Diagram
FLC	Forming Limit Curve
Al	Aluminium
Al-Mg	Aluminium-Magnesium
EDD	Extra Deep Drawing
IF	Interstitial Free
SPD	Severe Plastic Deformation
UFG	Ultrafine Grain
ARB	accumulative roll-bonding
HPT	high-pressure torsion
ECAP	equal channel angular pressing
THF	Tube Hydro forming
SHF	Sheet Hydro forming
IDDRG	International Deep Drawing Research Group
ID	Internal Diameter
OD	Outer Diameter
TRIP	Transformation Induced Plasticity
RTR	Room Temperature Rolling
CR	Cryogenic Rolling
CCR	Cryo-cross rolling
HCF	High Cycle Fatigue
AV	Annealing
HFIR	High Frequency Impacting And Rolling
YS	Yield Strength
UTS	Ultimate Tensile Strength

List of Symbol

Do	Initial blank Diameter
Dc	cup diameter,
%	Percentage
Dp	Punch Diameter
D_b	Blank Diameter
HV	Vickers's Hardness
MPa	Mega Pascal
°C	Degree centigrade
σ	True stress
ε	True strain
K	Strength coefficient
n	Strain hardening exponent
$\bar{R}$	Average plastic strain ratio
R	Plastic strain ratio
ΔR	Planar anisotropy
µm	Micron

List of Figures

FIGURE 1.1	Schematic illustration of cylindrical cup drawing of a circular sheet metal specimen……	2
FIGURE 1.2	Stretch forming process……...	2
FIGURE 1.3	Sheet metal bending operations. …….	3
FIGURE 1.4	A typical forming limit diagram……	5
FIGURE 1.5	A schematic showing conventional cold rolling and cryogenic rolling….	10
FIGURE 1.6	Classification of hydroforming technology…….	11
FIGURE 1.7	hydro-mechanical or counter pressure forming……...	12
FIGURE 1.8	punchless hydroforming or high-pressure forming…….	12
FIGURE 1.9	Some components formed by sheet hydroforming for industrial applications……..	13
FIGURE1.10	Principle of Deep drawing……..	15
FIGURE1.11	Range of Components produced in deep drawing……...	15
FIGURE1.12	Scheme of deep drawing process…….	16
FIGURE 2.1	Mechanism of grain refinement during cryorolling of aluminum alloys…	18
FIGURE 2.2	SEM images of Cu–Ni–Si alloy aged at 723 K for 24 h: a RTR sample, b CR sample……	19
FIGURE 2.3	The variation of Hardness with different rolling directions……	21
FIGURE 2.4	Comparison of forming limit diagrams and fracture curves for room temperature rolling and cryorolling conditions……...	24
FIGURE 2.5	Stress-strain curve for bending test for specimens A, B, and C……	27
FIGURE 2.6	: The forming limit diagram for different aging treatments of Aluminum Alloy 6061……...	29
FIGURE 3.1	The methodology used in the present work……	35
FIGURE 3.2	Rolling mill and experimental setup used for cold rolling and cryorolling.	36
FIGURE 3.3	Schematic showing rolling cycle of AA8011 alloy sheets……..	37
FIGURE 3.4	Cold Rolling…….	38
FIGURE 3.5	Cryorolling……...	39
FIGURE 3.6	Furnace used for annealing……..	39
FIGURE 3.7	Surface defects on rolled samples……	40
FIGURE 3.8	Hardness sample……..	42
FIGURE 3.9	Computerized Universal Testing M-100…….	44
FIGURE3.10	Tensile Test Specimens……...	44
FIGURE3.11	Directions in which samples were taken for determination of anisotropic parameters……	46
FIGURE3.12	Schematic diagram of the tooling arrangement for LDH……...	47
FIGURE3.13	The actual experimental setup used for LDH experiments on a 20-ton power press……..	48

FIGURE3.14	Fabricated dies and punch for LDH tests……	48
FIGURE3.15	Samples of different Rectangle width for LDH Test……	49
FIGURE3.16	Failure in the draw-bead region during testing of lower width samples…	50
FIGURE3.17	Samples of different width for FLD Test……...	50
FIGURE3.18	Laser marking machine……	51
FIGURE3.19	Tested FLD samples for determination of FLD……..	52
FIGURE3.20	Close-up view showing deformed grid used for measurement of strains in safe, necked and failed regions……	52
FIGURE3.21	The possible changes in shape of the grid pattern (ASTM E2218-15)……	53
FIGURE3.22	Tested drawing specimens for cold rolling and cryorolling with drawing ratio 2.0……	56
FIGURE3.23	Tested drawing specimens for cold rolling and cryorolling with drawing ratio 1.78……..	57
FIGURE3.24	Tested drawing specimens for cold rolling and cryorolling with drawing ratio 1.71……..	58
FIGURE3.25	Tested drawing specimens for cold rolling and cryorolling with drawing ratio 1.11……..	59
FIGURE3.26	Tested drawing specimens for cold rolling and cryorolling with drawing ratio 1.11……..	59
FIGURE3.27	Tested drawing specimens for square cup drawing of cold rolling and cryorolling……	60
FIGURE 4.1	Optical micrographs of AA8011 alloys (a) cold rolled (b) Cryorolled…...	62
FIGURE 4.2	Variation of hardness of AA8011 alloys for raw material, cold rolled and cryorolled…….	63
FIGURE 4.3	Variation of surface roughness of AA8011 alloys for cold rolled and cryorolled conditions……...	64
FIGURE 4.4	Tested tensile specimens at 0°C, 45°C and 90°C with respect to rolling direction for cold rolling and cryorolling……	65
FIGURE 4.5	(a), (b), (c) show how the Variations in Load vs CHT of the cold and cryorolled samples at at 0°C, 45°C and 90°C with respect to rolling direction……...	67
FIGURE 4.6	Variations in UTS, YS and elongation of the cold and cryorolled samples at 0°C, 45°C and 90°C of rolling direction……	69
FIGURE 4.7	LDH of cold rolled and cryorolled of AA8011 sheets……...	72
FIGURE 4.8	Forming Limit Diagram of cold rolled sheets…….	73
FIGURE 4.9	Forming Limit Diagram of cryorolled sheets……..	74
FIGURE4.10	Strain distribution in FLD samples of cold rolled and cryorolled of AA8011 sheets after annealing……	76
FIGURE4.11	Drawing of cold rolled and cryorolled of AA8011 sheets (blank dia 120mm, punch dia 70mm at 100kN)……...	77
FIGURE4.12	Drawing of cold rolled and cryorolled of AA8011 sheets (blank dia	77

200mm, punch dia 180mm at 80kN)……...
FIGURE4.13 Drawing of cold rolled and cryorolled of AA8011 sheets (blank dia 200mm, punch dia 180mm at 100kN)……. 78
FIGURE4.14 Drawing of cold rolled and cryorolled of AA8011 sheets (blank size 200mm x 200mm, punch size 100mm x 100mm at 100kN)……... 79

List of Tables

TABLE 3.1	Composition of alloying elements in weight % of AA8011……	35
TABLE 4.1	Hardness of cold rolled and Cryorolled samples of AA8011 alloy…….....	63
TABLE 4.2	Surface roughness values of AA8011 alloy sheets in different conditions….	64
TABLE 4.3	Tensile properties of AA8011 alloy sheets in different conditions…….	68
TABLE 4.4	Anisotropic parameters of AA8011 alloy sheets tested cold rolled and cryorolled conditions……..	72

List of Appendices

		Page No.
Appendix -A	Material Test Certificate…….	95
Appendix -B	Chemical Analysis Certificate……	96

CHAPTER 1

INTRODUCTION

1.1 Sheet Metal Forming Processes

Sheet metal is extensively used in the production of various industrial and consumer goods due to its ability to be formed into intricate shapes. A significant portion of consumer products and parts for automobile, airplane, and agricultural machinery are made of sheet metal. To produce parts with the correct shape, a variety of sheet metal forming techniques are used, including shearing, bending, stretch forming, deep drawing, etc. Every procedure has a distinct function and must produce a certain end result shape. While the metal may occasionally deform under combined tensile and compressive loads, in sheet metal forming operations, tensile stresses are applied primarily. Here is a quick description of some of these forming processes' principal features.

As seen in Figure 1.1, **deep drawing** is a sheet metal forming technique where a sheet metal blank is mechanically dragged radially into a forming die by a punch. When a drawn section in a cylindrical cup drawing is deeper than its diameter, the drawing technique is referred to as "deep" drawing [1]. Because deep drawing involves a large amount of metal flow, it must be administered carefully to prevent tearing, fracture, and creases.

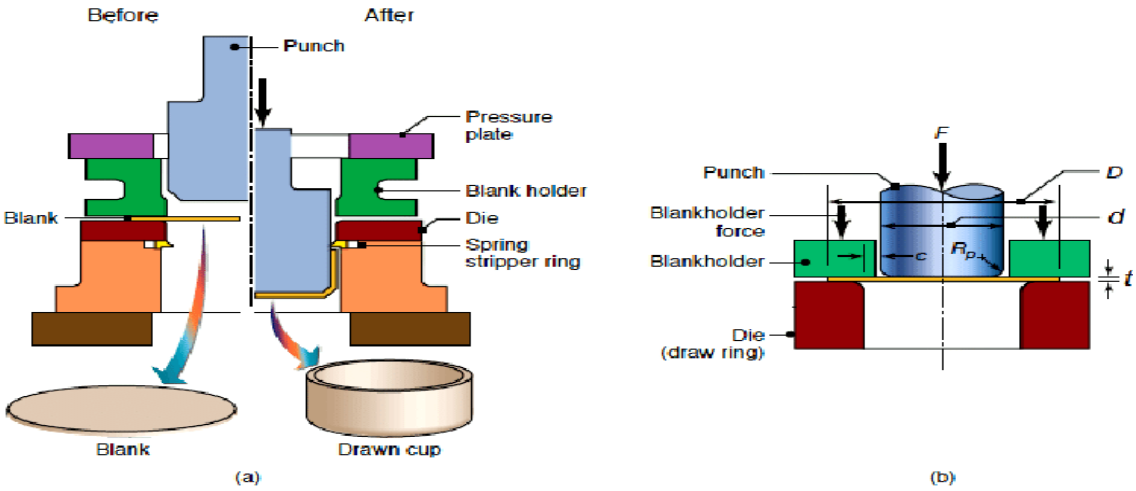

FIGURE 1.1 : Schematic illustration of cylindrical cup drawing of a circular sheet metal specimen [1]

Stretch forming involves fully clamping the sheet around its circumference, developing the shape at the expense of the thickness of the sheet. Figure 1.2 [2] presents a schematic set-up of stretch forming process. For stretch forming to work well and prevent flaws like excessive thinning and ripping of the formed portion, the die design is essential. The automobile and aircraft industries make substantial use of the stretch forming method to create pieces with huge radiuses of curvature (usually for uniform cross section) [3]

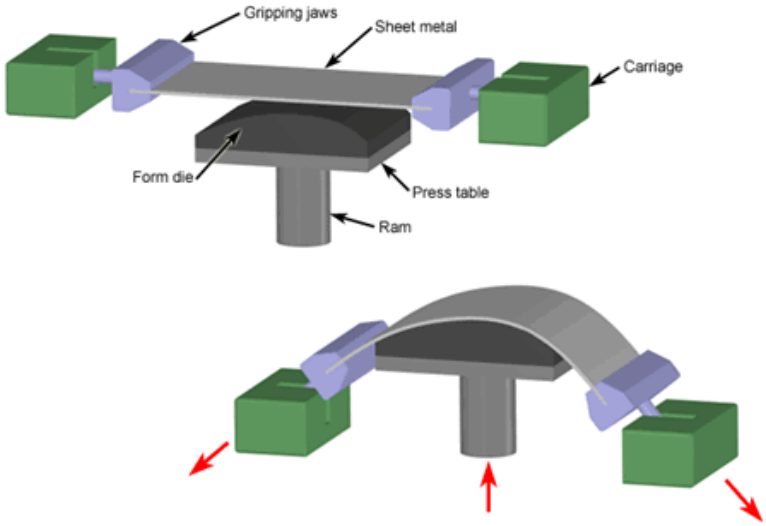

FIGURE 1.2 : Stretch forming process [2]

The technique of **bending** flat sheets into curved sections with little to no change in surface area along a linear axis known as the bending axis is known as sheet bending [1] Some common bending operations are shown in Figure 1.3 [1]

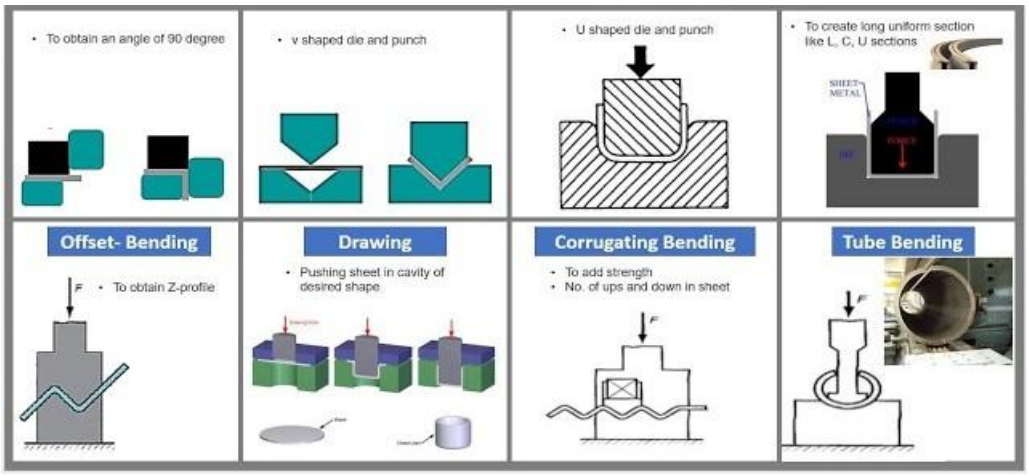

FIGURE 1.3 : Sheet metal bending operations [1]

Combining the afore mentioned procedures is necessary for complex sheet stampings. The majority of car panels combine drawing and stretching, which are also related to bending, unbending, and flanging [4].

1.2 Formability

A sheet metal's formability is its capacity to take on the necessary shape without breaking. Redesigning the part or altering the processing technique is a typical practice when a sheet metal part fails due to localized necking and fracture during manufacture. This ensures that the state of strain in the crucial zone does not exceed the limit of deformation [5]. The complicated boundary and metal die interfacial conditions, along with the challenge of characterizing the neck start and growth behavior; make it hard to predict such a failure. It is impossible to characterize or measure the formability of a single test for every kind of forming activity.

By calculating the limiting draw ratio (LDR), which is the ratio of the maximum initial blank diameter (D_0 max) that can be successfully drawn to the cup diameter (D_c), one can quantitatively determine the drawability of a sheet metal in deep drawing [6]. This test is known as Swift flat bottom cup test [7] When a blank is

deformed by a hemispherical bottom punch, the maximum dome height that may be reached at the beginning of necking or failure is what limits the formability of stretch forming. This test is known as the Limiting Dome Height Test (LDH). Additional common tests for determining formability under biaxial stretching conditions are the Erichsen cup test and the Olsen test [8]. The Fukui conical test simulates combined stretching and drawing in order to assess formability in a combined mode of deformation [9].

Formability of a sheet is often predicted or evaluated using a forming limit diagram (FLD) or forming limit curve (FLC), which is a graphical representation of the limit strains of a sheet metal in all potential modes of deformation. An essential tool for determining the limit spots at which necking or failure occurs in a sheet metal is the forming limit diagram, which was first proposed by Keeler and Goodwin [10]. On the surface of blanks deformed by various load paths, it is typically shown as major principle engineering strain vs. minor primary engineering strain.

Hecker [11] developed a standard method to determine limit strains in various phases of strain, wherein blanks of varying widths are deformed using a cylindrical punch with a hemispherical bottom of 101.6 mm diameter, until the blank exhibits evident failure or necking. Because the dies include a circular draw bead, the clamping area shrinks as the blank width lowers, changing the method of deformation. The circular grid approach is frequently used to calculate the strain on the deformed sample. A modified blank geometry for FLD evaluation was proposed by Nakazima [12].

Figure 1.4 depicts a typical FLD [1]. The safe region is shown by the combination of major and minor strain points below the curve, which indicates the maximum thickness at which a sheet can be manufactured without cracking or necking. The failure location is indicated by the strain data above the curve. The left-hand curve represents the limit stresses in the drawing processes' tension-compression mode. Limit stresses under biaxial tension are shown by the curve on the right (stretched). Limit strain under plane strain deformation is shown by the major strain value (Y-intercept) when the minor strain is zero. FLD is the name given to it. It is a crucial

component of the material's formability since it shows the FLD level. Forming limit diagrams have also been theoretically predicted [13] in order to rapidly determine the boundaries of a safe forming process. The safe working zone in sheet metal stampings is predicted using forming limit diagrams rather frequently. FLDs are utilized as failure criteria in FE simulations of sheet metal forming because they are a practical and helpful tool for die design and failure analysis in the production of sheet metal goods [14].

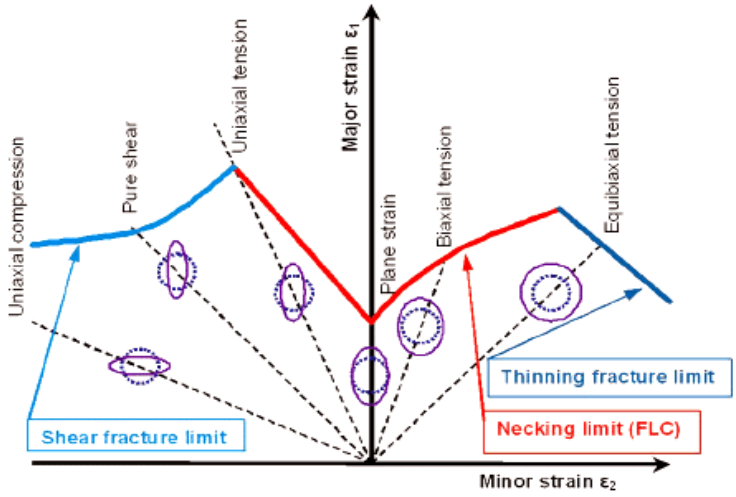

FIGURE 1.4 : A typical forming limit diagram [1]

A solid mix of strength and formability is necessary to create sheet metal items from cryorolled sheets. Although post-heat treatment after cryorolling improves formability to some degree, it takes a lot of time and may not always be practical to use in industry because of its lengthy cycle time. Furthermore, annealing parameters like as temperature and soaking time have a significant impact on formability, strength, and ductility. The strength decreases if these parameters are not appropriately selected, partially negating the cryorolling's function. An alternative method to improve both strength and formability of cryorolled sheet by warm forming after cryorolling without any post heat treatment is performed by Feyissa [15].

1.3 Factors Affecting Formability

A sheet's formability is dependent on numerous variables that interact in a highly intricate way. The following two categories of variables generally affect it: process variables like blank-holding force, friction (which is determined by the lubrication conditions), punch travel speed, etc. and design variables like die geometry, die corner radius, punch corner radius, clearance between punch and die, location and design of draw bead, etc. [16].

In every process involved in sheet metal forming, proper punch-die clearance is crucial [17]. In deep drawing, the space between the punch and the die should be 10–20% larger than the thickness of the sheet [18]. Less than that results in ironing. There are lower clearances available for bending and stretching. Reduced formability and fracture/tearing at the die entry or the bottom of the cup wall near the punch corner in deep drawing are caused by insufficient die corner and punch corner radii [19]. To prevent flaws like wrinkling and to regulate or limit the flow of material during forming, the draw bead's placement and design are crucial. An excessive amount of thinning and cracking at the draw bead could result from improper draw bead design [20].

Higher blank-holding forces cause the blank to tear at the die entry, whereas insufficient blank-holding forces produce wrinkling in deep drawing and stretch forming [21]. In sheet formation, lubrication has a significant impact on how strain is distributed. Although the strain state and local strains close to failure may remain same, better lubrication (reduced friction) encourages the distribution of load and strain more evenly across a specimen, permitting a greater cup depth [22]. Lubrication effectiveness is influenced by a variety of forming parameters, including die design, material characteristics, contact pressure, and forming speed [23]. Punch travel speed raises cause strain rate, which decreases formability.

1.4 Importance of Aluminum Alloys

Currently, when energy conservation and environmental preservation are paramount, there is a greater interest than ever in reducing weight in all types of transportation vehicles. Light metals and their alloys, including aluminum alloys, are becoming more and more popular in the automotive, marine, and other industries because of their significant potential for weight reduction [24]. Because aluminum alloys are denser than steel by about one-third, several of them have good strength to weight ratios. Heat treatment and work hardening of Al alloys can enhance their mechanical properties [25]. In addition to being non-toxic and having exceptional corrosion resistance in marine environments, aluminum alloys may be recycled using only 5% of the energy required to create aluminum from its ore [26].

Material selection and custom part design are the two fundamental strategies, and they are interrelated. In terms of materials, light metals and their alloys are increasingly being used in place of more conventional materials like steel. Although significant study has been done on the use of nonmetallic materials, aluminum, magnesium, and their alloys are the most promising materials. Aluminum alloys have been used in place of traditional steel grades in the production of auto body parts, and considerable attempts have been made to do so because to its superior corrosion resistance, reduced fuel usage, and potential for weight savings. Because of their appropriate mechanical properties, Al-Mg type alloy sheets are an affordable and promising material for sheet metal forming applications among other Al-alloys.

1.5 Limitations of Aluminum Alloys for Sheet Metal Forming

Although aluminum alloy sheets, as discussed in the preceding section, have a number of advantages over steel, they also have some significant drawbacks that limit their usage in intricate sheet forming applications. Among these restrictions are:

1) Compared to conventional grades of steel, which are widely utilized in the aerospace, shipbuilding, and automobile industries, aluminum alloys are less strong and ductile.

2) Compared to low carbon steel grades like Extra Deep Drawing (EDD) and Interstitial Free (IF) steels, among others, the formability of aluminum alloys is significantly lower. Aluminum alloys' LDR in deep drawing is typically 1.6–1.8, although EDD/IF steel sheets can attain LDRs of up to 2.1–2.3. Multi-stage deep drawing is used to produce huge LDR; this adds to the number of forming processes and raises the cost of tooling.

3) An aluminum panel has lower energy absorption, crash resistance, and dent resistance than a steel panel.

4) Aluminum alloys are more prone to wrinkling and cracking than other materials.

1.6 Applications of Aluminum Alloys

Structural Engineering:

Aluminium is a popular choice for building construction, bridges, and offshore structures due to its durability and recyclability.

Electrical Engineering:

It's used in power lines, electrical components like capacitors and antennae, and in the production of electronic devices.

Mechanical Engineering:

Aluminium alloys are used in various mechanical systems, including robotics, seawater desalination plants, and heat exchangers.

Transportation:

Aluminium's lightweight nature makes it ideal for aerospace applications, automotive bodies, and even train and ship construction.

Other Applications:

Aluminium is also found in packaging, food processing, energy generation (wind turbines, solar panels), and architectural applications like windows and doors.

1.7 Techniques for Enhancing Strength of Aluminum Alloys

Owing to the shortcomings of aluminum alloy sheets made using traditional techniques, stronger aluminum alloys are being developed using alternative techniques such Severe Plastic Deformation (SPD) processes. Using severe plastic deformation (SPD) procedures, ultrafine grain (UFG) structured materials with high strength can be produced.

Numerous accumulative roll-bonding (ARB), high-pressure torsion (HPT), cryogenic rolling, equal channel angular pressing (ECAP), and other SPD techniques have been developed [27]. One of the SPD methods that works well for producing aluminum alloys with greater strength in sheet form is cryorolling.

1.7.1 Cryogenic Rolling of Aluminum Alloys

The term cryogenic rolling, commonly referred to as cryorolling, describes the process of rolling metal at cryogenic temperatures using a liquid nitrogen bath as shown in Figure 1.5. This is one possible method for creating sheet-form nanostructured materials from their bulk equivalent. The majority of the literature reports that rolling pure metals and alloys at cryogenic temperatures suppresses dynamic recovery and increases the density of accumulated dislocations with each cryorolling pass. These dislocation cells then organize themselves into ultrafine-grained structures with high angle grain boundaries [28–30].

Because of this, sheet materials with ultra-fine grain structure can be created that are harder and more resilient than those made by traditional cold rolling. The process enables the creation of stronger sheets made of metals and alloys with ultrafine structures. [32].

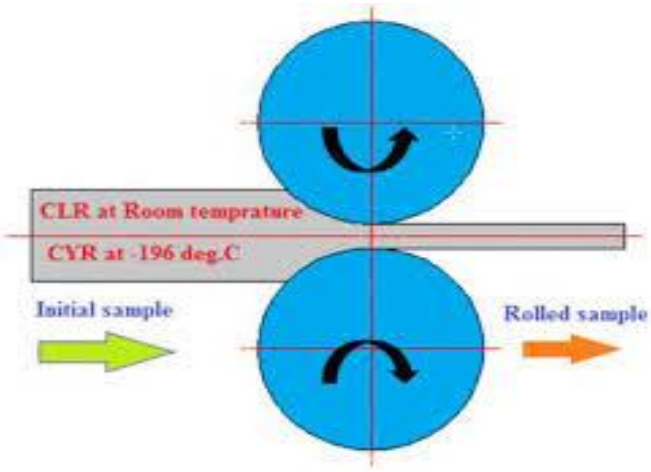

FIGURE 1.5: A schematic showing conventional cold rolling and cryogenic rolling.[31]

The literature has indicated that cryorolling has shown to be a successful method of strengthening a variety of aluminum alloys. After cryorolling, the right heat treatment can help achieve the required balance of strength and ductility. Nonetheless, in many aluminum alloys, the majority of these investigations [33–36] indicated improvements in mechanical characteristics as well as microstructural development. The formability of Al alloy sheets, a crucial factor in their formation, has not been examined in the context of cryo-rolled aluminum alloys.

Advantages of Cryorolling:

- Enhanced Strength and Hardness
- Ultra-Fine Grain Structure
- Reduced Dislocation Annihilation
- Reduced Plastic Deformation
- Retained Strain Hardening

1.7.2 Hydroforming

In the non-traditional metal forming method known as hydroforming, a suitable die is utilized to form a tube or sheet metal blank into the desired shape under fluid pressure. The material experiences enough stress from the applied fluid pressure for the metal to undergo plastic deformation. Hydroforming is broadly classified into

two major categories: tube hydroforming and sheet hydroforming [37]. As seen in Figure 1.6, sheet hydroforming can be further separated into hydro-mechanical forming and pure hydroforming. In the process of tube hydroforming, an axial force is frequently employed in addition to internal pressure to shape a pre-shaped seamless or welded tube into the shape of the die cavity[38]. A sheet metal blank is subjected to fluid pressure during the sheet hydroforming process, which modifies the metal's overall geometric shape. Fluid pressure is used to the part to obtain specific benefits in sheet hydroforming, or it can be utilized to substitute rigid tools[39].

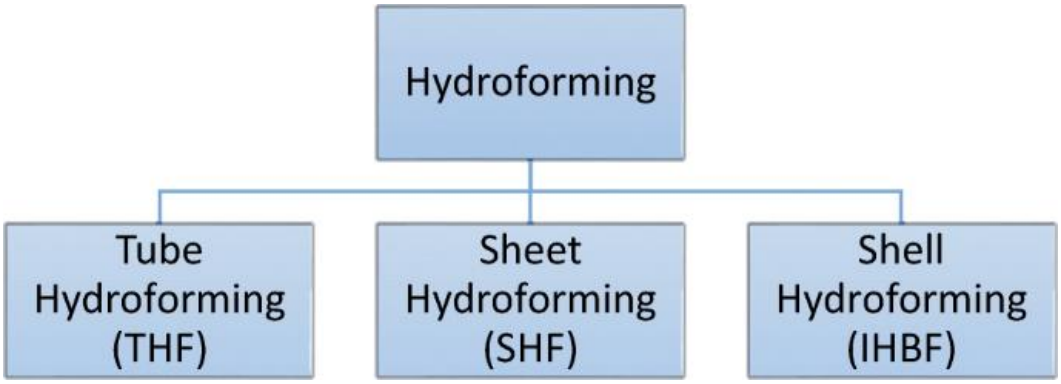

FIGURE 1.6 : Classification of hydroforming technology[40]

As illustrated in Figure 1.7, the latter method is also known as the hydro-mechanical deep drawing process or counter pressure deep drawing process. In this method, the punch moves against a regulated pressured fluid to deform the blank to its final shape [41]. High fluid pressure is utilized in pure sheet hydroforming (without a punch) to create the blank. It is schematically depicted in Figure 1.8 and entails applying high liquid pressure through a nozzle—typically through the blank holder—to the sheet metal blank in order to shape it into the shape of the die cavity until it takes on the final shape [42].

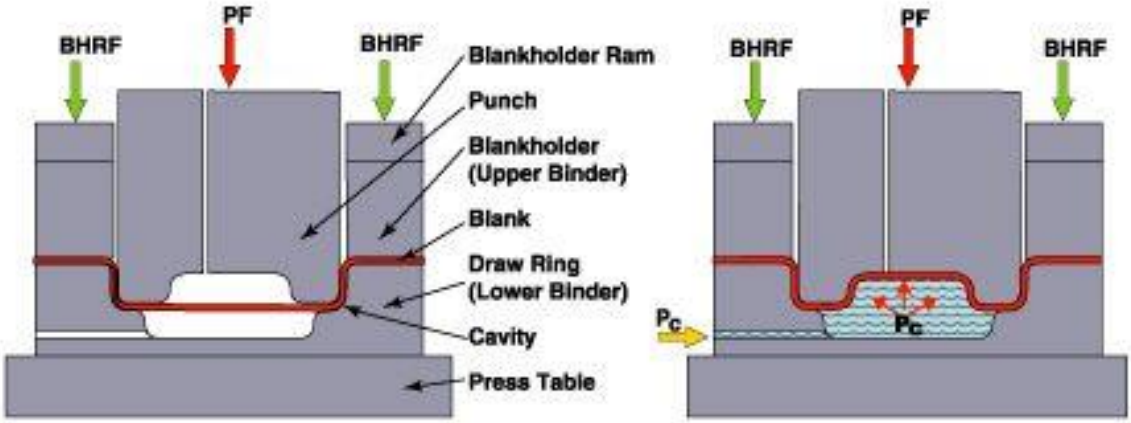

FIGURE 1.7: hydro-mechanical or counter pressure forming[40]

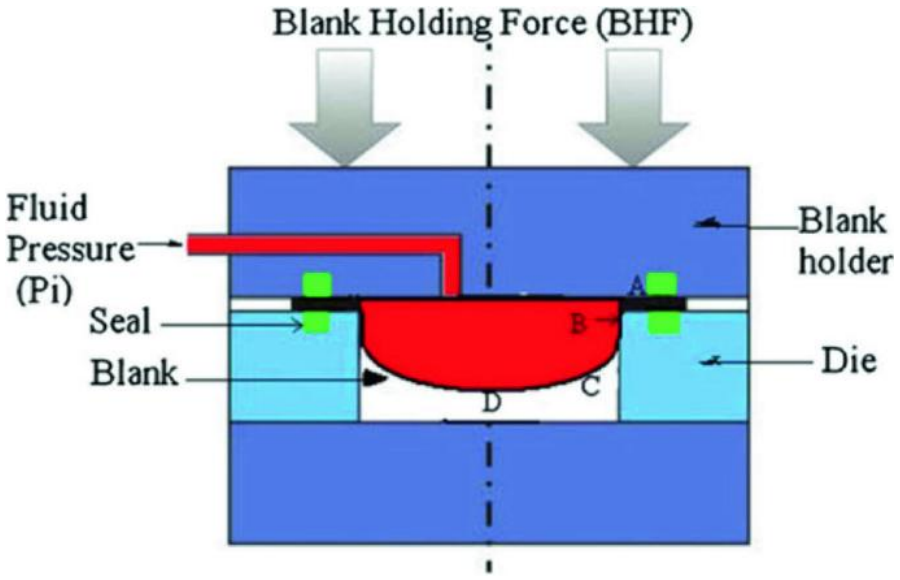

(b)

FIGURE 1.8 : punchless hydroforming or high-pressure forming[40]

Hydroforming techniques can be used to successfully form sheets and tubes into a wide variety of complex geometries [40, 43, 44]. Some of the components produced by sheet hydroforming are shown in Figure 1.9 [45] .



FIGURE 1.9 : Some components formed by sheet hydroforming for industrial applications [45]

1.7.3 Drawing Processes

Metalworking involves the transformation of metals into various parts and components. One of the prevalent metalworking techniques is metal drawing, where metal is pulled through a mold or die. Similar to the extrusion process, where metal is pushed through a die using a draw punch, metal drawing results in a final product with a depth equal to or greater than its width or radius. Known as deep drawing, this variant offers substantial cost savings and the ability to create high-strength, lightweight products, making it a favored choice for numerous manufacturers.

1.7.3.1 Deep Drawing:

Due of its significance in numerous industrial applications, the deep drawing method has been the subject of intense research during the past few decades. In order to investigate sheet metal forming operations, including materials, formability difficulties, tooling, and tribology, the International Deep Drawing Research Group (IDDRG) is attempting to bring together various research organizations from across

the world. Additionally, it coordinates global gatherings of scientists, academics, and industry professionals to exchange scientific knowledge about deep drawing and other sheet metal forming processes. With new alloy grades constantly hitting the market, the IDDRG and other worldwide industry and institutional research groups came to the conclusion that more ongoing research is crucial in the sheet forming process[46]

The use of lightweight materials like copper, magnesium, and aluminum in complex component configuration systems is growing quickly. Understanding the technical process and the factors that affect it, such as the type of lubricant, the clearance between the die and punch, the die and punch profile, the blank holding type, the blank holding force, the blank holding mechanism, the blank thickness, and the material properties, is crucial. In order to reduce design costs and rejections, there is also a need for rapid formability assessments for sheet metal, such as Forming Limit Diagrams (FLD) and Limiting Drawing Ratios (LDR). The difficulties with sheet forming are driving the development of new deep drawing production methods in the current decade. The designer must have a full understanding of the deep drawing process and its limits because it is a complicated plane strain deformation process that is subject to biaxial stresses and strains[46]. The principle of deep drawing is shown in Figure 1.10.

In deep drawing operation, a two-dimensional plane sheet, known as blank, transforms into a three-dimensional component. It involves forcing the blank gradually into the die cavity with a punch while holding the flange region between the blank holder and die shoulder[47] to regulate the flow of blank material [48].

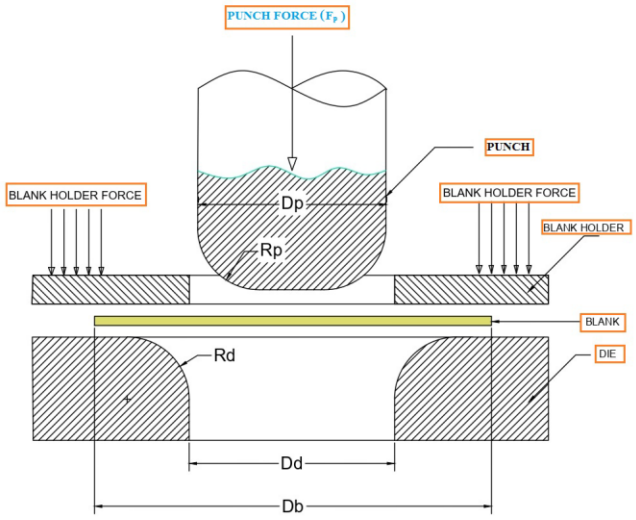

FIGURE 1.10: Principle of Deep drawing [48]



FIGURE 1.11: Range of Components produced in deep drawing [49–51]

Figure 1.11 shown some of the components that are typically created in deep sketching. Deep drawing is a multi-step process that starts with punching the blank into the die and finishes with the entire drawn cup being ejected through a die cavity.

The blank is exposed to a number of intricate stresses of various kinds, including circumferential compressive stresses at the entire flange section, bending stresses at the punch nose and die shoulder regions, and radial tensile stresses at the wall portion. The blank bends around the punch nose and die shoulder areas as a result of punch load. Different stages involved in deep drawing process are shown in Figure 1.12.

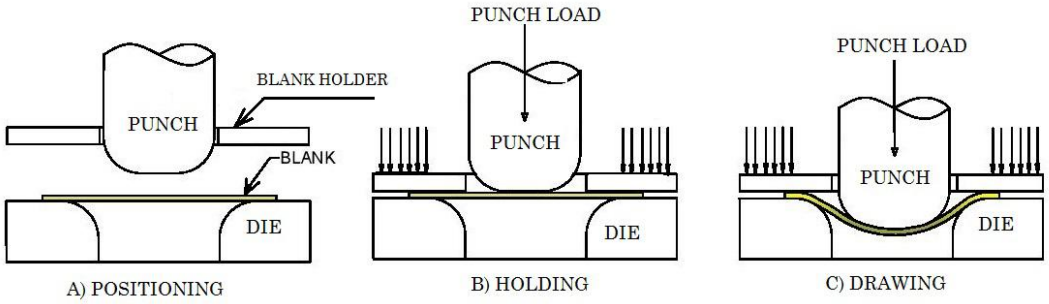

FIGURE 1.12: Scheme of deep drawing process[52]

As seen in Figure 1.12(c), the punch's downward motion causes the bent piece of the blank to move deeper into the die and create a shallow cup. The flange becomes a whole wall section of the cup at the end of the punch stroke, turning the shallow cup into a final cup [53]. Tensile stresses are applied to the vertical wall, circumferential compressive stresses are applied to the flange portion, and biaxial tensile stresses are applied to the bottom portion throughout the operation. It has been noted that during the deep drawing process, the cup's sidewall and flange sections flex. The friction force at the flange is crucial to deep drawing's successful operation. [46].

The blank material moves in the direction of the die cavity when the drawing force is greater than the frictional forces between the contacting surfaces of various tool parts. When the blank is pushed into the die hole while the material is prevented from doing so by frictional forces, a pulling tendency is created. The circumferential compression of the blank section at the flange region results in hoop compressive stresses and a propensity for wrinkle formation. The wrinkles are formed when the hold-down force is not sufficient or the frictional coefficient is less. Hence, the radial tension is the actual source for hoop compressive stresses [53].

Deep Drawing Advantages:

1. When compared to comparable production methods, tool construction costs are cheaper.
2. The method works well for goods that need to be very strong and light in weight.

   Additionally, the approach is advised for product geometries that cannot be produced using alternative production methods.
3. When creating large quantities, deep drawing is particularly advantageous because the cost per unit drops significantly as the number of units increases.
4. Good mechanical properties:

   The process can increase the strength of the material through work hardening, resulting in more durable parts.
5. Seamless and complex shapes:

   Deep drawing can produce parts with intricate geometries and without seams, which can improve the overall product quality and reduce the need for additional joining processes.
6. Good dimensional accuracy and consistency:

   Deep drawing can achieve high precision and consistency in the dimensions of the finished parts.

Deep Drawing Disadvantages:

1. The thickness of the material greatly influences the cost of processing.
2. The parts must be driven into the dies with the help of special sleeves.
3. Due to its low production rate, this procedure is expensive.
4. Limited shapes
5. High initial setup cost:

   The cost of tooling and setting up the deep drawing process can be significant, particularly for complex geometries, making it less suitable for small production runs.

CHAPTER 2

LITERATURE REVIEW

This chapter presents a review of the literature on the mechanism of the development of the ultrafine-grained structure in cryorolling and the related effects on mechanical properties, as the current work focuses on the development of ultrafine-grained (UFG) Al alloy sheets by cryorolling and then improving the formability of cryorolled sheets.

2.1 Microstructural Changes during Cryorolling

By suppressing dynamic recovery, the annihilation of dislocations is less ended when the deformation temperature decreases. Numerous authors have reported on this [30] [34], [35]. Figure 2.1 [55] shows the mechanism of grain refining during cryorolling.

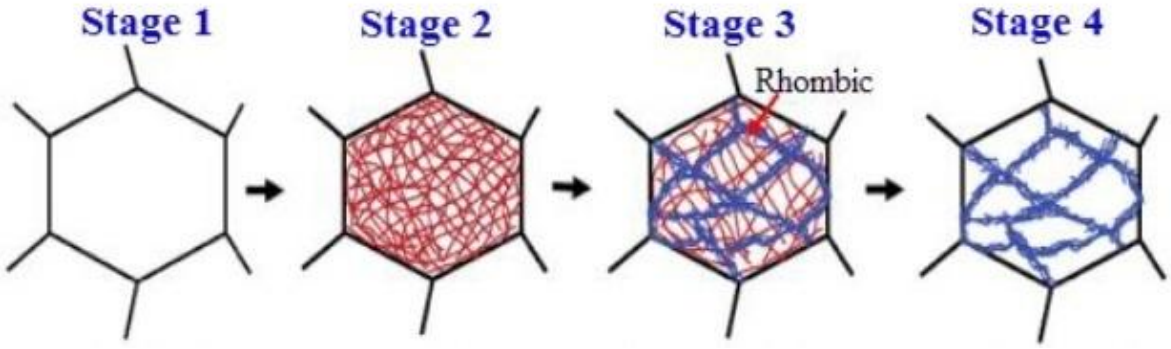

FIGURE 2.1 : Mechanism of grain refinement during cryorolling of aluminum alloys [55]

Work hardening linked to extreme plastic deformation results in a tangled microstructure, which then transforms into a somewhat ordered structure when cells begin to develop inside the grains. Dense dislocations make up the cell borders, and when these dislocations within the cells are annihilated, fine sub-grains with a little bit more misorientation are produced [55]. Precipitation hardening and solute strengthening are two additional mechanisms that lead to improved strengthening, though. Cryorolling has been done on the material following solid solution treatment, in which the solute atoms are dissolved in the matrix, as documented in the literature [56], [57], [58], [59], [60]. As a result of adiabatic heating in the sample, these solute atoms precipitate out of the matrix during rolling and create precipitates, or phases with unique crystal structures. The precipitated atoms or clusters holding down the dislocation movement provide higher flow stress. Numerous factors, such as the quenching temperature, ambient temperature, thickness reduction following each pass, the number of passes, and the duration between passes, affect the precipitation of solute atoms during room temperature rolling. The induced temperature, which fluctuates based on the previously listed parameters, determines the precipitation of solute atoms. As such, it exhibits a range of deformation behaviors during tensile testing. According to recent research by Wang et al. [61], as shown in Figure 2.2 precipitation in cryorolled Cu-Ni-Si alloys is greatly accelerated as long as there is greater dislocation density, which promotes more heterogeneous nucleation.

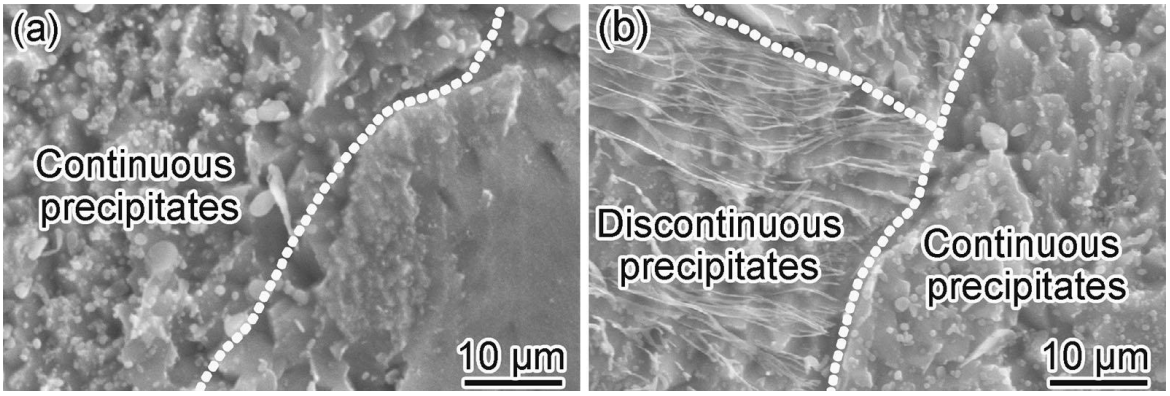

FIGURE 2.2: SEM images of Cu–Ni–Si alloy aged at 723 K for 24 h: a RTR sample, b CR sample[61]

Higher stored energy during the later stages of aging promotes recrystallization (it helps the creation of discontinuous precipitation). Following a brief annealing period, the cryorolled commercial pure aluminum samples' deformation behavior enhanced the materials' anisotropic characteristics. This has been linked to the enhanced micro-forming capabilities of UFG material as well as its distinct equiaxed, thermally stable microstructure made up of high-angle nanograins [62]. Peak shift and peak broadening were detected in the UFG AA1050 alloys produced by cryorolling, according to Sekhar et al. [63]. This was ascribed to the development of tiny grains and a higher density of defects than in cold rolling methods. The higher fracture toughness observed in the cryorolled and annealed samples compared to the cold rolled samples is supported by the fractographic features of cryorolled AA6082 alloys reported by Kumar et al. [64]. These features include shallow ridges, transgranular facets, flat circular and elongated dimples, small sized Si-rich precipitates, and high kernel average misorientation.

Rong Li et al [65] examined Using a high-purity argon environment and a vacuum induction melting furnace, an alloy with the composition Cu-1.79Ti-0.39Cr-0.1Mg (weight%) was created. The microstructure, texturing, and mechanical characteristics of the alloy were examined by the use of electron backscatter diffraction, transmission electron microscopy, and X-ray diffraction to compare the impacts of room temperature and cryogenic rolling.The findings demonstrate that, for any measured rolling reduction, the hardness of the cryogenically rolled alloy is 18–30 HV higher than that of the rolled alloy at ambient temperature as shown in Figure 2.3.

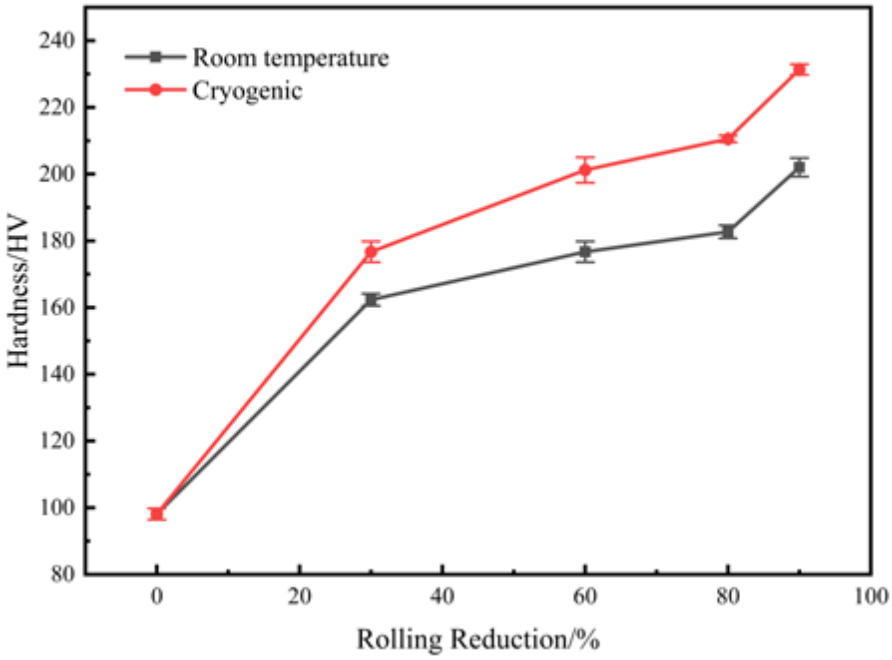

FIGURE 2.3: The variation of Hardness with different rolling directions

The alloy that was cryogenically rolled by 90% reduction has a yield strength of 723 MPa and a tensile strength of 796 MPa. The orientation density of the Brass texture grows as rolling reduction increases, but that of the Cube texture drops. Particularly during cryogenic rolling, the brass texture is desired, indicating that cross-slip is limited at the cryogenic temperature. The Cu-Ti-Cr-Mg alloy's dislocation densities rise dramatically during deformation, eventually reaching 23.03 x 10^{-14} m^2 and 29.98 x10^{-14} m^2 for the room temperature rolled alloy and cryogenically rolled alloy, respectively, following a 90% reduction. This discrepancy may be explained by the way that cryogenic temperatures hinder dynamic recrystallization and recovery. The dislocation and nano-twin creation are aided by the cryogenic temperature, which enhances the alloy's mechanical qualities.

2.2 Effect of Cryorolling on Mechanical Properties

There are conflicting reports regarding the qualities that cryorolling yields. Due to a larger dislocation density in the sheets than in cold-rolled sheets with the same

thickness reduction, cryorolling has undoubtedly increased strength and hardness; but, in the case of some Al alloys, it is often linked with a reduction in ductility [66], [67], [68], [69], [70], [71], [72], [73], [74]. Nonetheless, some researchers found that UFG and nanocrystalline metals like Zr, Cu, and steel have increased ductility and strength [75], [76], [77]. Higher strength and ductility in cryorolled Zr were reported by Shi et al. [76] as indicators of increased toughness, and this was explained by the motion of pre-existing high density of dislocations at high stress to create nano-grains and sub-grains. According to He et al. [78], the gliding of already-existing mobile dislocations and the controlled release of the Transformation Induced Plasticity (TRIP) effect allow for the great ductility and high yield strength that may be achieved in deformed and partitioned steels. Wang et al. [75] also observed high tensile ductility in pure Cu, treated similarly .

High strength and ductility are required for optimum toughness in materials intended for structural use. However, in most cases, ductility and strength in nano/ultrafine-grained materials are contradictory characteristics [79]. Improved strain hardening ability in nano/ultrafine-grained materials has been attained through the application of several techniques. The following are the key tactics: i) controlling the distribution of grain sizes [75], ii) creating nanotwins [80], iii) lowering the energy of the stacking fault and raising the solute content [81], and iv) constructing a gradient strucure [82]. Materials produced by cryorolling followed by brief annealing [83] and powder metallurgy approach [84] have demonstrated a strong mix of strength and ductility through bimodal and multimodal grain structure.

Sheets of the alloy AA5083 have been described and compared to cold-rolled and annealed sheets. This alloy was cryorolled in several passes to a final thickness of 1 mm (80% reduction with a true strain of 1.6) from sheets that were 5 millimeters thick. After cryorolling, a brief annealing at 275°C for 15 minutes would provide a suitable balance of strength and ductility, according to research on the effects of annealing temperature and duration on hardness[85]. The formability of cryorolled AA5083 alloy sheets was described in this paper. The mechanical characteristics of sheet samples that had been cryorolled and cold rolled with an 80% thickness decrease were compared. Using the limiting dome height test, formability in the

biaxial stretching mode was ascertained. Samples of cryorolled AA5083 alloy were partially annealed between 150°C and 300°C to increase formability without appreciably reducing strength. It was discovered that the ideal heat treatment temperature for attaining a reasonable balance of strength and formability was between 200 and 250°C[31].

In a comparison of the mechanical characteristics of cold-rolled and cryorolled AA8090 alloy sheets at a 70% reduction, the accumulation of strain in the rolling direction and the effects of cryorolling were found to be responsible for the cryorolled sheet's increased strength [86]. The process of annealing cryorolled commercially pure Al (strain: 0.75) at 275°C for 15 minutes produced ultrafine equiaxed grains with improved ductility, measuring less than 500 nm in diameter [87]. A novel mechanism for the enhancement of cryorolled sheets' ductility during tensile deformation was put forth by Yu et al. [68]. According to this, homogeneous elongation, void nucleation and growth, local necking, grain refinement till the mean grain size approaches the lowest possible mean grain size, and damage are the processes that cause the deformation and fracture of cryorolled sheets under tensile deformation. Additionally, they noticed that compared to rolled material at ambient temperature, the minimum feasible mean grain size in cryorolled material is smaller. Applying cryorolling and post-cryoroll aging treatment to an AA2014 aluminum alloy simultaneously improves its strength, ductility, and wear resistance [88]. Bhattacharjee et al. [89] have showcased a noteworthy characteristic of the cryorolled and annealed samples (AlCoCrFeNi2), which is their hierarchical microstructure. This property allows for the simultaneous increase of strength and ductility [89]. The cryorolling of AA5083 and AA1070 samples was compared by Dhal et al. [90]. Because of the balance between the dislocation annihilation caused by dynamic recovery and the dislocation accumulation during cryorolling, the tensile strength increment of AA5083 samples was significantly greater than that of AA1070 after cryorolling (dynamic recovery is more prominent in AA1070 due to its greater stacking fault energy compared to AA5083).

2.3 Effect of Cryorolling on Formability

The study of the formability characteristics of ultrafine-grained aluminum alloys has gained significant importance due to the significant alteration of hardening and anisotropic behavior of aluminum alloy sheets caused by microstructural features. Formability has generally been found higher in cryorolled as compared to cold rolled as shown in Figure 2.4[91], however post heat treatment may help.

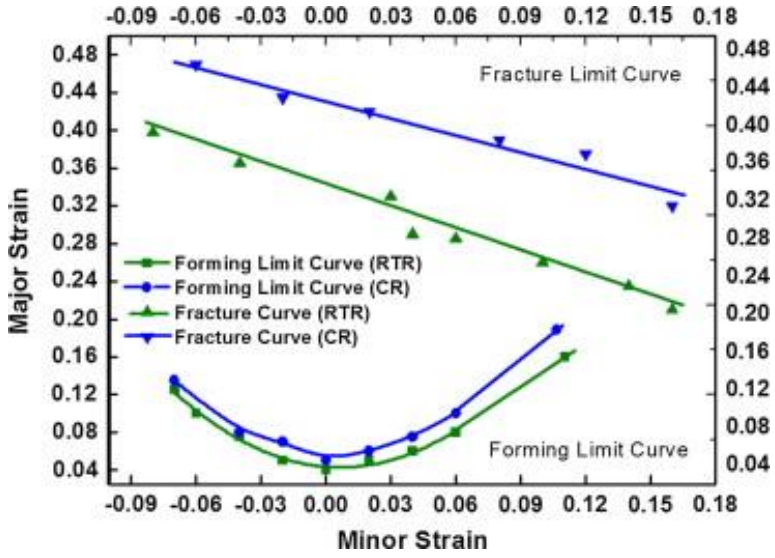

FIGURE 2.4: Comparison of forming limit diagrams and fracture curves for room temperature rolling and cryorolling conditions[91]

Low-temperature recovery heat treatment was used to increase the ductility of the ultrafine-grained aluminum alloy sheets [87] [92], [93]. In their investigation of the formability of cryorolled aluminum alloy sheets, Taylor et al. [94] found that annealing the sheets at 275°C for 120 and 2300 seconds enhanced the total elongation in uniaxial stress by 5%. When compared to the as-rolled condition, the limiting major strain improved by 40% in biaxial stretching mode. The strength and formability of cryorolled 2024 aluminum alloy were investigated by Weiss et al. [95] under biaxial stretching conditions at various aging sequences. Stretchability improved after 8 hours of aging at 150°C following cryorolling.

Using the Erichsen cupping test, the formability of cryorolled precipitate hardenable AA2024 alloy has been investigated [96]. Samples that were cryorolled and then heat treated for eight hours at 150°C had the best formability. When cold rolled and cryorolled AA6061 alloy sheets were tested for mechanical characteristics and formability, it was discovered that the cryorolled sheets had greater strength and hardness than the cold rolled sheets and the alloy in its as-received state [91]. Due to heterogeneous slip, cryorolled sheets demonstrated somewhat greater formability than cold rolled sheets in the as-rolled condition, despite the fact that both types of sheets have very poor ductility and formability. Thus, in order to use these alloys for applications that call for a good balance between strength and formability, a post-heat treatment must be performed following cryorolling. Formability in the as-rolled condition is covered in some published works [91], [97], [98], but no attempt has been made to define the formability of cryorolled sheets following post-heat treatment in all modes of deformation. The formability and fracture behavior of cold-rolled and cryorolled Al-3Mg-0.25Sc samples were described by Vigneshwaran et al. [99]. It was demonstrated that formability and fracture resistance were improved by void coalescence delays. In their investigation of the formability of cryorolled commercial pure aluminum at different reductions, Sekhar et al. [63] found that cryorolled samples had superior formability compared to cold rolled samples. It was thought that increased deformation before necking was caused by heterogeneous slide in cryorolled conditions. When Dhal et al. [90] investigated how alloy chemistry affected the characteristics of cryorolled AA5083 and AA1070 sheets, they discovered that AA5083 had better average anisotropy and a higher strain hardening exponent than AA1070, which improved formability features. These were ascribed to the impact of reduced stacking defect energy of AA5083 and incoherent magnesium solute atoms dispersed in aluminum matrix. Even after annealing at high temperatures, the anisotropic characteristics of the AA5083 alloy remained bigger than those of AA1070 because of the preservation of rolling texture at cryogenic temperatures.

Khalkho et al [100] The current project attempts to create aluminum metal matrix composites (AA7075) strengthened with different ratios of tantalum carbide (TaC)

utilizing a rheo stir casting technique, ranging from 0.1 to 0.5 weight percent. The consequences of secondary procedures like rolling under various circumstances and solutionizing heat treatment were further evaluated on the composite AA7075/0.5TaC. According to the microstructural investigation, the pining effect caused by the addition of TaC to the AA7075 matrix led to grain refinement. With an increase in TaC addition, a progressive improvement in the mechanical characteristics was noted. The composite with 0.5 weight percent TaC exhibited the maximum microhardness of 96 HV, yield strength (YS) of 171 MPa, and ultimate tensile strength (UTS) of 205 MPa, all due to the dispersion strengthening mechanism. The AA7075/TaC composites' densification and particle distribution were improved by the rheo stir casting technique. Through the use of homogenization treatment, the secondary phases were dissolved, resulting in precipitation hardening and increased hardness. Because dynamic recovery was suppressed, the cryo-rolled specimen with a 70% thickness reduction had the maximum hardness of 165 HV among all rolling methods. Analysis of the strengthening processes' impact on YS showed that the experimental YS is greater than the theoretical YS.

Abbas et al [101] The current study looked at the effects of annealing on the mechanical, chemical, and formability properties of 7075 alloy. During the bending test, the formability was attained. Mechanical and chemical qualities are represented by tests for tensile strength, hardness, microstructure, and corrosion. After preparing the test specimens for each test, they underwent an electrical furnace annealing heat treatment, where they were heated to 200°C and 300°C for two hours. Subsequently, the samples were permitted to reach room temperature within the furnace. The findings show that there was a roughly 50% loss in both hardness and tensile strength as shown in Figure 2.5. The symbol (A) being given to specimens that were not exposed to annealing heat treatment, and the symbols (B and C) being given to specimens that were heated to 200, and 300°C consequently, submerged at this temperature for two hours and then left to cool down in the furnace to room temperature to complete the annealing process. When compared to base metal, the specimens' bending strength was improved by about 30%, allowing them to bend at

an extremely high angle without breaking or cracking. The microstructure was stabilized and the second phase precipitate component was released using annealing heat treatment, which was carried out under carefully chosen conditions and temperatures.

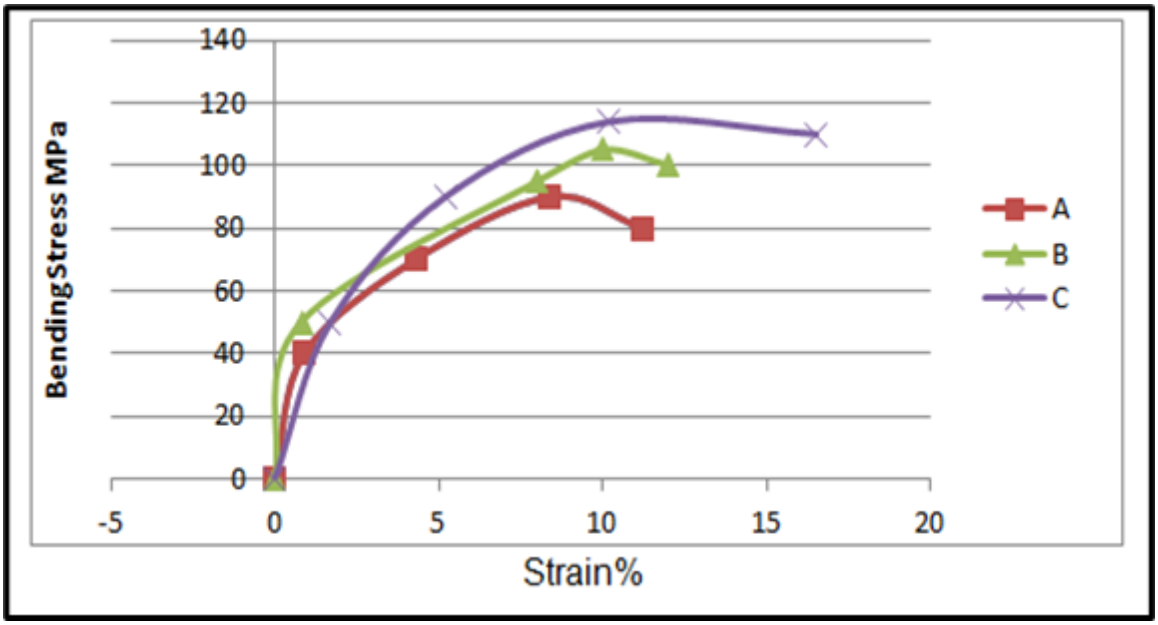

FIGURE 2.5: Stress-strain curve for bending test for specimens A, B, and C[101]

Wang et al [102] The performance and microstructure characterization of Al–Mg–Si alloys rolled at room temperature (RTR) and cryogenic rolling (CR) were methodically examined in this work. The outcome demonstrated that whereas the hardness of the RTR alloys rose at the early aging stage, the hardness of the CR alloys decreased. In the early aging period of the CR alloys, regression events were observed. Even after being subjected to the identical solid solution treatment, the CR alloys still showed some substructures, and their degree of recrystallization was noticeably lower than that of the RTR alloys. The strength and density of precipitates in the CR 75 alloy after 50 hours of age were greater than those in the other alloys; this suggested that the substructures aided in precipitation and precipitate growth. To show the precipitation contribution at various aging phases, a model of precipitation strength was used. The highest precipitation strengthening was attained by the CR 75 alloy, according to the results.

Pant et al [103] The current study examines the effects of ultrafine grain (UFG) Al 5052 alloy cryo-cross rolling (CCR) and annealing (CCR + AN) on high cycle fatigue (HCF). At liquid nitrogen temperature (− 196°C), Al 5052 alloy sheets were thinned to about 90% of their original thickness using the CCR technique. The CCR specimen was heated for 45 minutes at a temperature range of 100–250°C in order to examine the impact of heat treatment on mechanical qualities such as yield strength, tensile strength, and high cycle fatigue properties. Through the use of transmission electron microscopy, field emission scanning electron microscopy, and electron back scattered diffraction, the microstructure of each specimen as well as their combined effects were examined. In comparison to solution-treated alloy, the CCR sample has a greater HCF strength due to the establishment of a UFG-based microstructure and reduced grain size, which minimizes the possibility of stress concentration close to the fracture site. The CCR + AN alloy had remarkable HCF characteristics up to 100°C during annealing. This is explained by the precipitation interaction at grain boundaries, which enhances fracture development resistance. As the annealing temperature rises from (100–250°C), the HCF strength gradually falls because of grain coarsening brought on by recrystallization and the recovery process within the specified temperature range.

Sadeghi et al [104] investigate one of the most important severe plastic deformation techniques for producing aluminum sheets with exceptional formability limits is cryogenic rolling. The formability of AA6061 for cryogenic rolling both before and after artificial aging is characterized in the current work. Formability is measured using the Nakajima method, which is based on the ISO standard. The samples are aged between 100 and 150°C. It is discovered that the ideal temperature for attaining a reasonable balance between strength and formability is 150 ~C during artificial aging. Strength increased by up to 40% during artificial aging; after 50 hours of age at 150°C, the cryo-rolled sample's original value of 250 MPa climbed to 350 MPa. Formability also improved, particularly under multi-axial forming conditions as shown in Figure 2.6.

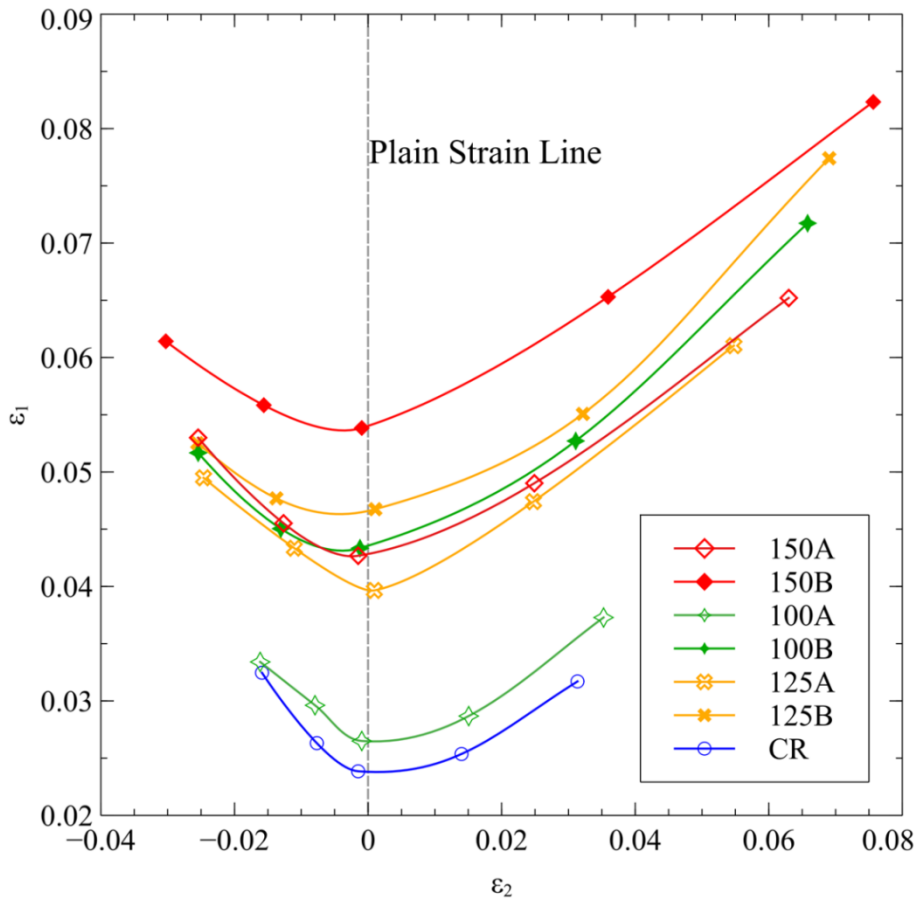

FIGURE 2.6: The forming limit diagram for different aging treatments of Aluminum Alloy 6061[105]

Zhang et al [106] examined how the microstructure, average microstrain, dislocation density, nanomicrohardness, tensile strength, and corrosion behavior of the 2A12 aluminum alloy were affected by the high frequency impacting and rooling (HFIR) treatment. It was successful to generate an SPD layer. As the static pressure rose, The top surface's average grain size shrank. As static pressure rises, so do nanomicrohardness, elastic modulus, and tensile strength. All of the samples, including the HFIR-free one, showed the best corrosion resistance when the aluminum alloy 2A12 was treated with 500N static pressure. The development of dense passive film, low surface roughness, compressive residual stress, tiny grain size, and these other factors were critical in enhancing the corrosion resistance. Abishkenov et al [107] The goal of this work is to determine how the microstructure and mechanical characteristics of the alloy are affected by cryorolling (at a

temperature of –150°C) in mill rolls that use shear alternating severe plastic deformation (SPD). The methods of rolling at room temperature (RTR) and cryorolling (CR) are compared. Based on an analysis of the samples' microstructure and mechanical characteristics, it was determined that CR guarantees the creation of ultra-fine grained (UFG) material, with an average grain size of 350 ÷ 500 nm. It also increases hardness by 162,2% (118 ± 2 HV) and Rm by 106,34% (293 ± 5 MPa).

2.4 Methods to Enhance Formability

Some of the methods which have been developed to enhance formability of sheets are briefly discussed below.

2.4.1 Warm Forming

In order to lessen flow stress and improve formability, warm forming involves forming metal at a temperature that is lower than the recrystallization temperature (between 0.3 and 0.5 times the material's absolute melting temperature) [108]. To a certain extent, warm forming combines the benefits of hot forming and cold working [108], [109].

2.4.2 Super plastic Forming

A non-traditional forming technique called superplastic forming is used to increase the ductility and formability of some Al and Ti alloys. The phenomenon known as superplasticity occurs when some materials, when subjected to regulated conditions, undergo extremely massive plastic deformation without experiencing localized necking in the tensile mode of deformation. Superplastic formation requires extremely low strain rates (10^{-2} to $10^{-}5s^{-1}$) and temperatures above recrystallization temperature [110]. Superplastic materials are characterized by very small grain size and high strain rate sensitivity (m>0.3) at increased temperatures [111], [112].

2.4.3 Viscous Pressure Forming

A type of semisolid, flowable, and viscous substance is applied to the blank as a pressure-carrying medium in the viscous pressure forming method [113]. It is thought that if the medium is applied to both sides of the sheet, it will stretch more evenly [114]. This method works well for many different applications and low volume production, particularly in the aerospace and astronautical industries.

2.4.4 Hydroforming

Similar to the viscous pressure forming method, the sheet hydroforming process uses a high-pressure liquid medium (often oil) to form the blank into the shape of the die cavity instead of a strain-rate-sensitive viscous pressure medium[113].

2.4.5 Incremental Forming

Incremental forming is a sheet metal forming technique that shapes parts by applying localized plastic deformation using a small, computer-controlled tool. It's a dieless process, meaning it doesn't require a die that matches the final part's shape, making it suitable for low-volume, customized production and rapid prototyping. It offers greater formability compared to traditional forming methods due to the localized nature of the deformation[115].

2.5 Summary of Literature Review

From the literature reviews, following points are summarized:

- There is a improved mechanical properties for 5053, 6061, 7075 cryorolled aluminium alloys when compared to cold rolled aluminium alloys.
- Importance of Cryorolling is to improve microstructure, mechanical properties for aluminium alloys.
- Annealing temperature after cryorolling can also affect the microstructure, mechanical properties for aluminium alloys.

- It is essential to understand the formability of materials, a Forming Limit Diagram of 7xxx & 8xxx series of Al alloys extremely useful for both industry and researchers.
- However, no efforts have been done in the past to study the drawing/bending operation of cryorolling sheet in metal forming.

2.6 Motivation and objectives of the Present Work

In recent years, the motor vehicle industry has been to find ways to reduce weight while still maintaining all other design and safety criteria in order to enhance fuel economy. Many aluminum alloys have the potential to replace steel in a variety of applications because of their exceptional strength to weight ratio. However, the fact that aluminum alloys are not as strong or formable as low- and extra-low carbon steels is one of the primary problems. The creation of processing techniques to boost the strength of Al-Mg alloys has been one of the primary topics of interest for academics over the last few decades. Cryorolling has been identified as one of the possible methods to create thin sheets of high strength, ultra-fine-grained aluminum alloys. Nonetheless, the cryorolled sheets' restricted ductility might make it challenging to use them for intricate stampings. You could utilize recovery annealing or partial annealing to get good ductility without significantly compromising strength. Thus, in order to use these alloys for applications that call for a good balance between strength and formability, a post-heat treatment must be performed following cryorolling. Formability of cryorolled sheets following post heat treatment in all modes of deformation has not been attempted to be characterized, despite the fact that some published research is available on the subject [91]. Considering the aforementioned, it has been proposed that combining cryorolling and conventional process improve the use of Al alloys for parts that need to have high strength and formability. The overall goal of this work is to develop high strength, ultrafine-grained aluminum alloy sheets (AA8011 alloy) by cryorolling, partially annealing the sheets, and then study the formability of the cryorolled sheet.

This research aimed to develop technique, a novel technique for industrial growth. However, the novelty of this research is to develop a novel technique for metal such as ferrous and Non-ferrous metals. This method has produced a material with improved mechanical properties and a uniformly distributed structure.

The exact goals of the current research project are as follows:

I. To study the rolling process of cold rolled and Cryorolled 8011 Al alloy sheet.

II. Characterization of Mechanical Properties, Microstructure and Surface roughness of the Cryorolled 8011Al alloy sheet.

III. Determination of formability of 8011 Al alloy sheet by limiting dome height test.

IV. Study formability in Drawing process of Cold rolled and Cryorolled Al alloy sheet.

CHAPTER 3

MATERIAL PROCESSING AND CHARACTERIZATION

The methodology that has been adopted for carrying out the required experimental work in the present research work is presented in this chapter. The detailed description of materials used in the present work, characterization of mechanical properties and microstructure and experimental evaluation of formability and surface roughness is presented here.

3.1 Material Selection

Aluminum alloys of 8xxx series are work-hardenable and hence they are cold worked in order to increase their strength. They are potential materials for applications in automobiles, manufacture for packaging, satellite, aluminum foil, which can be used in bottle caps, radiator, anti-theft cover [116] Because of its low density, ideal plasticity and strength, and ease of surface processing, pure aluminum and aluminum alloys have found widespread application in the construction, packaging, transportation, electronic, mechanical and electrical manufacturing, aerospace, and petrochemical industries in recent years. Additionally, they are simple to work with in terms of plate, foil, pipe, bar, type, line, etc. As a result, behind iron and steel, pure aluminum and aluminum alloys are used as the second most common metals worldwide. Thus, in this work, AA8011 alloy sheet in as received H14 condition having 3mm thickness has been used. Table 3.1 shows the chemical composition of the AA8011 sheets as determined by spectroscopy.

TABLE 3.1: Composition of alloying elements in weight % of AA8011

AA8011	Aluminum (Al)	Chromium (Cr)	Copper (Cu)	Iron (Fe)	Magnesium (Mg)	Manganese (Mn)	Silicon (Si)	Titanium (Ti)	Zinc (Zn)	Nickel (Ni)
	98.58	0.002	0.020	0.66	0.012	0.061	0.63	0.020	00	0.003

3.2 Methodology

The entire research technique used to conduct the necessary experimental study in order to meet the suggested objectives, shown as flow chart in Figure 3.1.

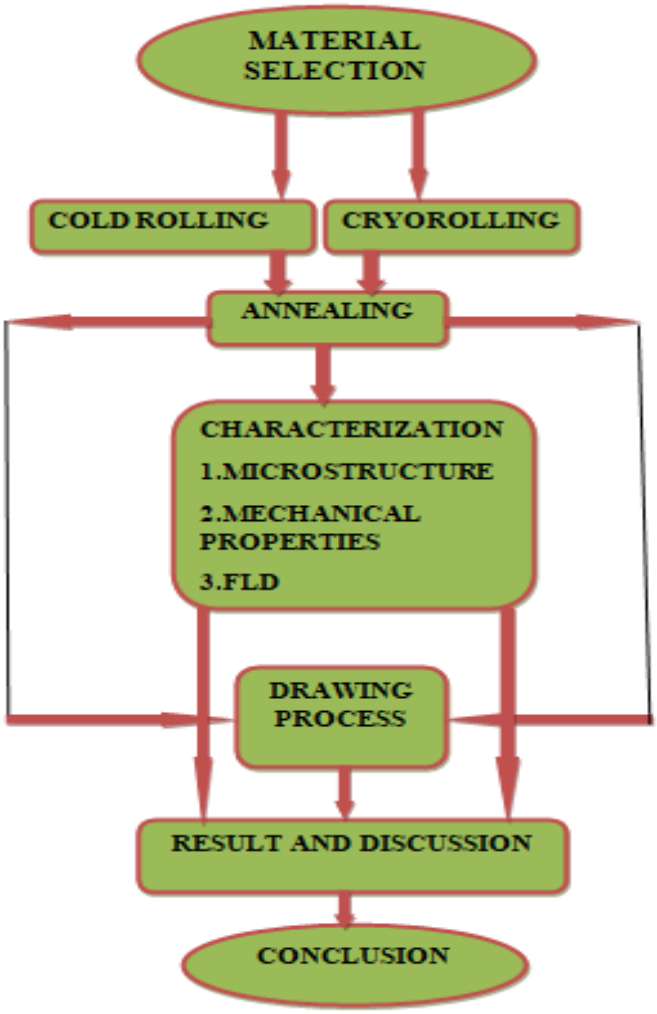

FIGURE 3.1 : The methodology used in the present work

3.3 Cold rolling and Cryorolling

The experimental setup having the rolling mill and liquid nitrogen container used for cryorolling and cold rolling are shown in Figure 3.2. A 4-high rolling mill with work rolls diameter of 200 mm and having speed of 50 rpm have been used for experimental work. A samples of 200mm x 200mm x 3mm AA8011 aluminium alloys sheet have been prepared from 2440mm x 1220mm sheet.



FIGURE 3.2 : Rolling mill and experimental setup used for cold rolling and cryorolling

A rolling samples has been passed through a 4 high rolling mill as shown in Figure 3.3. A schematic process shows rolling cycle for cold rolling and cryorolling. In cryorolling liquid nitrogen bath is used. Multiple passes have been required in rolling process to get the desired thickness of 1mm from 3mm thick sheet.

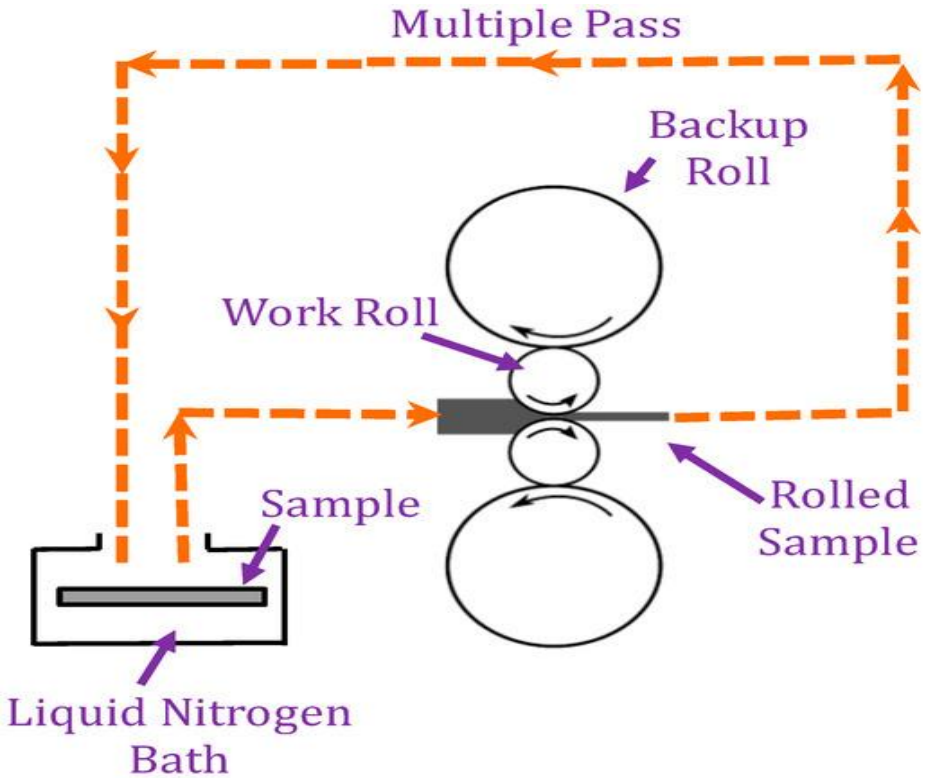

FIGURE 3.3 : Schematic showing rolling cycle of AA8011 alloy sheets

In cold rolling samples of 3mm thick AA8011 alloy sheet have been rolled. In cold rolling it required 4 no of passes to reduce thickness of 3mm AA8011 alloy sheet to 1 mm thickness. The size of sample after rolling is 200mm x 600mm x 1mm. Figure 3.4 represent the various passes of cold rolling. So in each pass, approximately 25% reduction in thickness has been take place.



FIGURE 3.4 : Cold Rolling

In cryorolling initially the samples of 3mm thick AA8011 alloy sheet have been dipped into the liquid nitrogen bath for a 40–45 minutes of time to reach the necessary cryogenic temperature (-196°C) of samples. Temperatures of cryo-cooled samples have been measured using digital temperature measurement gun. Cryo-cooled samples have been rolled through a 4 high rolling mill. In cryorolling we required 6 no of passes to reduce the thickness of 3mm AA8011 alloy sheet to 1 mm thickness, during each pass it is required to dip the samples into liquid nitrogen bath for 10-15 min to achieve the cryo-cooled temperature. In each pass, approximately 15-17% reduction in thickness. Figure 3.5 represent the various passes of cryo rolling.



FIGURE 3.5 : Cryorolling

To obtain stable microstructure and to improve formability rolled sheets were exposed to annealing[15].

A cold rolled and cryorolled samples have been annealed at a temperature of 200°C in furnace as shown in Figure 3.6. After annealing the samples have been air cooled in atmosphere.



FIGURE 3.6 : Furnace used for annealing

3.4 Rolling Defects

After cold rolling and cryorolling some of the defects observed during experimentation is presented as follows.

Initially when sample has been pass through rolling mill the deflection of rolls occurred by the high forces of rolling and due to the imperfection of the roll gaps variation the defects like wavy edges and rolling marks on rolled sheet have been occur as shown in Figure 3.7. Due to compressive load which results in the variation of thickness and rolling marks have been observed. By maintaining the rolling speed and roll gap variations the defects have been neglected and final roll product have been achieved.

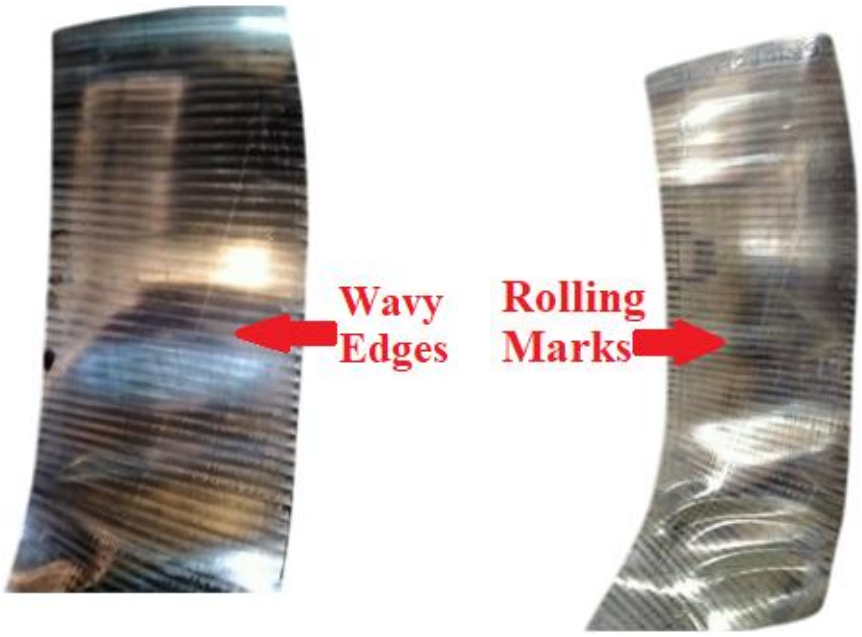

FIGURE 3.7 : Surface defects on rolled samples

3.5 Characterization of Microstructure and Mechanical Properties

3.5.1 Microstructure

The rolled samples' optical microstructure was analyzed using ASTM E3:11(RA2017) and ASTM E407:07(2015) test methods in order to look at the

deformed microstructure and grain boundary properties. Physical characteristics like strength, toughness, ductility, hardness, corrosion resistance, high/low temperature behavior, or wear resistance can all be significantly impacted by a material's microstructure, whether it be metal, polymer, ceramic, or composite. In turn, these characteristics dictate how these materials are used in industrial settings.

Nanostructure is the term used to describe microstructure at scales smaller than those that can be seen with optical microscopes, whereas crystal structure refers to the arrangement of individual atoms. Ultrastructure is the term used to describe the nanostructure of biological specimens. The various flaws in a microstructure, whether present or missing, largely determine how it affects a material's mechanical and physical characteristics. Although these flaws can take many different shapes, pores are the most common. Even if those pores are crucial in defining a material's properties, so is the material's composition. In actuality, several phases can coexist for a variety of materials. These stages have distinct characteristics and, with proper management, can stop the material from breaking.

3.5.2 Hardness

- A material's (specimen's) mechanical resistance to mechanical indentation by a harder body (indenter) is known as its hardness. The indenter is made of diamond, the hardest natural material (industrial diamond).Strength, which is a material's resistance to deformation and separation, is defined differently than hardness. A material's hardness is not one of its basic physical characteristics. However, some materials move in different hardness ranges. Heat has the ability to alter hardness, hence after a heat treatment; a work piece may acquire a new (higher) hardness rating. Static force application methods are commonly used for metal hardness testing. Either the size or depth of the depression that the indenter leaves behind is measured. Depth measuring techniques and optical measurement techniques are distinguished for static procedures in hardness testing. Depth measurement methods

measure the residual indentation depth of the indenter. The Rockwell method is the only standardized depth measurement method (see ISO 6508, ASTM E18). Besides these, there are non-standardized depth measurement methods: Brinell (HB) and Vickers for depth (HV).

- The indenter's remaining indentation size is measured using optical means. The Brinell (ISO 6506, ASTM E10), Knoop (ISO 4545, ASTM E92, ASTM E384), and Vickers (ISO 6507, ASTM E92, ASTM E384) hardness tests are examples of standardized optical hardness testing techniques.
- The remaining indentation size of the indenter is measured using optical techniques. The Brinell hardness test (ISO 6506, ASTM E10), the Knoop hardness test (ISO 4545, ASTM E92, ASTM E384), and the Vickers hardness test (ISO 6507, ASTM E92, ASTM E384) are standards for optical hardness testing.

- As an alternative, techniques that apply dynamic force can also be applied to the hardness test. For instance, the Leeb rebound hardness test method (ISO 16589, ASTM A965), which gauges a ball indenter's rebound height, is one of them.

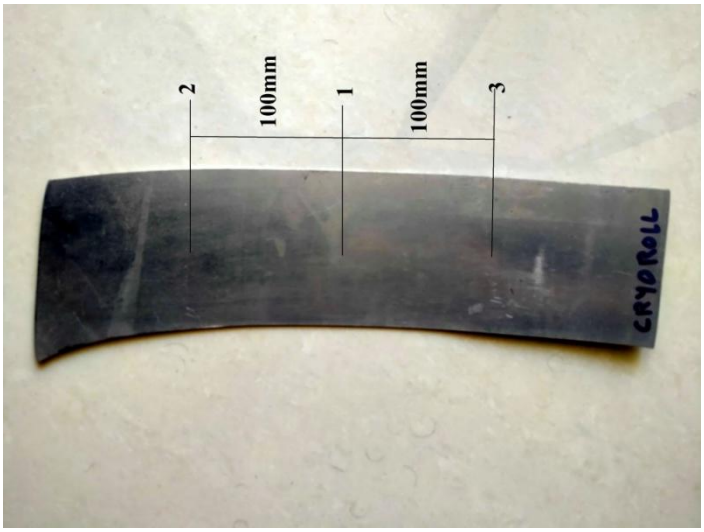

FIGURE 3.8: Hardness sample

Hardness test were performed as per ASTM E18-22 on the cold rolled and cryorolled samples after thickness reduction upto 1mm using Vickers cum superficial hardness testing machine and the hardness values were recorded at three different points as shown in Figure 3.8 and average of these values has been used.

3.5.3 Surface Roughness Measurement

Surface roughness or roughness is defined as the irregularities, which are inherent in the production process (e.g. cutting tool or abrasive grit). Surface roughness is quantified by the deviations in the direction of the normal vector of a real surface from its ideal form. If these deviations are large, the surface is rough; if they are small, the surface is smooth. These distinctions are therefore qualitative not quantitative yet are of considerable importance as defining them this way is well established and functionally sound. Surface roughness is produced only by the method of manufacture resulting from the process rather than the machine. Marks can be left by the tool or grit itself: these will be of a periodic nature for some processes and more random in others. There is also a finer structure formed by tearing of the part during machining, the build-up of debris at the edge and small blemishes in the tool tip. Waviness, however, is attributed to the individual machine, imbalance in the grinding wheel, lead screw inaccuracy and lack of rigidity. Form errors are often caused by the part not being held firmly enough or a slideway not being straight, or heat generated during the process that can cause a surface to bend. It should be emphasized that these three characteristics are never found in isolation. Most surfaces are the result of a combination of the effects of surface roughness, waviness and form.

Surface roughness test were performed as per ASTM D7127:2017 on the cold rolled and cryorolled samples after thickness reduction upto 1mm. Average surface roughness (Ra), also known as arithmetic average, is the most commonly used parameter because it provides a simple value for judging the surface quality of a part accept/reject decision it is usually expressed in microns. The average surface roughness was measured using a surface roughness testing machine marsurf PS1

(DMSPL/07/11) and the Surface roughness values were recorded at five different points and average of these values has been used.

3.5.4 Tensile test

Tensile test specimens from the sheets have been prepared by laser cutting as per ASTM E8/E8M-22 standard as shown in Figure 3.10 and tested along at 0º, 45º, and 90º to the rolling direction . An Computerized Universal Testing M-100 has been used for tensile testing. A view of the tensile test being conducted on an Computerized Universal Testing M-100 as shown in Figure 3.9.



FIGURE 3.9: Computerized Universal Testing M-100



FIGURE 3.10: Tensile Test Specimens

The load elongation data from the tensile tests on cryorolled and cold rolled specimens were recorded, and the engineering stress-strain curves were plotted. YS, UTS, and percentage elongation are examples of standard tensile qualities that have been calculated. The material's yield strength was calculated at 0.2% offset strain. Since the material follows the power-law of strain hardening $\sigma = K\varepsilon^{n}$, the real stress($\sigma$)-true strain ($\varepsilon$) curves plotted using the engineering stress – engineering

strain data were used to calculate the coefficients in the equation, strength coefficient (K) and strain hardening exponent (n). The $\sigma - \varepsilon$ data from the homogeneous plastic deformation zone (before to the commencement of necking) was used to create the $log\sigma - log\varepsilon$ graphs. From the best fit line on the $log\sigma - log\varepsilon$ plot, these parameters were extracted using the linear regression (least square) approach.

3.5.5 Anisotropy

The rolling direction affects the properties of sheet metals both within and normal to the sheet plane. This characteristic, referred to as anisotropy, is caused by the rolled sheet metals' crystalline texture. Anisotropy is measured by the plastic strain ratio (R), which is the ratio of actual strain in width to true strain thickness in a uniaxial tensile test. As seen in Figure 3.11, it is ascertained by taking samples at 0º, 45º, and 90º to the rolling direction. By using [114] one can find the average plastic strain ratio ($\bar{R}$).

$$\bar{R} = \frac{R_0 + 2*R_{45} + R_{90}}{4}$$

where R_o, R_{45} and R_{90} are plastic strain ratios determined at 0°, 45º and 90º to the rolling direction respectively.

As the literature review points out, $\bar{R}$ has a significant impact on the drawability of sheets in deep drawing. Better drawability is achieved with higher $\bar{R}$ [115].

The planar anisotropy ΔR is defined as follows:

$$\Delta R = \frac{R_0 - 2*R_{45} + R_{90}}{2}$$

Deep sketching results in earing. The R-value [116] can be used to determine the size and location of the ears in a deep drawing of a cylindrical cup.



FIGURE 3.11: Directions in which samples were taken for determination of anisotropic parameters

3.5.6 Limiting Dome Height Test

The sample height measured in biaxial tension up to necking or failure is known as the limiting dome height. The test setup consists of upper and lower dies with draw-beads, as depicted in the schematic in Figure 3.12. A view of experimental set-up for LDH tests on the 20-ton capacity double action hydraulic press is shown in Figure 3.13, the tooling was put together on a double action hydraulic press. All the experiments were conducted in dry condition (without lubrication) with a punch velocity of 10 mm/min. Some trial experiments were conducted to identify optimum blank holding force this has been found to be in the range of 80 to 100kN. The tooling for punch diameter, which consists of a hemispherical bottom punch, a die and a blank holder was designed. The tools were fabricated using die steel (D2) in a CNC machining centre. D2 steel is a high carbon and high chromium steel and it is commonly used for making cold working tools because of its excellent wear and abrasion resistance along with high strength and hardness. A circular draw bead was provided on the die and the blank holder to restrict the flow of metal from the flange

region into the die and to ensure that only the portion within the die opening was deformed by the punch. The fabricated punch and dies as shown in Figure 3.14. Samples of varying widths were distorted using a cylindrical punch with a 50 mm diameter and a hemispherical bottom until necking or fracture was noticed in order to determine limit stresses in various modes of deformation. In all the LDH experiments, care was taken to stop the test at the onset of a visible necking or initiation of fracture. For improved repeatability, each width was tested on a minimum of three samples.

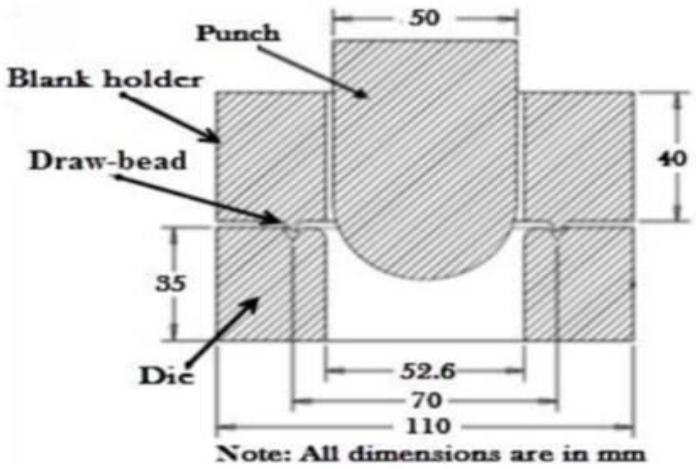

FIGURE 3.12: Schematic diagram of the tooling arrangement for LDH[117]



FIGURE 3.13: The actual experimental setup used for LDH experiments on a 20-ton power press

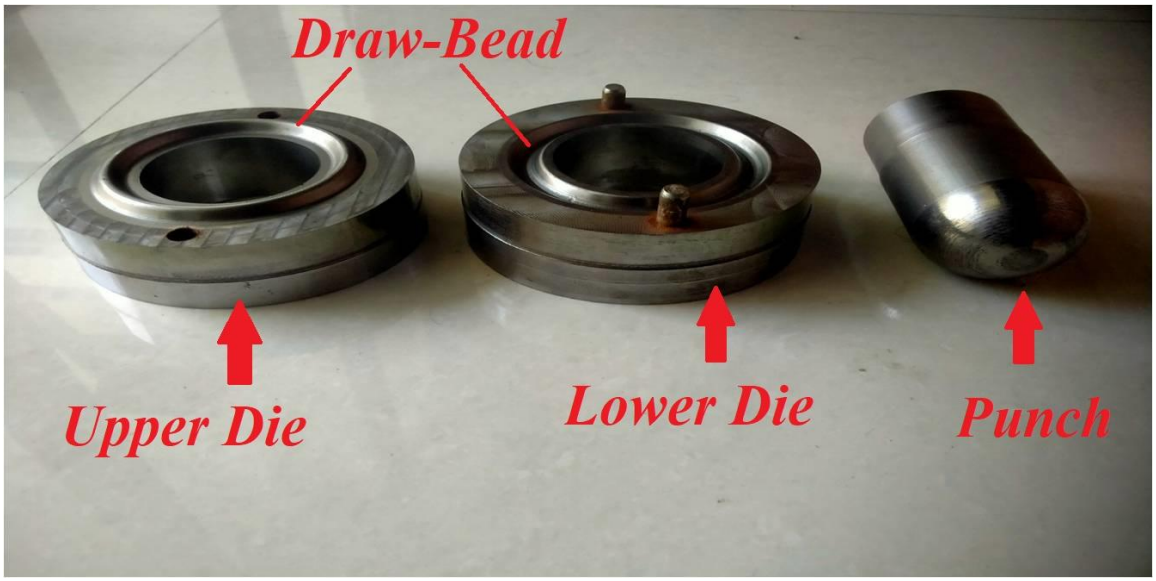

FIGURE 3.14: Fabricated dies and punch for LDH tests

As seen in Figure 3.15, rectangular samples with a constant length of 100 mm and a decreasing width of 20 mm were tested. The size of the LDH sample was decreased by half due to limitations on the size of samples that could be rolled, and as a result, the punch diameter was lowered to 50mm rather than the typical punch diameter of 101.6mm as advised by Ghosh and Hecker [117].

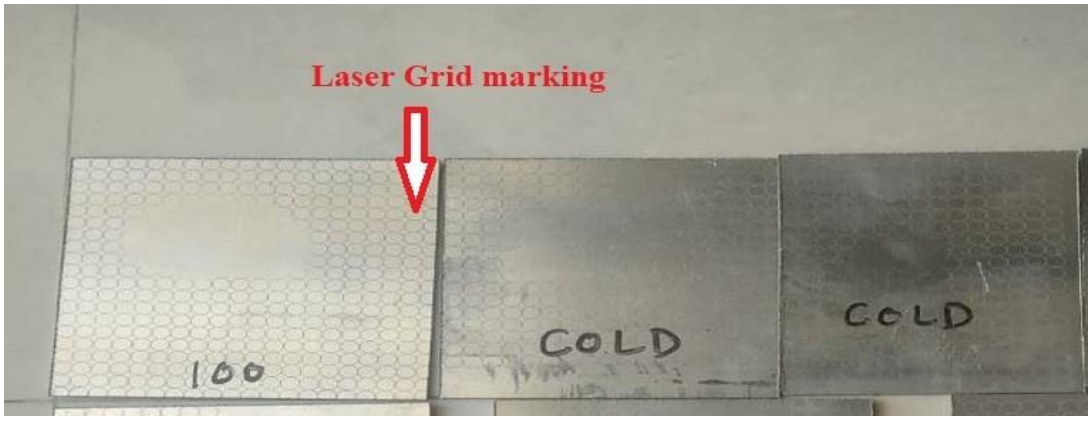

FIGURE 3.15: Samples of different Rectangle width for LDH Test

To stretch the sheet specimen over the punch, it was first clamped between the die and the blank holder.. The extent of drawing in during punch stretching depends on the width of the blank. Since the draw bead diameter is 70mm, draw-in occurs in specimens with width less than 70mm (as there is no complete clamping). As the width decreases, the drawing component increases and stretching component decreases. The samples with width more than 50 mm were tested successfully but when samples with lower width (40mm, 30mm and 20mm) were tested, crack/failure was observed near the draw bead after a certain amount of deformation (Fig. 3.16). It was due to insufficient material in the clamping area and hence it could not support the load applied. Therefore, specimens of lower width were prepared with a slight modification in the geometry with a larger clamping area using geometry according to the Nakazima approach [12]. The enlargement of clamping area of specimens enabled a better material flow over the die radius during deformation and hence prevented failure at the draw bead. The specimens with modified shape were as

shown in Figure 3.17. The experiments were done successfully with the modified blank design with smaller widths and the deformed samples are shown in Fig. 3.19.

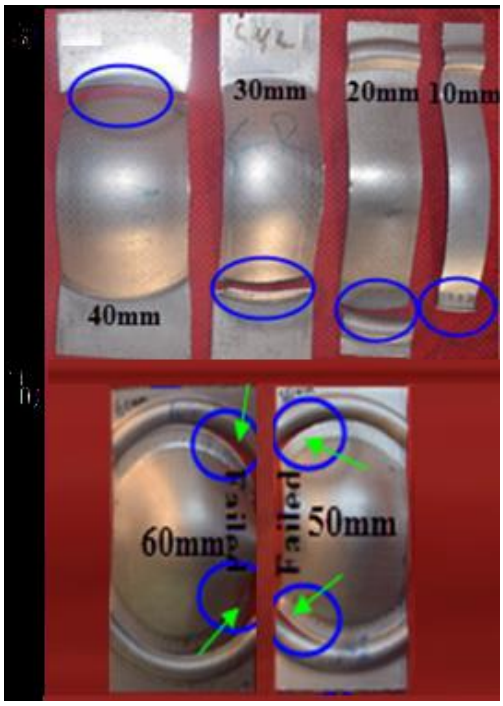

FIGURE 316: Failure in the draw-bead region during testing of lower width samples

A laser marking machine as shown in Figure 3.18 was used to grid mark the blanks with circles of 5.00 mm in diameter and 0.5 mm between neighboring circles

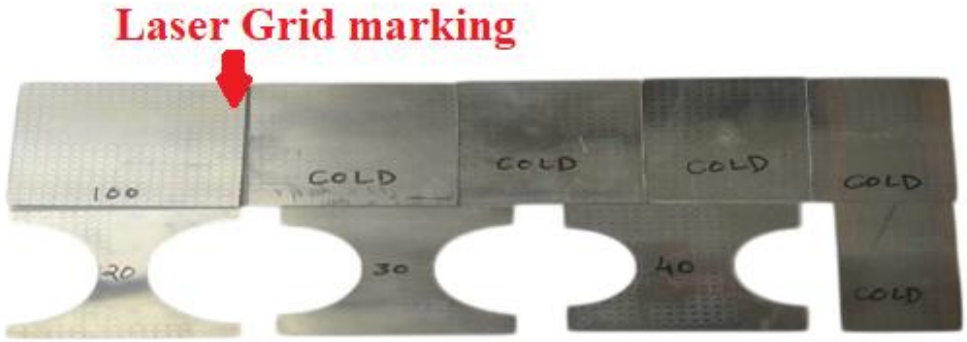

FIGURE 3.17: Samples of different width for FLD Test

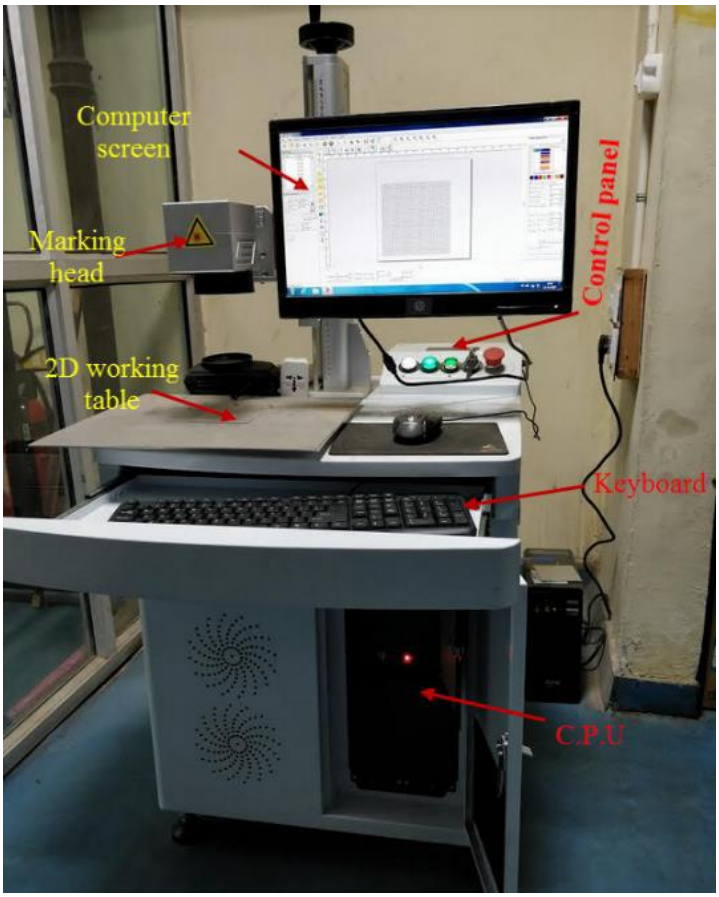

FIGURE 3.18: Laser marking machine

Figure 3.19 displays several example samples following testing. Following deformation, the ellipses' major and minor diameters—selected from the tested samples' safe, necked, and failed regions were measured using the Toolmakers microscope in order to plot and build limit diagrams, as seen in Figure 3.20. By measuring the major and minor diameters of the ellipses in the region of necking/failure in accordance with ASTM E2218, the major and minor stresses on the surface of the deformed specimens were identified. Figure 3.21[118] illustrates potential modifications to the grid pattern's shape brought about by forming operations on metallic sheet.

Major Strain = $[(L_f-L_o)/L_o] \times 100$…….[118]

Minor Strain = $[(W_f-W_o)/W_o] \times 100$…… ….[118]

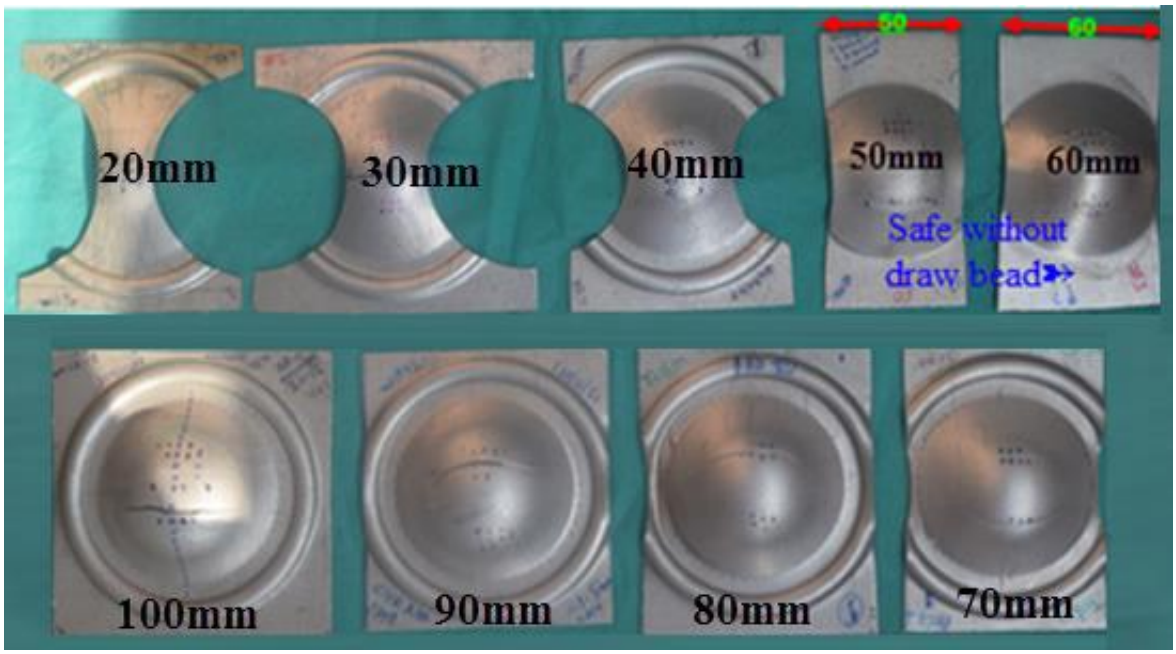

FIGURE 3.19: Tested FLD samples for determination of FLD

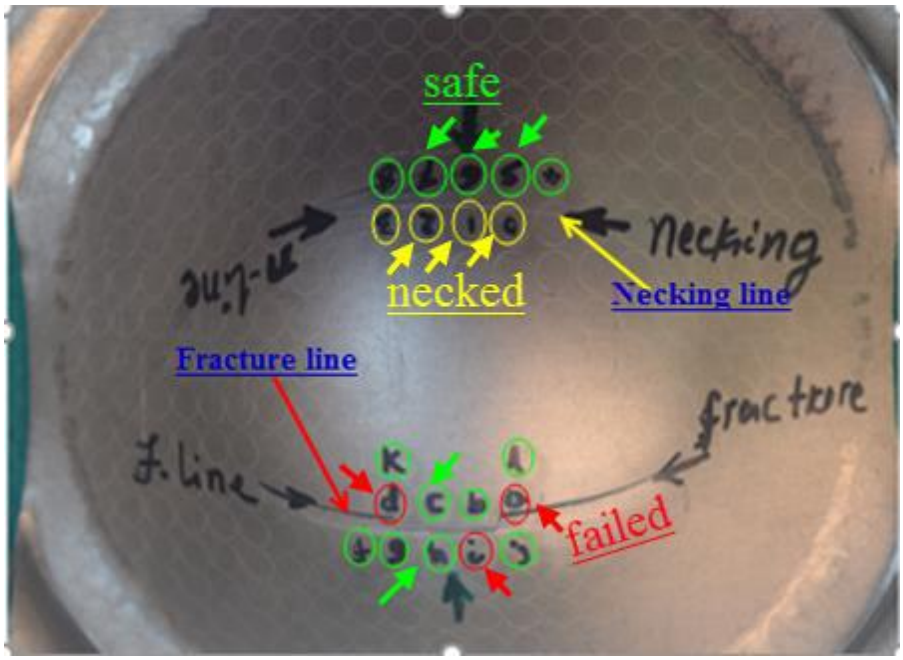

FIGURE 3.20: Close-up view showing deformed grid used for measurement of strains in safe, necked and failed regions

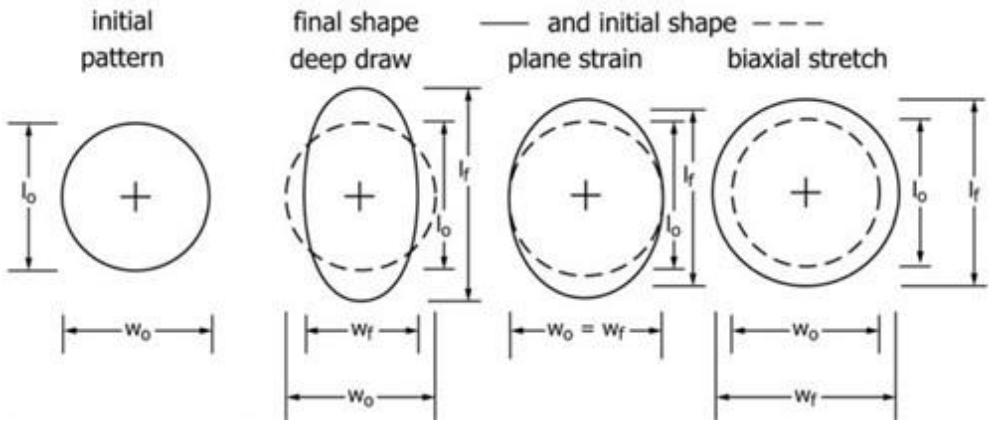

FIGURE 3.21: The possible changes in shape of the grid pattern (ASTM E2218-15) [118]

3.5.7 Forming Limit Diagram

Forming limit diagram is an important tool for prediction of failure in sheet metal forming. Forming limit diagrams of low carbon steel, AA 8011 alloy and annealed brass sheets with nearly same grain size were determined experimentally. Experimental procedure developed by Hecker (1975) was followed to determine forming limit diagrams Forming Limit Diagrams (FLDs) of cold-rolled and cryorolled sheets were found in this investigation by applying the Ghosh and Hecker [116] approach. Experiments were conducted using the same tooling setup that was used in LDH tests (discussed earlier) with 50 mm diameter hemispherical bottom punch. The specimen width was adjusted in increments of 10 mm from 20 mm to 90 mm in order to obtain limit strains in all potential modes of deformation (bi-axial stretching, plane strain stretching and draw-in forming modes) in order to calculate FLDs using the same equipment. For every width, three to four samples were tested in order to account for result scatter. A circular grid with a diameter of 5 mm was laser-marked onto thin sheet metal samples of all widths. All of the samples' limit strain values under different deformations were measured using the LDH test, and major and minor strain plots were created. Between the necking and the safe region, The Limiting curve has been plotted between necking and safe region. So from the results of LDH test the forming limit diagram have been plotted.

3.5.8 Strain Measurement

The analysis of strain distribution has been conducted on both cold-rolled and cryorolled samples of the tested LDH samples. An essential aspect of researching a sheet's formability is examining the distribution of strain inside the sample during deformation. To analyze the distribution of strain, tested samples of each width from both cold-rolled and cryorolled sheets were chosen.

Major and minor strains were measured for each ellipse along the samples' longitudinal axis (which passes through the "pole," or center of the dome), in order to examine the strain distribution profiles in the tested samples. Using the deformed grid on the tested samples, the major and minor strains were assessed (in the LDH and FLD tests). The distortion of the blanks caused the circles to become into ellipses. The ellipses' major and minor diameters were measured using a traveling microscope made by a digital tool manufacturer. By orienting the sample under the microscope so that the grid under observation was almost flat, an approximation of the 3D length on the distorted surface was made. All of the necessary ellipses' major and minor diameters were obtained by repeating this process, and the corresponding major and minor strains were computed.

3.5.9 Drawing Process

The metal drawing process is a fundamental manufacturing technique that transforms metal materials into desired shapes and structures through the application of force. Widely used in various industries, such as automotive, aerospace, and construction, metal forming encompasses a diverse range of methods, including bending, stamping, rolling, extrusion, and forging. These processes involve manipulating the metal's shape, size, and mechanical properties without removing material, offering significant advantages in terms of material utilization and structural integrity[119].

The same experimental set-up has been used for drawing operation of 1mm thick cold rolled and cryorolled AA8011 which is used for limiting dome height test.

To study and compare drawability of the cold rolled and cryorolled AA8011 sheets samples have been drawn using the conventional forming technique. The tools (die, punch and binder) have been fabricated in order to draw the cylindrical/square cups with different blank size and different punch size.

Cup Height After Deep Drawing (h):

$$D^2 = (d_p-2r_p)^2 + 4d_p(h-r_p) +2\pi r_p(d_p-0.7r_p)\ldots\ldots\ldots\ldots[120]$$

Punch diameter, *dp (mm)*
Punch nose radius, *rp (mm)*
Blank (sheet) diameter, *D (mm)*

Drawing Ratio (DR): it is measure of the severity of a deep drawing operation.

Drawing Ratio(DR) = Blank Diameter(Db) / Punch Diameter(Dp)……..…..[120]

Db: blank diameter
Dp: punch diameter

The greater the ratio, the more severe the operation.

The range of DR $\leq$ 2.

For the drawing of 1mm thick AA8011 cold rolled and cryorolled sheet a double action hydraulic press of 20-ton capacity is used. Blank holding force in the range of 80-100kN was applied on the upper die/binder to prevent material draw-in from the flange region.

Drawing Ratio: 2.0

To study the effect of drawing ratio a drawing ratio of 2.0 has been used having blank diameter 140mm, punch diameter 70mm and 100kN force is applied to deformed the sample Which is shown in Figure 3.22. From the Figure 3.22, it is observed that at drawing ratio of 2.0 all sample failure have been occur.



(a) Cold rolled (b) Cryorolled

FIGURE 3.22: Tested drawing specimens for cold rolling and cryorolling with drawing ratio 2.0

Drawing Ratio: 1.78

As the drawing ratio of 2.0 all samples have failed so a drawing ratio of 1.78 has been studied with blank diameter 125mm, punch diameter 70mm and 100kN force is applied to deformed the sample Which is shown in Figure 3.23. From the Figure 3.23, it is observed that at drawing ratio of 1.78 all sample failure have been occur.



(a) Cold rolled (b) Cryorolled

FIGURE 3.23: Tested drawing specimens for cold rolling and cryorolling with drawing ratio 1.78

Drawing Ratio: 1.71

To study the variation of punch diameter a 70mm punch diameter and 100kN force have been used to deformed a blank diameter of 120mm sample having thickness of 1mm AA8011 cold rolled and cryorolled sample as shown in Figure 3.24. A deformed samples shows marginal difference in cup height of cold rolled and

cryorolled samples. The height of cup for cold rolled sample is found to be 38.36mm while the height of cup for cryorolled sample is 40.54mm.So the height in cryorolled sheet is observed 2.174mm higher as compared to cold rolled sheet with a drawing ratio 1.71.



(a) Cold rolled (b) Cryorolled

FIGURE 3.24: Tested drawing specimens for cold rolling and cryorolling with drawing ratio 1.71

Drawing Ratio: 1.11

The sample of 200mm blank diameter and punch diameter 180mm with a applied force of 80kN by hydraulic press have been successfully deformed in cup shape as shown in Figure 3.25 for 1mm thick AA8011 cold rolled and cryorolled samples. The height of cup for cold rolled sample is 12.58mm while the height of cup for cryorolled sample is 14.30mm. So the height in cryorolled sheet is 1.72mm higher as compared to cold rolled sheet with a drawing ratio 1.11.



(a) Cold rolled (b) Cryorolled

FIGURE 3.25: Tested drawing specimens for cold rolling and cryorolling with drawing ratio 1.11

When applied a 100kN of force to the sample having blank diameter 200mm and punch diameter 180mm have been successfully deformed in cup shape having more depth of cup as compared to 80kN force as shown in Figure 3.26. The height of cup for cold rolled sample is 20.77mm and the height of cup for cryorolled sample is found to be 21.68mm. So the height of cryorolled sample is 0.91mm higher as compared to cold rolled sample with a drawing ratio 1.11.



(a) Cold rolled (b) Cryorolled

FIGURE 3.26: Tested drawing specimens for cold rolling and cryorolling with drawing ratio 1.11

Square Cup Drawing

The cold rolled and cryorolled samples have been tested for square cup. A blank size of 200mm x 200mm & punch size of 100mm x 100mm with a load of 100kN have been used for forming a square cup. A square cup has been drawn successfully as shown in Figure 3.28. The height of cup for cold rolled sample is 36.40mm while the height of cup for cryorolled sample is 39.85mm. It shows that in cryorolled sheet is 3.45mm higher as compared to cold rolled sheet.



(a) Cold rolled (b) Cryorolled

FIGURE 3.27: Tested drawing specimens for square cup drawing of cold rolling and cryorolling

CHAPTER 4

RESULT AND DISCUSSION

Results obtained from the experimental work on determination of microstructure, mechanical properties and anisotropy of cold rolled and cryorolled AA8011 alloy sheet using uni-axial tensile tests and characterization of formability using limiting dome height, forming limit diagrams and strain distribution profiles are presented and discussed in this chapter. The results obtained on surface roughness are also compared for cold rolled and cryorolled AA8011 alloy sheet.

4.1 Microstructure and Mechanical Properties of Rolled Sheets

4.1.1 Microstructure

As discussed in Chapter 3, The cold rolled and cryorolled samples have been examined for Optical microstructure as per ASTM E3:11(RA2017) and ASTM E407:07(2015). The material has an equiaxed, fully recrystallized grain structure with an average size in the cold rolled and cryorolled condition, according to the optical microstructure (Figure 4.1). There are noticeable variations in the microstructural characteristics of the cryorolled and cold rolled samples. Grain structure with inner dislocation-free formation has been formed as a result of annealing. Recovery annealing has resulted in a significant decrease in dislocation density. The density of dislocations is crucial to the material's strength.

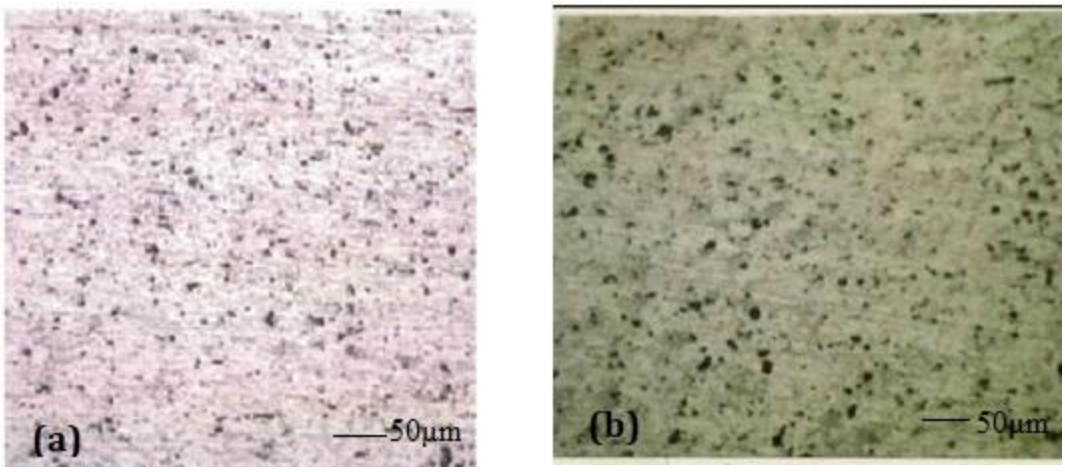

(a) Cold rolled(500X) (b) Cryorolled(500X)

FIGURE 4.1: Optical micrographs of AA8011 alloys (a) cold rolled (b) Cryorolled

The result of the cryorolled sample is a bimodal grain structure (Figure 4.1(b)), where ultrafine recovered granules and extremely fine recrystallized grains are the constituents of the recrystallized grains. It is anticipated that during deformation, the recrystallized grains will accommodate dislocations, increasing the ductility. Grain boundary misorientation has increased and the percentage of low angle grain boundaries has reduced after annealing. There is no evidence of recrystallized grains and merely regained grain structure with a reduced degree of fineness in the cold-rolled sample (Figure 4.1(a)).

4.1.2 Hardness

Vickers Hardness test have been performed for raw material, cold rolled and cryorolled samples as per as per ASTM E92-22 .The hardness value recorded at three different points and average value shown in Table 4.1.

Figure 4.2 shows the comparison of hardness for the AA8011 alloy of Raw material, cold rolled and cryorolled samples. The hardness values of the raw material, cold rolled and cryorolled were observed as 45.3, 53.40 and 61.36Hv As will be explained below, the suppression of dynamic recovery, increased dislocation density, and grain refinement compared to room temperature rolling give cryorolled sheets a somewhat greater hardness value than cold rolled sheets.

TABLE 4.1: Hardness of cold rolled and Cryorolled samples of AA8011 alloy

Conditions	Hardness in HV			Average
Raw Material	42.3	48.1	46.2	45.3
Cold Rolled	49.2	55.2	55.8	53.40
Cryo Rolled	61.0	64.1	59.0	61.36

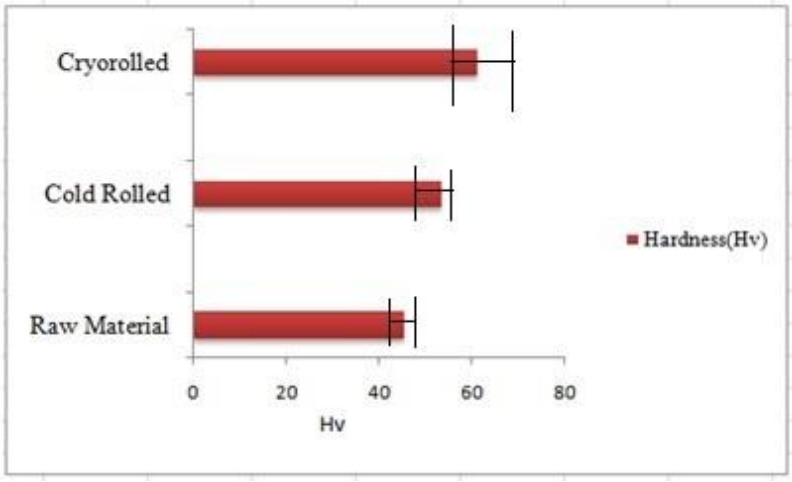

FIGURE 4.2: Variation of hardness of AA8011 alloys for raw material, cold rolled and cryorolled conditions

After a 3mm thickness to 1mm thickness, the hardness values of cryorolled material are 15% more than those of cold rolled sheets. Higher dislocation density is what contributes to the increased hardness of cryorolled sheets. Pure metals and alloys are rolled at cryogenic temperatures, which inhibit dynamic recovery and causes the density of accumulated dislocations to rise with the number of passes.

4.1.3 Surface Roughness Measurement

Surface Roughness measured as per ASTM D7127:2017 on the cold rolled and cryorolled samples after thickness reduction upto 1mm at five different locations using Surface roughness testing machine PS1(DMSPL/07/11). Figure 4.3 shows the average surface roughness value for 1mm 8011 aluminum alloys that have been cryorolled and cold rolled. The Surface Roughness value recorded at five different points and average value shown in Table 4.2. The average roughness value of cold

rolled sample is 0.959 µm and the average roughness value of cold rolled sample is 0.509 µm. From the result it is concluded that cryorolled sample have better surface finish compared to cold rolled samples.

TABLE 4.2: Surface roughness values of AA8011 alloy sheets in different conditions

Observed Value Ra (µm)	Average Ra (µm)	Conditions
1.162, 0.892, 0,933, 1.014, 0.792	0.959	Cold rolled
0.381, 0.861, 0.564, 0.246, 0.491	0.509	Cryorolled

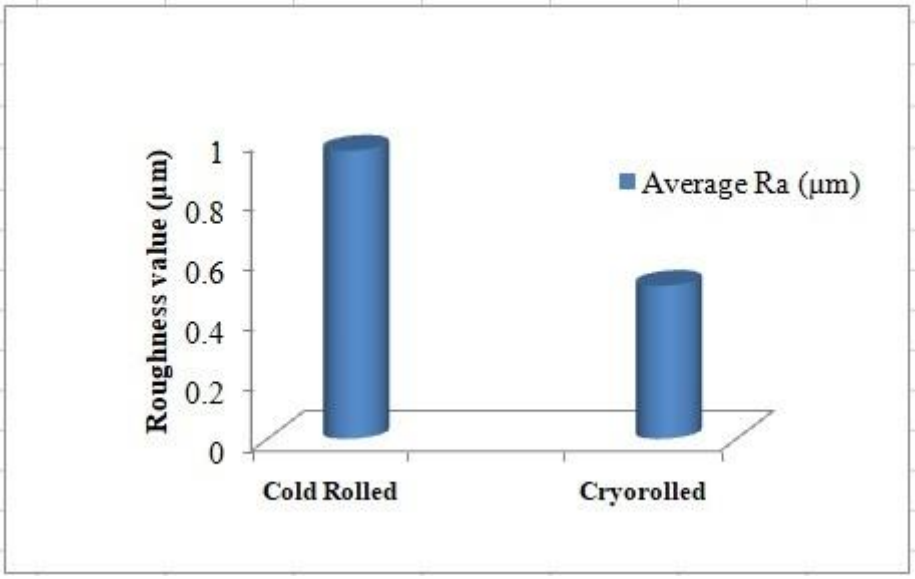

FIGURE 4.3: Variation of surface roughness of AA8011 alloys for cold rolled and cryorolled conditions

4.1.4 Tensile Test

The tested tensile specimens at 0ºC, 45ºC and 90ºC with respect to rolling direction for cold rolling and cryorolling are shown in Figure 4.4.



FIGURE 4.4: Tested tensile specimens at 0°C, 45°C and 90°C with respect to rolling direction for cold rolling and cryorolling

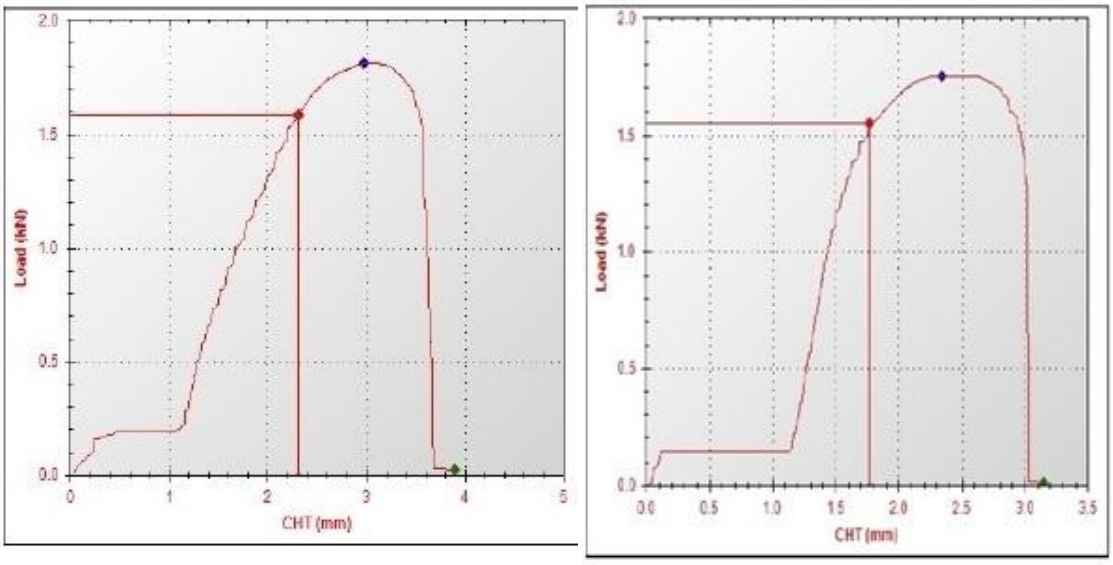

(a) Cold Rolled (b) Cryorolled

FIGURE.4.5 (a) Load vs CHT at for cold rolled and cryorolled sheet at 0°C with respect to rolling direction

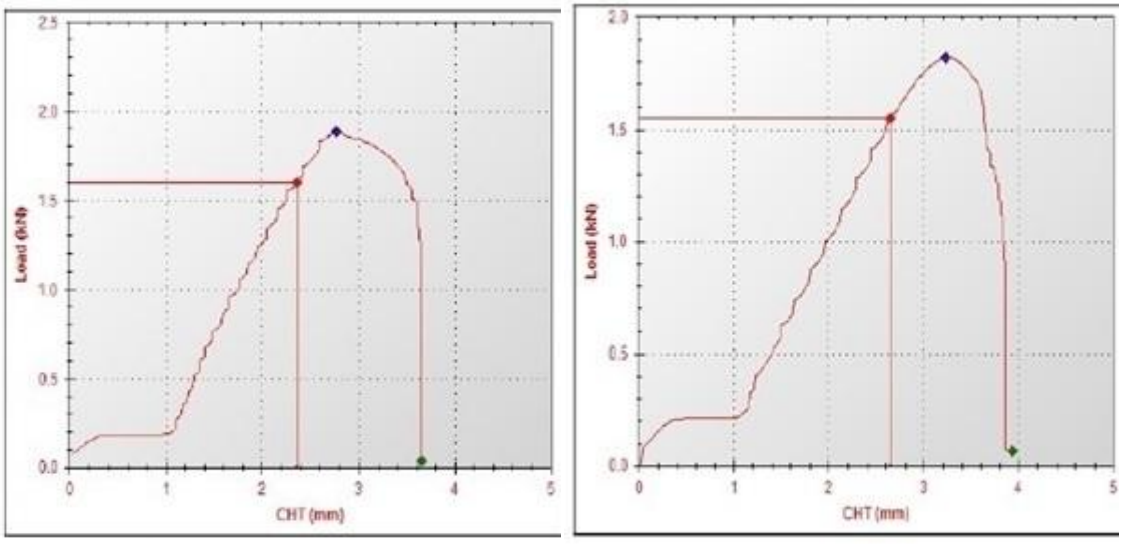

(a) Cold Rolled (b) Cryorolled

FIGURE.4.5 (b) Load vs CHT at for cold rolled and cryorolled sheet at 45°C with respect to rolling direction

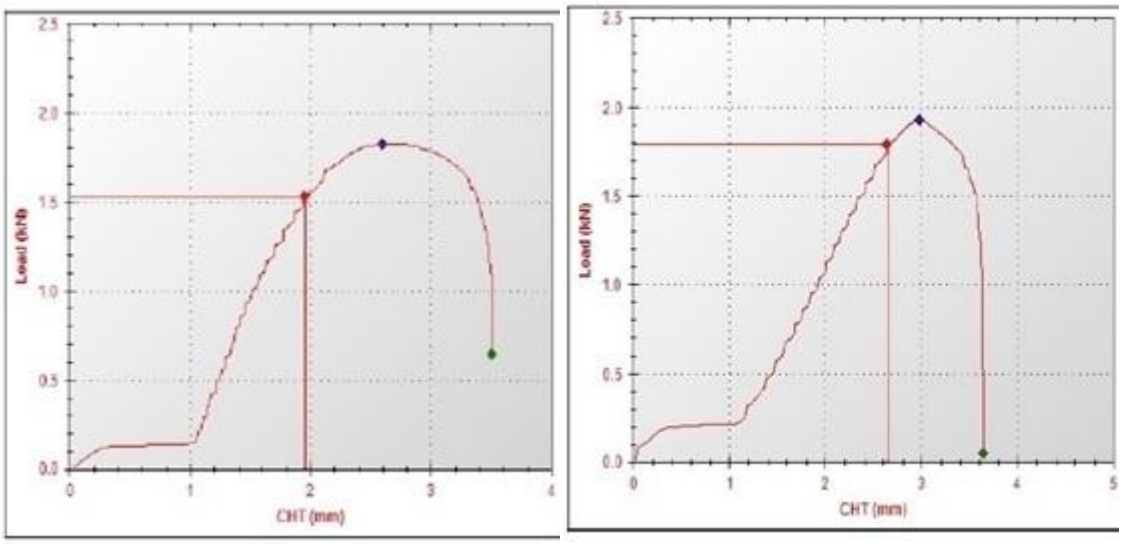

(a) Cold Rolled (b) Cryorolled

FIGURE.4.5 (c) Load vs CHT at for cold rolled and cryorolled sheet at 90°C with respect to rolling direction

FIGURE 4.5: (a), (b), (c) show how the Variations in Load vs CHT of the cold and cryorolled samples at 0°C, 45°C and 90°C with respect to rolling direction.

Figure 4.5 shows how the Variations in Load vs CHT of the cold and cryorolled samples at 0°C, 45°C and 90°C with respect to rolling direction. From the Figure 4.5(a,b,c) it has been observed that the cryorolled samples exhibits slightly higher load as compared to cold rolled samples.

Tensile samples of raw material, cold rolled and cryorolled sheets after annealing were tested and the results found for YS, UTS and % elongation in 0º, 45º, and 90º to rolling direction are shown in Table 4.3.

From the tensile test result, the sheet has a high density of dislocations in its as-rolled state. Dislocation density is found to grow further when processing temperatures are lowered to cryogenic temperatures due to the suppression of dynamic recovery. Table 4.3 shows that in comparison to cold rolling, this produced greater strength and hardness in all three testing directions (0º, 45º, and 90º to rolling direction).

TABLE 4.3: Tensile properties of AA8011 alloy sheets in different conditions

Conditions	Orientation With respect to Rolling direction	YS (N/mm^2)	UTS (N/mm^2)	Total elongation (%)
Raw Material		94.268	98.175	1.20
Cold Rolled	0°	117.507	134.613	2.84
	45°	123.472	145.234	3.44
	90°	120.114	143.131	3.06
Cryorolled	0°	134.648	151.761	3.72
	45°	128.857	150.722	3.94
	90°	154.161	165.762	3.98

High strain hardening ability materials are favored for forming applications because they can prevent early stage necking and localized deformation. Despite having a high density of dislocations, which gives ultrafine-grained materials their high strength, their capacity for significant plastic deformation is somewhat restricted. Several tactics have been tried to improve the work hardening ability of these materials, including the insertion of nano-sized precipitates and the formation of a bimodal grain structure through post-heat treatment. Grain boundary characteristics and the amount of dislocations present have a considerable impact on work hardening ability.

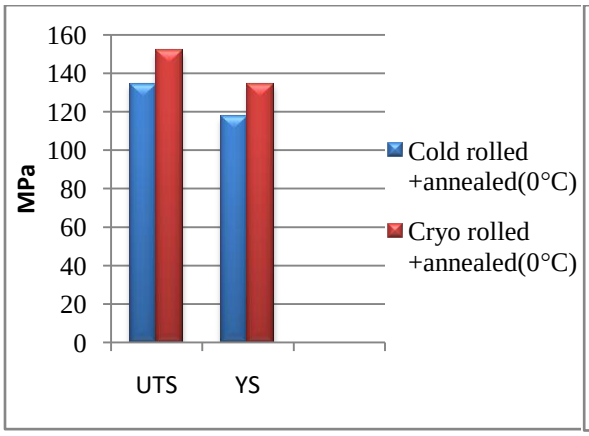

(a) Comparison of UTS and YS for cold rolled and cryorolled sheet at 0ºC of rolling direction

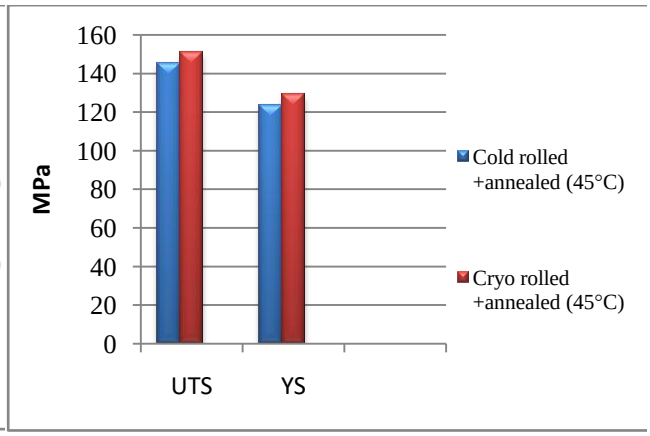

(b) Comparison of UTS and YS for cold rolled and cryorolled sheet at 45°C of rolling direction

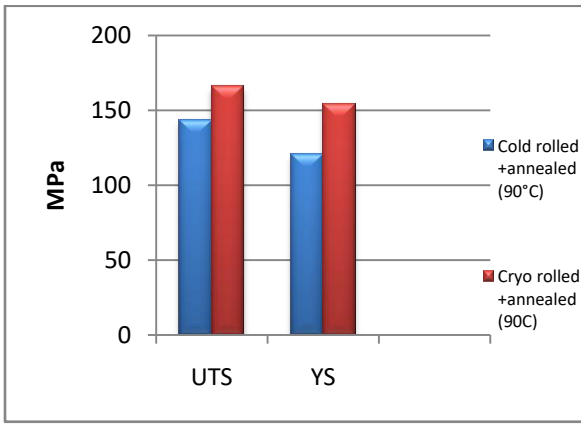

(c) Comparison of UTS and YS for cold rolled and cryorolled sheet at 90°C of rolling direction

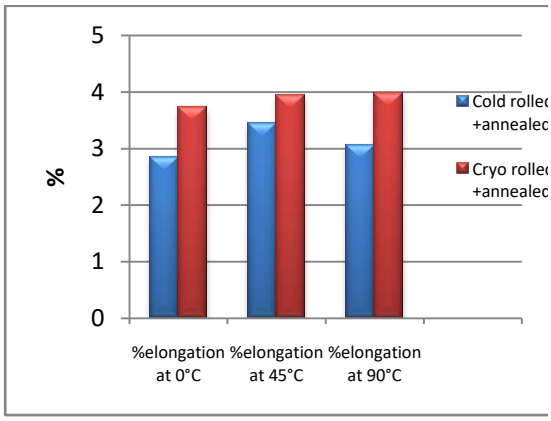

(d) Comparison of %Elongation for cold rolled and cryorolled sheet at 0°C , 45°C and 90°C of rolling direction

FIGURE 4.6: Variations in UTS, YS and elongation of the cold and cryorolled samples at 0°C, 45°C and 90°C of rolling direction.

For cryorolled and cold rolled samples, Figure 4.6 illustrates how the % elongation, YS, and UTS change with rolling direction. In both the rolled and annealed regimes, cryorolled sheets have shown somewhat higher YS and UTS. It is clear that cryorolling, followed by annealing, results in improved strength and roughly equivalent ductility. Because of this, cryorolled sheets are more resilient than cold rolled ones. The reason why cryorolled sheets are stronger than cold-rolled sheets

while still having about the same ductility can be attributed to the bimodal microstructure in cryorolled samples as was previously discussed.

The comparison of UTS and YS for cold-rolled and cryorolled sheets at 0° with regard to rolling direction is shown in Figure 4.6 (a). YS 117.507 (MPa) and UTS 134.613 (MPa) are found in cold-rolled annealed sheets at 0°, whereas YS 134.648 (MPa) and UTS 151.761 (MPa) are found in cryo-rolled anneaves. According to the YS and UTS values for both cold-rolled and cryorolled annealed sheets, the cryorolled annealed sheet has a 15% rise in YS and a 13% increase in UTS when compared to the cold-rolled annealed sheet.

The comparison of UTS and YS for cold-rolled and cryorolled sheets at 45° with regard to rolling direction is shown in Figure 4.6 (b). YS 123.472 (MPa) and UTS 145.234 (MPa) are found in cold-rolled annealed sheets at 45°, whereas YS 128.857 (MPa) and UTS 150.722 (MPa) are found in cryorolled confined sheets. It is inferred from these YS and UTS values for both cold rolled and cryorolled-annealed sheets that, in comparison to cold rolled annealed sheets, there is a 4% increase in YS and a 4% rise in UTS for cryorolled-annealed sheets.

The comparison of UTS and YS for cold-rolled and cryorolled sheets at 90° with regard to rolling direction is shown in Figure 4.6 (c). YS 120.114 (MPa) and UTS 143.131 (MPa) are found in cold-rolled annealed sheets at 90°, whereas YS 154.161 (MPa) and UTS 165.762 (MPa) are found in cryo-rolled anneaves. According to these YS and UTS values for both cold-rolled and cryorolled-annealed sheets, the YS and UTS of the cryorolled-annealed sheet are 28% and 16% higher, respectively, than those of the cold-rolled annealed sheet.

The percentage elongation for cold-rolled and cryorolled sheets at 0°C, 45°C, and 90°C with regard to rolling direction is compared in Figure 4.6 (d). Cold-rolled annealed sheets exhibit 2.84% elongation at 0°, whereas cryo-rolled annealed sheets exhibit 3.72% elongation. These elongation values for cold-rolled and cryorolled-annealed sheets indicate that the elongation of cryorolled annealed sheets is 30% more than that of cold-rolled annealed sheets. Cold-rolled annealed sheets exhibit 3.44% elongation at 45°, whereas cryo-rolled annealed sheets exhibit 3.94%

elongation. These elongation measurements for cold rolled and cryorolled-annealed sheets show that the elongation of the cryorolled-annealed sheet is 15% more than that of the cold rolled annealed sheet. Cold-rolled annealed sheets exhibit an elongation of 3.06% at 90°, whereas cryo-rolled annealed sheets exhibit an elongation of 3.98%. These elongation measurements for cold rolled and cryorolled-annealed sheets show that the elongation of the cryorolled-annealed sheet is 30% more than that of the cold rolled annealed sheet.

Anisotropy

As mentioned earlier, anisotropy in sheet metals is an important phenomenon which influences formability, especially in operations such as drawing. The anisotropic parameters (R_0, R_{45} and R_{90}), normal anisotropy ($\bar{R}$) and planar anisotropy (ΔR), evaluated by uniaxial tensile tests in the present study for both cryorolled and cold rolled sheets are presented in Table 4.4. From the table, it can be observed that the normal anisotropy ($\bar{R}$) of is higher in cryorolled sheet than that of AA8011 cold rolled sheet. Usually, for good drawability, values of R greater than 1 are desirable as high R indicates higher resistance to thinning in the cup wall during deep drawing . Better drawability is achieved with higher $\bar{R}$ [114]. R is maximum at 45° to rolling direction and minimum in parallel to rolling direction. Planar anisotropy (ΔR) indicates the extent of variation of properties within the plane of the sheet and ideally it should be zero to prevent defects like earing in deep drawing. Planar ratio ΔR value which is negative indicates the possible occurrence of little earing during deep drawing of these sheets. From the result, it is found that $\bar{R}$ value is slightly higher in cryorolled samples as compared to cold rolled samples.

TABLE 4.4: Anisotropic parameters of AA8011 alloy sheets tested cold rolled and cryorolled conditions

Anisotropic parameter	Cold rolled	Cryorolled
R_0	0.9	0.94
R_{45}	0.92	0.95
R_{90}	0.88	0.92
$\bar{R}$	0.9	0.94
ΔR	-0.03	-0.02

4.2 Limiting Dome Height Test

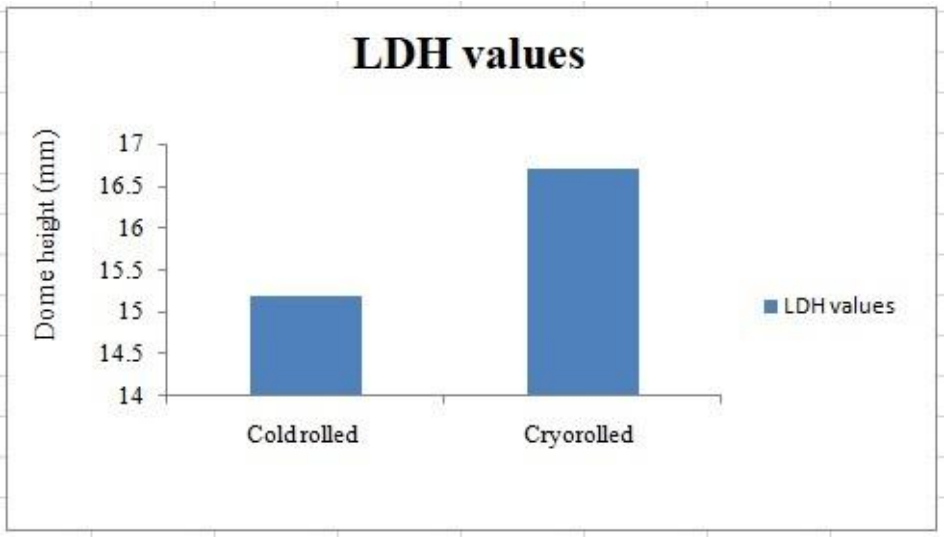

FIGURE 4.7: LDH of cold rolled and cryorolled of AA8011 sheets

According to Figure 4.7 Although the difference was minor, the cryorolled samples showed a slightly greater limiting dome height than the cold-rolled samples, suggesting that they have superior stretchability. The limiting dome height of the cryorolled samples was 9% greater than that of the cold-rolled samples.

4.3 Forming Limit Diagram

The forming limit diagrams (FLDs) of cold rolled and cryorolled AA8011 materials determined using Hecker's method, as explained in Section 3.2, are shown in Figures 4.8 and Figures 4.9. The curves represent the limit strains up to which these sheet metals can be formed in different modes of deformation (stretching, plane strain stretching and draw–in forming modes). The strains measured from safe, necked and failed regions are shown with different symbols. The forming limit curves show that cryorolled samples has higher plane strain intercept (value of e1 when e2 is zero) and overall limit strains than cold rolled AA8011 alloy. However, the difference is very small. The range of 15-17% is the FLDo for both cold rolled and cryorolled sheets. Because of inconsistent results and the practical difficulty of obtaining precise strains at the commencement of necking, an exact value cannot be determined. Comparing the results to typical cold rolled sheets, it is evident that increased strength can be achieved without sacrificing formability through cryorolling and a brief annealing step.

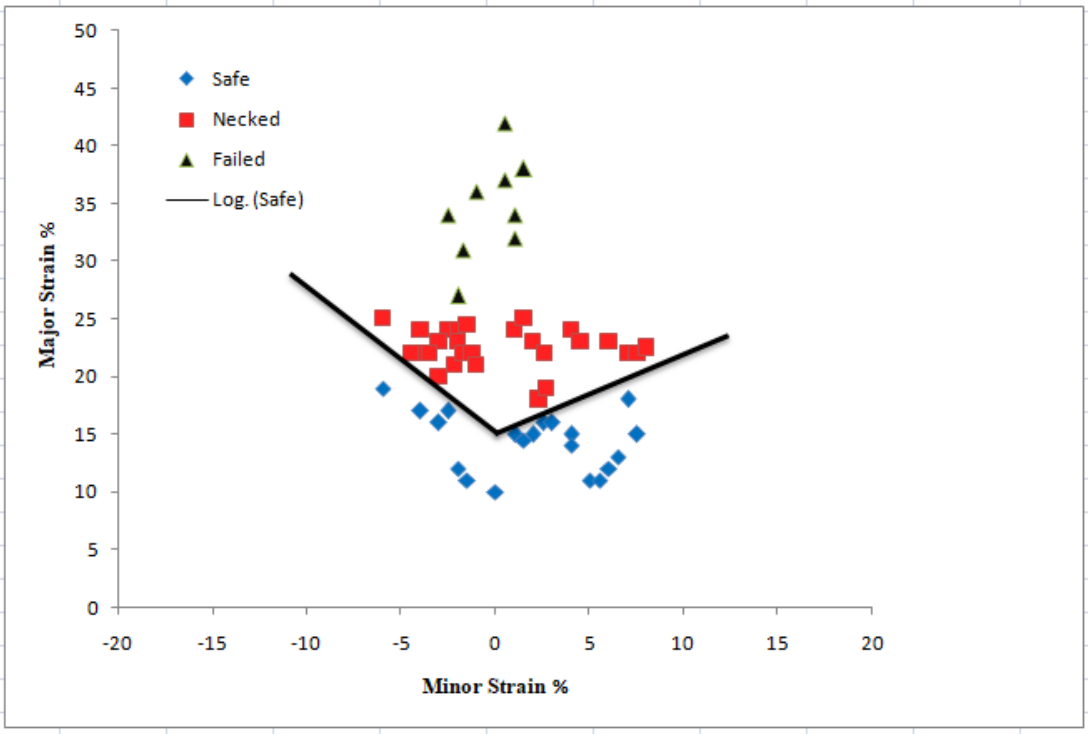

FIGURE 4.8: Forming Limit Diagram of cold rolled sheets

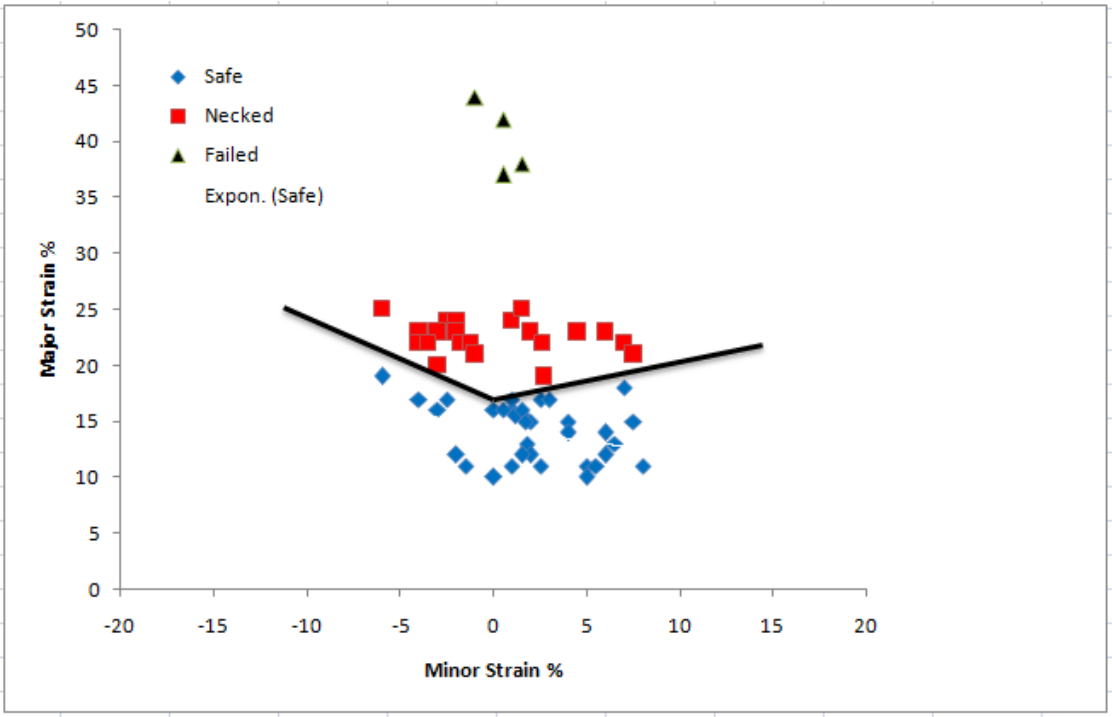

FIGURE 4.9: Forming Limit Diagram of cryorolled sheets

4.4 Strain Measurement

Figure 4.10 displays the changes in major and minor stresses as a function of distance from the pole for sheet metal specimens evaluated for FLD determination that had the same length but variable width. In every sample, there are two peaks, one on either side of the pole. The location of the highest peak has been determined to be the site of fracture or necking. In both situations, the separation between strain peaks is nearly equal. The values of minor strains are much higher for higher widths (90, 80, and 70 mm), indicating a higher degree of biaxiality. It has been noted that the peak strains achieved in cryorolled and cold rolled samples do not significantly differ from one another. For blank widths of 50 mm and 60 mm, minor strain reduced with width and became almost nil at all points, indicating a near plane-strain condition. In this circumstance, the peak limit strains have been shown to be the lowest. Using an ultrasonic thickness gauge, the maximum thinning of examined samples that were cryorolled and cold rolled was determined to be between 25 and 28%. In every sample, the thinning is always greatest at the regions that correlate to

the peak major strain, suggesting that excessive thinning, followed by localized necking and fracture, was the cause of the failure. In cryorolled samples, the thinning at the necking region is somewhat bigger than in cold rolled samples.

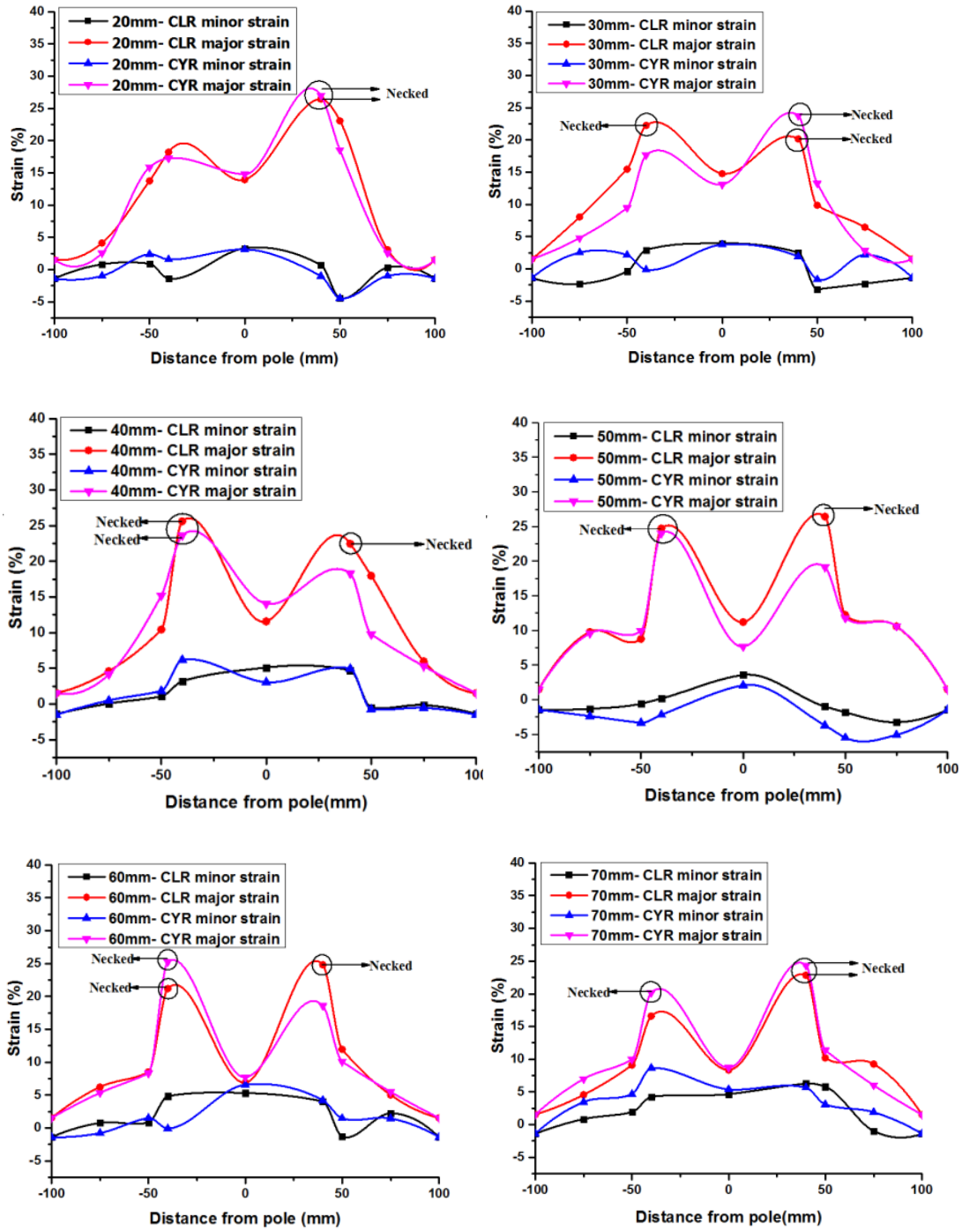

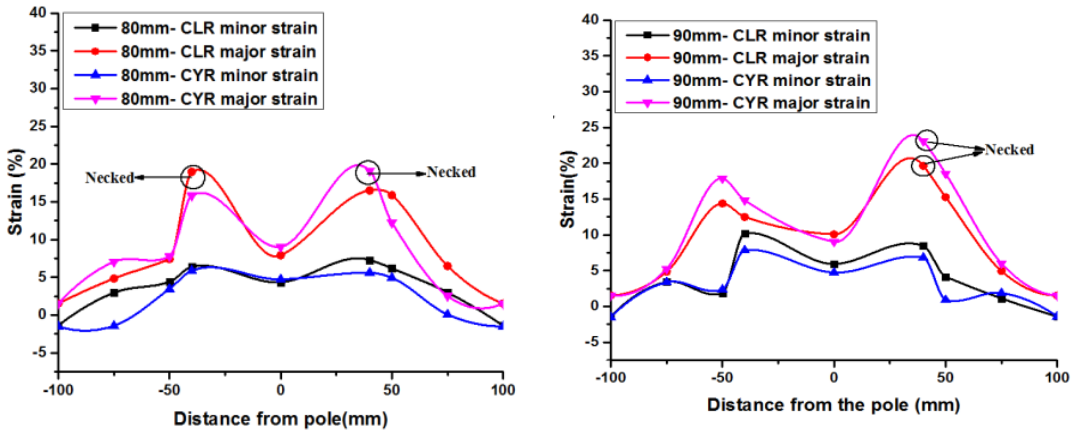

FIGURE 4.10: Strain distribution in FLD samples of cold rolled and cryorolled of AA8011 sheets after annealing

4.5 Drawing Process

The drawing operations performed with various punch size and blank size. The samples with drawing ratio 2 and 1.78 have not drawn successfully. Samples with drawing ratio 1.71 cup is formed successfully.

As shown in Figure 4.11 When applied 100kN force to 1mm thick AA8011 cold rolled and cryorolled sheet with blank diameter 120mm and punch diameter 70mm the cup shape can be formed with a marginal difference in cup height of cold rolled and cryorolled samples. The cryorolled samples exhibited slightly higher cup height than the cold rolled samples, indicating that they have better drawability. The cryorolled samples exhibited 5.36% higher limiting dome height than the cold rolled samples with a drawing ratio 1.71.

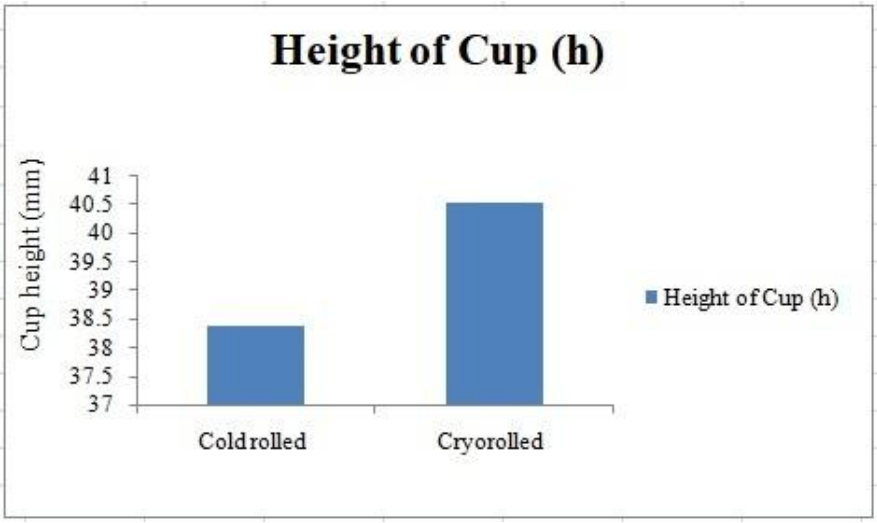

FIGURE 4.11: Drawing of cold rolled and cryorolled of AA8011 sheets
(blank dia 120mm, punch dia 70mm at 100kN)

As shown in Figure 4.12 When applied 80kN force to 1mm thick AA8011 cold rolled and cryorolled sheet with blank diameter 200mm and punch diameter 180mm the cup shape can be formed with a marginal difference in cup height of cold rolled and cryorolled samples. Indicating superior drawability, the cryorolled samples showed a slightly larger cup height than the cold rolled samples. The limiting dome height of the cryorolled samples was 12% more than that of the cold-rolled samples.

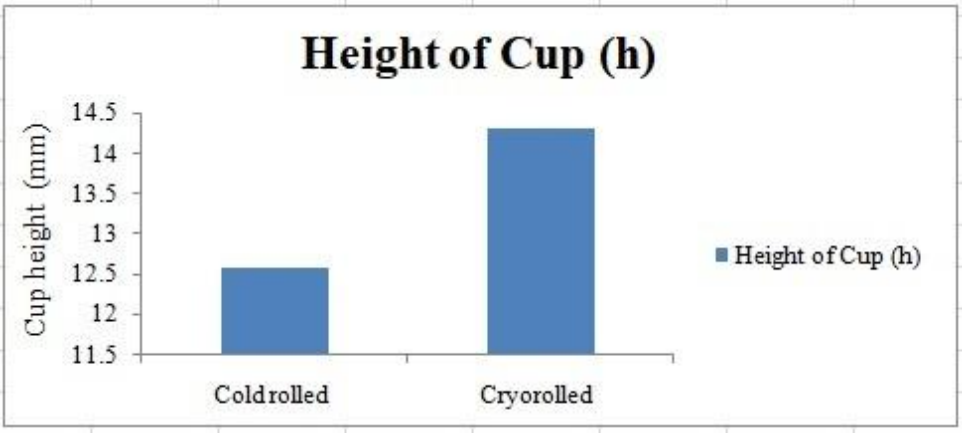

FIGURE 4.12: Drawing of cold rolled and cryorolled of AA8011 sheets
(blank dia 200mm, punch dia 180mm at 80kN)

As shown in Figure 4.13 When applied 100kN force to 1mm thick AA8011 cold rolled and cryorolled sheet with blank diameter 200mm and punch diameter 180mm the cup shape can be formed with a marginal difference in cup height of cold rolled and cryorolled samples. The cryorolled samples exhibited slightly higher cup height than the cold rolled samples, indicating that they have better drawability. The cryorolled samples exhibited 4.2% higher limiting dome height than the cold rolled samples.

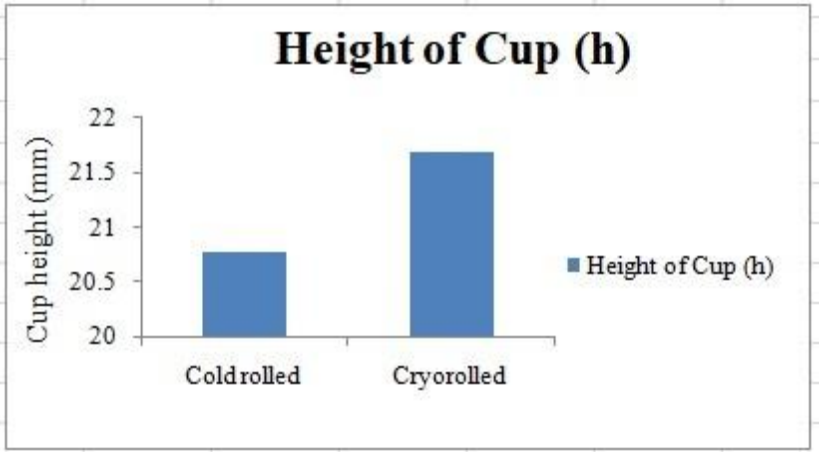

FIGURE 4.13: Drawing of cold rolled and cryorolled of AA8011 sheets (blank dia 200mm, punch dia 180mm at 100kN)

As shown in Figure 4.14 When applied 100kN force to 1mm thick AA8011 cold rolled and cryorolled sheet with blank size 200mm x 200mm and punch size 100mm x 100mm the square cup shape can be formed with a marginal difference in cup height of cold rolled and cryorolled samples. The cryorolled samples exhibited slightly higher cup height than the cold rolled samples, indicating that they have better drawability. The cryorolled samples exhibited 8.7% higher limiting dome height than the cold rolled samples.

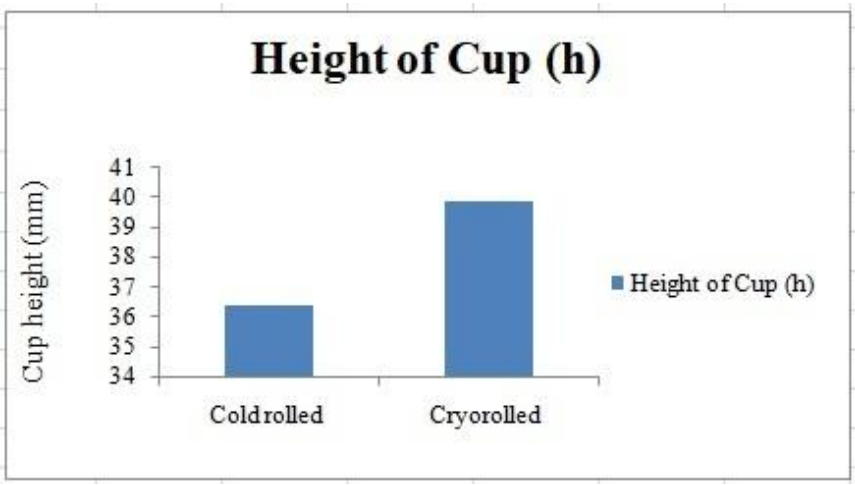

FIGURE 4.14: Drawing of cold rolled and cryorolled of AA8011 sheets
(blank size 200mm x 200mm, punch size 100mm x 100mm at 100kN)

So from these drawing operations it has been observed that with a drawing ratio 1.71 the cold rolled and cryorolled sheets have been drawn successfully.

4.6 Summary

It has been observed that in comparison to cold rolled and annealed sheets, it has been found that cryorolling the AA8011 alloy and then annealing it at a temperature of 200℃ results in increased strength without sacrificing ductility. This is explained by the bimodal microstructure of cryorolled samples, which is not present in cold rolled sheets and consists of some relatively larger grains from recrystallization and ultrafine granules from recovery. The cryorolled samples showed a slightly greater limiting dome height than the cold rolled ones, suggesting superior stretchability. The formability of cryorolled sheets is generally comparable to that of cold rolled sheets, as demonstrated by nearly similar limit strains in the three modes of deformation (biaxial tension, plane-strain, and tension-compression). For both cryorolled and cold rolled sheets, the plane-strain intercept (value of major strain when the minor strain is zero) ranges from 16–17%. There is marginal difference in the peak strains measured in cold-rolled samples as compared to cryorolled samples. The strain distributions in tested samples are non-uniform (having two peaks on either side of the pole) along the longitudinal direction. under comparison to tension-

compression, the sheets exhibited a greater degree of biaxiality under pure tension. There is a improved drawability with different punch size and blank size in cryorolled sheet as compared to cold rolled sheet. It is concluded that, in sheet metal forming applications, cryorolling AA8011alloy sheets followed by annealing treatment (with a bimodal grain structure) can yield parts with greater strength than traditional sheets without sacrificing formability. The unique contribution of this research is to development of Forming Limit Diagram of Cold rolled and Cryorolled 8011 Al alloy sheet by Limiting Dome Height Test. Also there is Comparative study of Formability in Drawing process for both Cold rolled and Cryorolled 8011 Al alloy sheet.

CHAPTER 5

CONCLUSION AND SCOPE OF FUTURE WORK

5.1 Conclusion

In the present work, AA8011 alloy sheets have been cryorolled to produce ultrafine-grained sheets with higher strength and hardness than conventional cold rolled sheets. In order to combine two unconventional processes—cryorolling and drawing operation—and create sheet metal parts with a combination of increased strength and improved formability, the formability of cryorolled sheets in the drawing operation of cylindrical/square cups has been investigated and compared with conventional forming. The findings and analysis discussed in the first two chapters have led to the following conclusions.

1) Cold rolling process required 4 no of pass for thickness reduction of 3mm to 1mm of AA8011 while cryorolling required 6 no of pass for thickness reduction of 3mm to 1mm of AA8011. Number of pass increases in cryorolling due to increase in hardness of cryorolled sheet.

2) The mechanical properties of cryorolled 8011 Al alloys samples improved as compared to conventional cold rolled sheet. At 0°C YS increased 13% and UTS increased 12%, at 45°C YS increased 5% and UTS increased 4%, at 90°C YS increased 22% and UTS increased 14%.

3) The average plastic strain ratio ($\bar{R}$) of cryorolled samples is 2.12% higher as compared to cold rolled sample. Higher value of plastic strain ratio ($\bar{R}$) indicate Better drawability of sheet.

4) Microstructure in cryorolled samples consisting of ultrafine-grains due to recrystallization and it can be obtained by a proper choice of annealing time and temperature.

5) It has been found that cryorolling of AA 8011 alloy sheets with thickness reduction followed by annealing at a temperature of 200°C for a 45min gives higher strength without loss of ductility as compared to cold rolled annealed sheets.

6) The Hardness of cryorolled 8011 aluminium Al alloys improved 12-13% as compared to conventional cold rolled sheet.

7) The surface roughness of cryorolled 8011 aluminium Al alloys improved 40-45% as compared to conventional cold rolled sheet.

8) The cryorolled samples exhibited 9% higher limiting dome height than the cold rolled samples, indicating better stretch ability.

9) In drawing operation of cold rolled and cryorolled AA8011 alloy sheet at drawing ratio 1.71 the cup have been drawn successfully.

10) In Drawing operation cup height of cryorolled 8011 aluminium alloys sheet improved 5-7% as compared to conventional cold rolled sheet. It shows that drawability increases with cryorolled.

11) In Forming Limit Diagram the value of FLD_o is higher in cryorolled sheet as compared to cold rolled sheet.

12) It can be concluded that cryorolling of AA8011 alloy sheets followed by annealing treatment can be used for sheet metal forming applications to produce parts with higher strength and better drawability than conventional sheets with increase in formability.

5.2 Scope of Future Work

1) The present work can also be extended to investigate the effect of annealing temperature at different time for cryorolled 8011 Al alloys and compared with conventional cold rolled.

2) The present work can also be extended to investigate the sub-grain size for cold rolled annealed and cryorolled annealed samples through EBSD micrographs or TEM.

3) Finite Element Analysis (FEA) analysis has been carried out to predict formability of cryorolled Al alloy sheets to make comparison with cold rolled samples.

4) The present work can also be extended to investigate the effect of bending operations and evaluate spring back effect for cryorolled 8011 Al alloys and compared with conventional cold rolled.

5) The present work can also be extended for other aluminium alloys such as AA5052 and AA7075.

6) The present work can also be extended to investigate fatigue and corrosion behavior of cryorolled and annealed sheets and compared with conventional cold rolled.

7) Statistical validation of results (e.g., standard deviation/error bars, ANOVA) will add more credibility and explore industrial-scale implementation and cost-benefit analyses of cryorolling.

REFERENCES

[1] Kalpakjian and Schmid, *Manufacturing Processes for Engineering Materials*. Pearson Education. Chicago, 2016.

[2] "http://www.metalformingmagazine.com/magazine/article.asp?aid=9501." Jun. 10, 2015. [Online]. Available: http://www.metalformingmagazine.com/magazine/article.asp?aid=9501.

[3] M. Kleiner, M. Geiger, and A. Klaus, "'Manufacturing of Lightweight Components by Metal Forming,'" *CIRP Annals-Manufacturing Technology*, p. 52(2), pp. 521-542., 2003.

[4] J. Hu, Z. Marciniak, and J. Duncan, *Mechanics of Sheet Metal Forming,*. Butterworth-Heinemann. London., 2002.

[5] W. F. Hosford and J. L. Duncan, "Sheet metal forming: A review," *JOM*, vol. 51, no. 11, pp. 39–44, Nov. 1999, doi: 10.1007/s11837-999-0221-5.

[6] S. L. Semiatin, E. Marquard, and H. Lampman, *Metalworking: Sheet Forming*, vol. 14B. ASM Handbook. Ohio., 2006.

[7] H. Swift, "'The Mechanism of a Simple Deep-Drawing Operation,'" *Sheet Metal Industries*, vol. 31(330), pp. 817-828., 1954.

[8] S. S. Hecker, "'A Cup Test for Assessing Stretchability,'" *Metals Engineering Quarterly*, vol. 14(4), pp. 30-36., 1974.

[9] B. Dorel, *Sheet Metal Forming Processes: Constitutive Modelling and Numerical Simulation,*. Springer. New York., 2010.

[10] S. P. Keeler, and W. A. Backofen, "'Plastic Instability and Fracture in Sheets Stretched over Rigid Punches,'" *ASM Transaction Quarterly*, vol. 56(1), pp. 25-48., 1963.

[11] S. S. Hecker, "Formability of Aluminum Alloy Sheets," *Journal of Engineering Materials and Technology*, vol. 97, no. 1, pp. 66–73, Jan. 1975, doi: 10.1115/1.3443263.

[12] K. Nakazima, T. Kikuma, and K. Hasuka, "'Study on the Formability of Steel Sheets,'" *Yawata Tech Rep*, pp. 678-680., 1971.

[13] M. C. Butuc, J. J. Gracio, and A. B. da Rocha, “A theoretical study on forming limit diagrams prediction,” *Journal of Materials Processing Technology*, vol. 142, no. 3, pp. 714–724, 2003, doi: https://doi.org/10.1016/S0924-0136(03)00813-6.

[14] S. Ahmadi, A. R. Eivani, and A. Akbarzadeh, “Experimental and analytical studies on the prediction of forming limit diagrams,” *Computational Materials Science*, vol. 44, no. 4, pp. 1252–1257, 2009, doi: https://doi.org/10.1016/j.commatsci.2008.08.008.

[15] D. R. Satish, F. Feyissa, and D. R. Kumar, “Cryorolling and warm forming of AA6061 aluminum alloy sheets,” *Materials and Manufacturing Processes*, vol. 32, no. 12, pp. 1345–1352, Sep. 2017, doi: 10.1080/10426914.2017.1317352.

[16] J. F. Siekirk, “‘Process Variable Effects on Sheet Metal Quality,’” *Journal of Applied Metalworking*, vol. 4(3), pp. 262-269., 1986.

[17] J. A. Soares, M. L. Gipiela, S. F. Lajarin, and P. V. P. Marcondes, “Study of the punch–die clearance influence on the sheared edge quality of thick sheets,” *The International Journal of Advanced Manufacturing Technology*, vol. 65, no. 1, pp. 451–457, Mar. 2013, doi: 10.1007/s00170-012-4184-2.

[18] S. Subramonian, T. Altan, B. Ciocirlan, and C. Campbell, “Optimum selection of variable punch-die clearance to improve tool life in blanking non-symmetric shapes,” *International Journal of Machine Tools and Manufacture*, vol. 75, pp. 63–71, 2013, doi: https://doi.org/10.1016/j.ijmachtools.2013.09.004.

[19] S. RAJU, G. GANESAN, and R. KARTHIKEYAN, “Influence of variables in deep drawing of AA 6061 sheet,” *Transactions of Nonferrous Metals Society of China*, vol. 20, no. 10, pp. 1856–1862, 2010, doi: https://doi.org/10.1016/S1003-6326(09)60386-1.

[20] A. Hedrick, “‘Controlling Flow and Obtaining Stretch in Deep Draw Operations,’” *Stamping Journal(USA)*, vol. 12(2), pp. 30-34., 2000.

[21] I. Suchy, *Handbook of Die Design*,. McGraw-Hill. New York., 2006.

[22] A. K. Gupta and D. R. Kumar, “Formability of galvanized interstitial-free steel sheets,” *Journal of Materials Processing Technology*, vol. 172, no. 2, pp. 225–237, 2006, doi: https://doi.org/10.1016/j.jmatprotec.2005.10.016.

[23] J. Hiam, and A. Lee, “‘Factors Influencing the FLC of Sheet Steel,’” *Sheet Metal Industries*, vol. 50, pp. 400-411., 1978.

[24] J. R. Davis, *Aluminum and Aluminum Alloys*,. ASM International. Ohio., 1993.

[25] j Hirsch, *Aluminium Alloys: The Physical and Mechanical Properties. Volume 1*. Wiley_Vch. Weinheim., 2008.

[26] D. R. Askeland, and P. P. Phulé, *The Science and Engineering of Materials*,. Springer. Stamford., 2006.

[27] A. Azushima *et al.*, “Severe plastic deformation (SPD) processes for metals,” *CIRP Annals*, vol. 57, no. 2, pp. 716–735, 2008, doi: https://doi.org/10.1016/j.cirp.2008.09.005.

[28] Y. Wang, T. Jiao, and E. Ma, “Dynamic Processes for Nanostructure Development in Cu after Severe Cryogenic Rolling Deformation,” *MATERIALS TRANSACTIONS*, vol. 44, no. 10, pp. 1926–1934, 2003, doi: 10.2320/matertrans.44.1926.

[29] D. K. Yang, P. Cizek, D. Fabijanic, J. T. Wang, and P. D. Hodgson, “Work hardening in ultrafine-grained titanium: Multilayering and grading,” *Acta Materialia*, vol. 61, no. 8, pp. 2840–2852, 2013, doi: https://doi.org/10.1016/j.actamat.2013.01.018.

[30] H. L. Yu, C. Lu, A. K. Tieu, G. H. J., A, and S. H. Zhang, “‘Special Rolling Techniques for Improvement of Mechanical Properties of Ultrafine-Grained Metal Sheets: A Review,’” *Advanced Engineering Materials*, vol. 18(5), pp. 754-769., 2015.

[31] F. Taye, “Characterization of Mechanical Properties and Formability of Cryorolled Aluminium Alloy Sheets,” 2014.

[32] S. Cheng, Y. H. Zhao, Y. T. Zhu, and E. Ma, “Optimizing the strength and ductility of fine structured 2024 Al alloy by nano-precipitation,” *Acta Materialia*, vol. 55, no. 17, pp. 5822–5832, 2007, doi: https://doi.org/10.1016/j.actamat.2007.06.043.

[33] Y. Zhao, Y. Zhu, and E. Ma, “Optimizing the strength and ductility of fine structured 2024 Al alloy by nano-precipitation,” *Acta Materialia - ACTA MATER*, vol. 55, pp. 5822–5832, Oct. 2007, doi: 10.1016/j.actamat.2007.06.043.

[34] D. Singh, P. Nageswararao, and R. Jayaganthan, “‘Microstructural Studies of Al 5083 Alloy Deformed through Cryorolling,’” *Advanced Materials Research*, vol. 585, pp. 376-380., 2012.

[35] K. G. Krishna, K. Sivaprasad, K. Venkateswarlu, and K. C. H. Kumar, “Microstructural evolution and aging behavior of cryorolled Al–4Zn–2Mg alloy,” *Materials Science and Engineering: A*, vol. 535, pp. 129–135, 2012, doi: https://doi.org/10.1016/j.msea.2011.12.052.

[36] K. Gopala Krishna, N. Singh, K. Venkateswarlu, and K. C. Hari Kumar, “Tensile Behavior of Ultrafine-Grained Al-4Zn-2Mg Alloy Produced by Cryorolling,” *Journal of Materials Engineering and Performance*, vol. 20, no. 9, pp. 1569–1574, Dec. 2011, doi: 10.1007/s11665-011-9843-1.

[37] M. Koç, *Hydroforming for Advanced Manufacturing*. Woodhead Publishing. Cambridge., 2008.

[38] “‘http://www.inoxveneta.it/en/tube-hydroforming/.’”

[39] “‘http://www.kltauto.com/images/product/automotive/exhaust-Sys-Big.jpg.’”

[40] H. Singh, “Fundamentals of Hydroforming,” *of Manufacturing Engineers. Michigan.*, 2003.

[41] “‘http://www.americanhydroformers.com/category/what-is-sheet-hydroforming.’”

[42] H. Palaniswamy, A. Yadav, S. Kaya, and T. Altan, "'New Technologies to Form Light Weight Automotive Components,'" *4th International Conference and Exhibition on Design and Production of Machines and Dies/Molds*, pp. 21-23., 2007.

[43] L. H. Lang *et al.*, "Hydroforming highlights: sheet hydroforming and tube hydroforming," *Journal of Materials Processing Technology*, vol. 151, no. 1, pp. 165–177, 2004, doi: https://doi.org/10.1016/j.jmatprotec.2004.04.032.

[44] S. H. Zhang, Z. R. Wang, Y. Xu, Z. T. Wang, and L. X. Zhou, "Recent developments in sheet hydroforming technology," *Journal of Materials Processing Technology*, vol. 151, no. 1, pp. 237–241, 2004, doi: https://doi.org/10.1016/j.jmatprotec.2004.04.054.

[45] "https://www.helandermetal.com/hydroforming-services."

[46] C. S. R. Araveeti, "INTRODUCTION TO DEEP DRAWING," May 2023, doi: 10.13140/RG.2.2.18467.43049.

[47] S. Kalpakjian, S. Schmid, and V. Sekar, *Manufacturing Engineering and Technology*. 2013.

[48] R. A Chennakesava, "Formability of High Temperature and High Strain Rate Superplastic Deep Drawing Process for AA2219 Cylindrical Cups.," *International Journal of Advanced Research*, vol. 3(10), pp. 1016-1024, 2015.

[49] R. AC Sekhara, R. S, and R. P Ravinder, "Experimental Study on Strain Variation and Thickness Distribution in Deep Drawing of Axisymmetric Components.".

[50] "http://www.braxtonmfg.com/parts.htm."

[51] "http://www.fondex.fr/en/deep-drawing.html/."

[52] "https://in.pinterest.com/pin/658229301764248066/."

[53] I. Ihsan Khalaf, "Process analysis and design in micro deep drawing utilizing a flexible die." PhD thesis, University of Glasgow, 2014.

[54] C. Vic, B. S, L. A, and M. S, *Principles of engineering manufacture*. Butterworth-Heinemann,.

[55] A. Dhal, S. K. Panigrahi, and M. S. Shunmugam, "Insight into the microstructural evolution during cryo-severe plastic deformation and post-deformation annealing of aluminum and its alloys," *Journal of Alloys and Compounds*, vol. 726, pp. 1205–1219, 2017, doi: https://doi.org/10.1016/j.jallcom.2017.08.062.

[56] P. N. Rao, D. Singh, and R. Jayaganthan, "Effect of annealing on microstructure and mechanical properties of Al 6061 alloy processed by cryorolling," *Materials Science and Technology*, vol. 29, no. 1, pp. 76–82, Jan. 2013, doi: 10.1179/1743284712Y.0000000041.

[57] S. K. Panigrahi and R. Jayaganthan, "Influence of solutes and second phase particles on work hardening behavior of Al 6063 alloy processed by cryorolling," *Materials Science and*

Engineering: A, vol. 528, no. 7, pp. 3147–3160, 2011, doi: https://doi.org/10.1016/j.msea.2011.01.010.

[58] S. K. Panigrahi and R. Jayaganthan, "Effect of annealing on precipitation, microstructural stability, and mechanical properties of cryorolled Al 6063 alloy," *Journal of Materials Science*, vol. 45, no. 20, pp. 5624–5636, Oct. 2010, doi: 10.1007/s10853-010-4627-9.

[59] L. W. Quan, W. N. Mu, L. Kang, X. Ma, P. Han, and M. L. Huang, "The Effect of Cryorolling on the Microstructure of Al-Cu-Mg Alloy," in *The 15th International Conference on Aluminium Alloys*, in Materials Science Forum, vol. 877. Trans Tech Publications Ltd, Jan. 2017, pp. 188–193. doi: 10.4028/www.scientific.net/MSF.877.188.

[60] D. Singh, P. N. Rao, and R. Jayaganthan, "Effect of deformation temperature on mechanical properties of ultrafine grained Al–Mg alloys processed by rolling," *Materials & Design*, vol. 50, pp. 646–655, Sep. 2013, doi: 10.1016/j.matdes.2013.02.068.

[61] W. Wang *et al.*, "Influence of Cryorolling on the Precipitation of Cu–Ni–Si Alloys: An In Situ X-ray Diffraction Study," *Acta Metallurgica Sinica (English Letters)*, vol. 31, no. 10, pp. 1089–1097, Oct. 2018, doi: 10.1007/s40195-018-0781-x.

[62] A. Dhal, P. S. K., and Shunmugam. M. S., "'Deformation Behaviour and Fracture Mechanism of Ultrafine-Grained Aluminium Developed by Cryorolling.' (AIMTDR)," pp. 31-52., 2019, doi: https://doi.org/10.1007/978-981-13-0378-4.

[63] K. C. Sekhar and R. Narayanasamy, "Mechanical Properties and formability of Cryorolled Commercial Pure Aluminium at various reductions," *Materials Today: Proceedings*, vol. 5, no. 2, Part 2, pp. 6888–6896, 2018, doi: https://doi.org/10.1016/j.matpr.2017.11.350.

[64] N. Kumar, G. M. Owolabi, R. Jayaganthan, and O. O. Ajide, "Plane stress fracture toughness of cryorolled 6082 Al alloy," *Theoretical and Applied Fracture Mechanics*, vol. 95, pp. 28–41, 2018, doi: https://doi.org/10.1016/j.tafmec.2018.02.011.

[65] R. Li, Z. Xiao, Z. Li, X. Meng, and X. Wang, "Work Hardening Behavior and Microstructure Evolution of a Cu-Ti-Cr-Mg Alloy during Room Temperature and Cryogenic Rolling," *Materials*, vol. 16, no. 1, p. 424, Jan. 2023, doi: 10.3390/ma16010424.

[66] D. Singh, P. N. Rao, and R. Jayaganthan, "Microstructures and impact toughness behavior of Al 5083 alloy processed by cryorolling and afterwards annealing," *Int J Miner Metall Mater*, vol. 20, no. 8, pp. 759–769, Aug. 2013, doi: 10.1007/s12613-013-0794-4.

[67] S. K. Panigrahi and R. Jayaganthan, "A study on the mechanical properties of cryorolled Al–Mg–Si alloy," *Materials Science and Engineering: A*, vol. 480, no. 1, pp. 299–305, 2008, doi: https://doi.org/10.1016/j.msea.2007.07.024.

[68] H. Yu *et al.*, "A new insight into ductile fracture of ultrafine-grained Al-Mg alloys," *Scientific Reports*, vol. 5, no. 1, p. 9568, Apr. 2015, doi: 10.1038/srep09568.

[69] H. Yu *et al.*, "Microstructure evolution of accumulative roll bonding processed pure aluminum during cryorolling," *Journal of Materials Research*, vol. 31, Mar. 2016, doi: 10.1557/jmr.2016.70.

[70] Y. B. Lee, D. H. Shin, K.-T. Park, and W. J. Nam, "Effect of annealing temperature on microstructures and mechanical properties of a 5083 Al alloy deformed at cryogenic temperature," *Scripta Materialia*, vol. 51, no. 4, pp. 355–359, 2004, doi: https://doi.org/10.1016/j.scriptamat.2004.02.037.

[71] T. Shanmugasundaram, B. S. Murty, and V. Subramanya Sarma, "Development of ultrafine grained high strength Al–Cu alloy by cryorolling," *Scripta Materialia*, vol. 54, no. 12, pp. 2013–2017, Jun. 2006, doi: 10.1016/j.scriptamat.2006.03.012.

[72] S. K. P. P. N. Rao and R. Jayaganthan, "Effect of annealing and aging treatment on mechanical properties of ultrafine grained Al 6061 alloy," *Materials Science and Technology*, vol. 26, no. 3, pp. 371–374, 2010, doi: 10.1179/174328409X443227.

[73] P. N. Rao, A. Kaurwar, D. Singh, and R. Jayaganthan, "Enhancement in Strength and Ductility of Al-Mg-Si Alloy by Cryorolling followed by Warm Rolling," *Procedia Engineering*, vol. 75, pp. 123–128, 2014, doi: https://doi.org/10.1016/j.proeng.2013.11.027.

[74] P. Das, R. Jayaganthan, and I. V. Singh, "Tensile and impact-toughness behaviour of cryorolled Al 7075 alloy," *Materials & Design*, vol. 32, no. 3, pp. 1298–1305, Mar. 2011, doi: 10.1016/j.matdes.2010.09.026.

[75] Y. Wang, M. Chen, F. Zhou, and E. Ma, "High tensile ductility in a nanostructured metal," *Nature*, vol. 419, no. 6910, pp. 912–915, Oct. 2002, doi: 10.1038/nature01133.

[76] Y. Shi *et al.*, "Extraordinary Toughening by Cryorolling in Zr," *Advanced Engineering Materials*, vol. 16, no. 2, pp. 167–170, 2014, doi: https://doi.org/10.1002/adem.201300153.

[77] I. A. Ovid'Ko, and T. G. Langdon, "'Enhanced Ductility of Nanocrystalline and Ultrafine-Grained Metals,'" *Reviews on Advanced Materials Science,* vol. 30(2), pp. 103-111., 2012.

[78] B. B. He *et al.*, "High dislocation density–induced large ductility in deformed and partitioned steels," *Science*, vol. 357, no. 6355, pp. 1029–1032, 2017, doi: 10.1126/science.aan0177.

[79] R. O. Ritchie, "The conflicts between strength and toughness," *Nature Materials*, vol. 10, no. 11, pp. 817–822, Nov. 2011, doi: 10.1038/nmat3115.

[80] Y. Wei *et al.*, "Evading the strength–ductility trade-off dilemma in steel through gradient hierarchical nanotwins," *Nature Communications*, vol. 5, no. 1, p. 3580, Apr. 2014, doi: 10.1038/ncomms4580.

[81] L. Lu, M. L. Sui, and K. Lu, "Superplastic Extensibility of Nanocrystalline Copper at Room Temperature," *Science*, vol. 287, no. 5457, pp. 1463–1466, 2000, doi: 10.1126/science.287.5457.1463.

[82] K. Lu, “Making strong nanomaterials ductile with gradients,” *Science*, vol. 345, no. 6203, pp. 1455–1456, 2014, doi: 10.1126/science.1255940.

[83] V. A. Pozdnyakov, “Ductility of nanocrystalline materials with a bimodal grain structure,” *Technical Physics Letters*, vol. 33, no. 12, pp. 1004–1006, Dec. 2007, doi: 10.1134/S1063785007120061.

[84] M. S. Oskooie, H. Asgharzadeh, and H. S. Kim, “Microstructure, plastic deformation and strengthening mechanisms of an Al–Mg–Si alloy with a bimodal grain structure,” *Journal of Alloys and Compounds*, vol. 632, pp. 540–548, 2015, doi: https://doi.org/10.1016/j.jallcom.2015.01.229.

[85] F. Feyissa, D. R. Kumar, and P. N. Rao, “Characterization of Microstructure, Mechanical Properties and Formability of Cryorolled AA5083 Alloy Sheets,” *Journal of Materials Engineering and Performance*, vol. 27, pp. 1614–1627, 2018, [Online]. Available: https://api.semanticscholar.org/CorpusID:139371605

[86] K. S. V. B. R. Krishna *et al.*, “Mechanical behavior and void coalescence analysis of cryorolled AA8090 alloy,” *The International Journal of Advanced Manufacturing Technology*, vol. 93, no. 1, pp. 253–259, Oct. 2017, doi: 10.1007/s00170-016-8863-2.

[87] N. Rangaraju, T. Raghuram, B. V. Krishna, K. P. Rao, and P. Venugopal, “Effect of cryo-rolling and annealing on microstructure and properties of commercially pure aluminium,” *Materials Science and Engineering: A*, vol. 398, no. 1, pp. 246–251, 2005, doi: https://doi.org/10.1016/j.msea.2005.03.026.

[88] I. Jaseem *et al.*, “Synergetic Effect of Cryorolling and Postroll Aging on Simultaneous Increase in Wear Resistance and Mechanical Properties of an Al–Cu Alloy,” *Journal of Tribology*, vol. 140, no. 6, p. 061607, May 2018, doi: 10.1115/1.4040162.

[89] T. Bhattacharjee *et al.*, “Simultaneous Strength-Ductility Enhancement of a Nano-Lamellar AlCoCrFeNi2.1 Eutectic High Entropy Alloy by Cryo-Rolling and Annealing,” *Scientific Reports*, vol. 8, no. 1, p. 3276, Feb. 2018, doi: 10.1038/s41598-018-21385-y.

[90] A. Dhal, S. K. Panigrahi, and M. S. Shunmugam, “Influence of alloy chemistry on the deformation behaviour and anisotropic properties of aluminium ultra-fine-grained thin sheets,” *Journal of Physics: Conference Series*, vol. 1063, no. 1, p. 012067, Jul. 2018, doi: 10.1088/1742-6596/1063/1/012067.

[91] K. C. Sekhar, R. Narayanasamy, and K. Velmanirajan, “Experimental investigations on microstructure and formability of cryorolled AA 5052 sheets,” *Materials & Design*, vol. 53, pp. 1064–1070, 2014, doi: https://doi.org/10.1016/j.matdes.2013.08.008.

[92] N. Kumar, P. N. Rao, J. Rengaswamy, and H.-G. Brokmeier, “Effect of cryorolling and annealing on recovery, recrystallisation, grain growth and their influence on mechanical and corrosion behaviour of 6082 Al alloy,” *Materials Chemistry and Physics*, vol. 165, Sep. 2015, doi: 10.1016/j.matchemphys.2015.09.014.

[93] S. K. Panigrahi and R. Jayaganthan, “A Study on the Combined Treatment of Cryorolling, Short-Annealing, and Aging for the Development of Ultrafine-Grained Al 6063 Alloy with Enhanced Strength and Ductility,” *Metallurgical and Materials Transactions A*, vol. 41, no. 10, pp. 2675–2690, Oct. 2010, doi: 10.1007/s11661-010-0328-x.

[94] A. S. Taylor, M. Weiss, T. Hilditch, N. Stanford, and P. D. Hodgson, “Formability of cryo-rolled aluminium in uniaxial and biaxial tension,” *Materials Science and Engineering: A*, vol. 555, pp. 148–153, 2012, doi: https://doi.org/10.1016/j.msea.2012.06.044.

[95] M. Weiss, A. S. Taylor, P. D. Hodgson, and N. Stanford, “Strength and biaxial formability of cryo-rolled 2024 aluminium subject to concurrent recovery and precipitation,” *Acta Materialia*, vol. 61, no. 14, pp. 5278–5289, 2013, doi: https://doi.org/10.1016/j.actamat.2013.05.019.

[96] A. S. Taylor, M. Weiss, T. Hilditch, P. Hodgson, and N. Stanford, “Cryo-Rolling and Formability of 2024 Aluminium,” in *Light Metals Technology 2013*, in Materials Science Forum, vol. 765. Trans Tech Publications Ltd, Sep. 2013, pp. 434–438. doi: 10.4028/www.scientific.net/MSF.765.434.

[97] A. S. Taylor, M. Weiss, T. Hilditch, N. Stanford, and P. D. Hodgson, “Formability of cryo-rolled aluminium in uniaxial and biaxial tension,” *Materials Science and Engineering: A*, vol. 555, pp. 148–153, Oct. 2012, doi: 10.1016/j.msea.2012.06.044.

[98] K. Chandra Sekhar, R. Narayanasamy, and K. Venkateswarlu, “Formability, fracture and void coalescence analysis of a cryorolled Al–Mg–Si alloy,” *Materials & Design*, vol. 57, pp. 351–359, May 2014, doi: 10.1016/j.matdes.2013.12.077.

[99] S. Vigneshwaran, K. Sivaprasad, R. Narayanasamy, and K. Venkateswarlu, “Formability and fracture behaviour of cryorolled Al-3 Mg-0.25 Sc alloy,” *Materials Science and Engineering: A*, vol. 721, pp. 14–21, 2018, doi: https://doi.org/10.1016/j.msea.2018.02.072.

[100] J. S. Khalkho, D. B. Karunakar, and S. Vidyasagar, “Effect of Aging and Rolling on Microstructure and Mechanical Properties of AA7075/TaC Composites,” *J. of Materi Eng and Perform*, Jan. 2023, doi: 10.1007/s11665-022-07788-z.

[101] N. Malik Abbas, Zahraa Thamer Abdulwahid, Asmaa Ali Hussien, S.V. Konovalov, and Hamid M. Mahan, “Formability, Mechanical and Chemical Properties Assessment for High Strength AA7075 Subjected to Annealing Heat Treatment,” *JT*, vol. 5, no. 1, pp. 16–21, Mar. 2023, doi: 10.51173/jt.v5i1.1107.

[102] X. Wang, Y. Liu, and Y. Huang, “Improving Precipitation in Cryogenic Rolling 6016 Aluminum Alloys during Aging Treatment,” *Materials*, vol. 16, no. 9, p. 3336, Apr. 2023, doi: 10.3390/ma16093336.

[103] R. Pant, A. Joshi, S. Singh, and A. Raturi, “Influence of Cryo-cross Rolling and Post-Rolled Annealing on Microstructure and High Cycle Fatigue Properties of Al-5052 Alloy,” *Metallography, Microstructure, and Analysis*, vol. 12, no. 3, pp. 505–514, Jun. 2023, doi: 10.1007/s13632-023-00961-3.

[104] A. Sadeghi, E. Kozeschnik, and F. R. Biglari, “Investigation of the Formability of Cryogenic Rolled AA6061 and Its Improvement Using Artificial Aging Treatment,” *Journal of Manufacturing and Materials Processing*, vol. 7, no. 2, 2023, doi: 10.3390/jmmp7020054.

[105] A. Sadeghi, E. Kozeschnik, and F. R. Biglari, “Investigation of the Formability of Cryogenic Rolled AA6061 and Its Improvement Using Artificial Aging Treatment,” *JMMP*, vol. 7, no. 2, p. 54, Feb. 2023, doi: 10.3390/jmmp7020054.

[106] H. Zhang, B. Guo, X. Zhao, and C. Chen, “Microstructure and corrosion behavior of 2A12 aluminum alloys by high frequency impacting and rooling,” *CIRP Journal of Manufacturing Science and Technology*, vol. 41, pp. 328–337, Apr. 2023, doi: 10.1016/j.cirpj.2023.01.001.

[107] A. M., A. Z., N. K., U. L., and K. S., “Micromechanical properties of cryo-rolled (CR) aluminum alloy Al0,6Mg0,35Si,” *METALURGIJA*, vol. 61, pp. 700–702, 2022.

[108] S. Toros, F. Ozturk, and I. Kacar, “Review of warm forming of aluminum–magnesium alloys,” *Journal of Materials Processing Technology*, vol. 207, no. 1, pp. 1–12, 2008, doi: https://doi.org/10.1016/j.jmatprotec.2008.03.057.

[109] D. Li and A. K. Ghosh, “Biaxial warm forming behavior of aluminum sheet alloys,” *Journal of Materials Processing Technology*, vol. 145, no. 3, pp. 281–293, 2004, doi: https://doi.org/10.1016/j.jmatprotec.2003.07.003.

[110] L. Ceschini, and A. Afrikantov, “‘Superplastic Forming (SPF) of Materials and SPF Combined with Diffusion Bonding: Technological and Design Aspects,’” *Metallurgical Science and Tecnology*, vol. 10(3)., 2013.

[111] F. K. Abu-Farha and M. K. Khraisheh, “An integrated approach to the Superplastic Forming of lightweight alloys: towards sustainable manufacturing,” *International Journal of Sustainable Manufacturing*, vol. 1, no. 1–2, pp. 18–40, 2008, doi: 10.1504/IJSM.2008.019225.

[112] D. V. Wilson, “Strain-rate sensitivity and effects of strain rate in sheet forming,” *Metals Technology*, vol. 7, no. 1, pp. 282–292, 1980, doi: 10.1179/030716980803287297.

[113] J. Liu and Z. Wang, “Prediction of wrinkling and fracturing in viscous pressure forming (VPF) by using the coupled deformation sectional finite element method,” *Computational Materials Science*, vol. 48, no. 2, pp. 381–389, 2010, doi: https://doi.org/10.1016/j.commatsci.2010.01.029.

[114] J. Liu, M. Ahmetoglu, and T. Altan, “Evaluation of sheet metal formability, viscous pressure forming (VPF) dome test,” *Journal of Materials Processing Technology*, vol. 98, no. 1, pp. 1–6, 2000, doi: https://doi.org/10.1016/S0924-0136(99)00299-X.

[115] “Incremental Forming.”

[116] Cui, Junjun, Chen, Liqing, Li, Yanfei, Liu, Jiahua, and Xie, Jiaqi, “Effects of annealing treatment on mechanical properties of 8011 aluminum alloy after cryogenic rolling,” *Metall. Res. Technol.*, vol. 116, no. 2, p. 219, 2019, doi: 10.1051/metal/2018067.

[117] W. F. Hosford, and R. M. Caddell, *Metal Forming: Mechanics and Metallurgy,*. Cambridge University Press. New York., 1993.

[118] W. Truszkowski, *The Plastic Anisotropy in Single Crystals and Polycrystalline Metals,*. PWN. Krakow., 2001.

[119] T. Altan, and A. E. Tekkaya, *Sheet Metal Forming: Fundamentals*. ASM International. Ohio., 2012.

[120] A. K. Ghosh and S. S. Hecker, "Failure in thin sheets stretched over rigid punches," *Metallurgical Transactions A*, vol. 6, no. 5, pp. 1065–1074, May 1975, doi: 10.1007/BF02661361.

[121] ASTM International, *"Standard Test Method for Determining Forming Limit Curves 1,"* vol. 1. 2014.

[122] A. Chennakesava Reddy, "CONVENTIONAL DEEP DRAWING VS INCREMENTAL DEEP DRAWING," *MED, JNTUH*, Aug. 2018.

[123] M. Janka, S. Emil, V. Samuel, and M. Peter, "Evaluation of Drawability of Selected Types of Steel Sheets," *The International Journal of Engineering and Science (IJES)*, vol. 10, no. 11, pp. 24–29, 2021.

LIST OF PUBLICATIONS

List of Publications

1) Manish N Parmar, Dr.A.B.Dhruv **"Analyze the effect of Cryorolling on Mechanical Properties and Microstructure of AA8011 "** Nanotechnology Perceptions , ISSN 1660-6795, vol 20 No. S15, pp. 3821-3830, (2024).

2) Manish N Parmar, Dr.A.B.Dhruv **"Study the Effect of Cryogenic Rolling on Mechanical Properties of Aluminium Alloys: A Review"** International Journal for Multidisciplinary Research (IJFMR), E-ISSN: 2582-2160 , Volume 7, Issue 1, January-February 2025, https://doi.org/10.36948/ijfmr.2025.v07i01.35493

3) Manish N Parmar, Dr.A.B.Dhruv **"Characterization of Mechanical Properties of Cryorolled AA8011 Alloys Sheet"** Tuijin Jishu/Journal of Propulsion Technology, ISSN 1001-4055, vol 44 No. 5, pp. 2595-2603, (2023).

4) Manish N Parmar, Dr.A.B.Dhruv **"Futuristic Trends in Cryogenic Rolling"** IIP Series, Volume 3, Book 1, Chapter 4, e-ISBN: 978-93-5747-742-0, pp. 46-57, (2024).

Appendices

Appendix A-Material Test Certificate

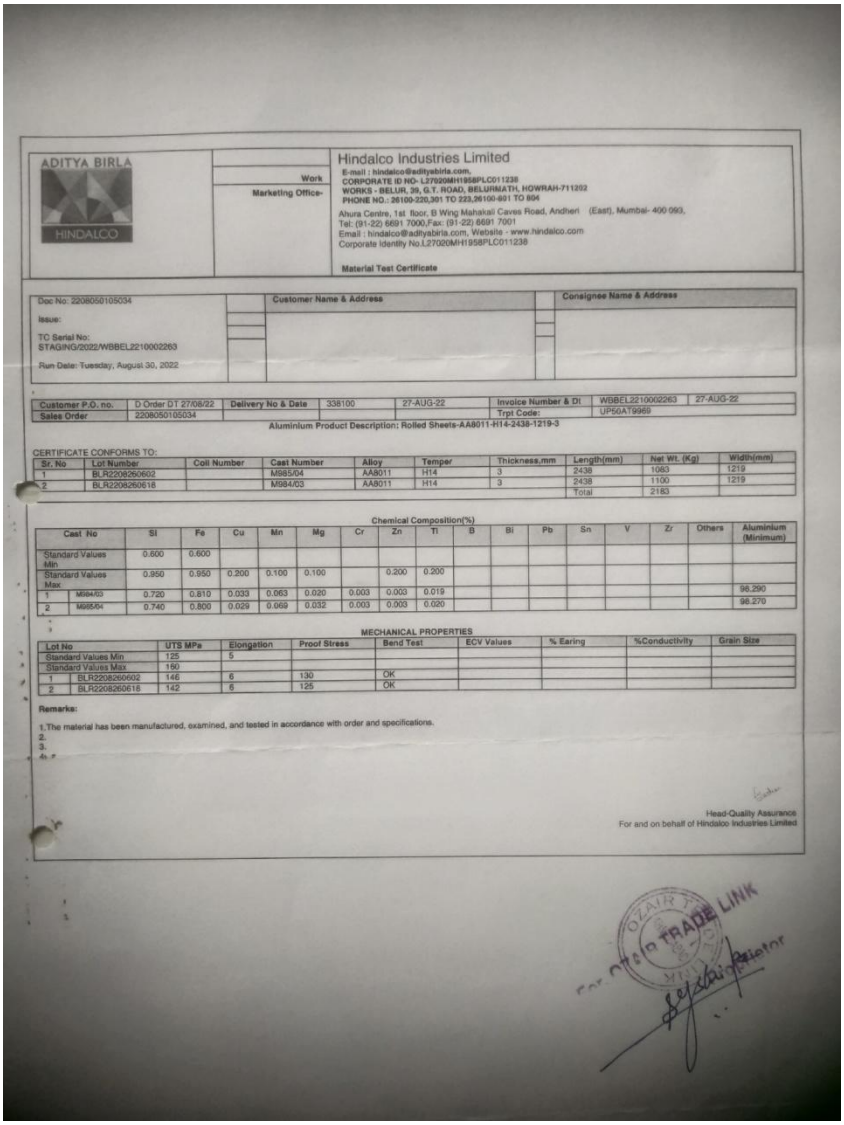

ADITYA BIRLA
HINDALCO

Hindalco Industries Limited
E-mail : hindalco@adityabirla.com,
CORPORATE ID NO- L27020MH1958PLC011238
WORKS - BELUR, 39, G.T. ROAD, BELURMATH, HOWRAH-711202
PHONE NO.: 26100-220,301 TO 223,26100-691 TO 804
Ahura Centre, 1st floor, B Wing Mahakali Caves Road, Andheri (East), Mumbai- 400 093,
Tel: (91-22) 6691 7000,Fax: (91-22) 6691 7001
Email : hindalco@adityabirla.com, Website - www.hindalco.com
Corporate Identity No.L27020MH1958PLC011238

Work
Marketing Office-

Material Test Certificate

Doc No: 2208050105034
Issue:
TC Serial No:
STAGING/2022/WBBEL2210002263
Run Date: Tuesday, August 30, 2022

Customer Name & Address

Consignee Name & Address

Customer P.O. no.	D Order DT 27/08/22	Delivery No & Date	338100	27-AUG-22	Invoice Number & DI	WBBEL2210002263	27-AUG-22
Sales Order	2208050105034				Trpt Code:	UP50AT9969	

Aluminium Product Description: Rolled Sheets-AA8011-H14-2438-1219-3

CERTIFICATE CONFORMS TO:

Sr. No	Lot Number	Coil Number	Cast Number	Alloy	Temper	Thickness,mm	Length(mm)	Net Wt. (Kg)	Width(mm)
1	BLR2208260602		M985/04	AA8011	H14	3	2438	1060	1219
2	BLR2208260618		M984/03	AA8011	H14	3	2438	1100	1219
							Total	2183	

Chemical Composition(%)

Cast No		Si	Fe	Cu	Mn	Mg	Cr	Zn	Ti	B	Bi	Pb	Sn	V	Zr	Others	Aluminium (Minimum)
Standard Values Min		0.600	0.600														
Standard Values Max		0.950	0.950	0.200	0.100	0.100		0.200	0.200								
1	M984/03	0.720	0.810	0.033	0.063	0.020	0.003	0.003	0.019								98.290
2	M985/04	0.740	0.800	0.029	0.069	0.032	0.003	0.003	0.020								98.270

MECHANICAL PROPERTIES

Lot No		UTS MPa	Elongation	Proof Stress	Bend Test	ECV Values	% Earing	%Conductivity	Grain Size
Standard Values Min		125	5						
Standard Values Max		160							
1	BLR2208260602	146	6	130	OK				
2	BLR2208260618	142	6	125	OK				

Remarks:

1.The material has been manufactured, examined, and tested in accordance with order and specifications.
2.
3.

Head-Quality Assurance
For and on behalf of Hindalco Industries Limited

Appendix B- Chemical Analysis Certificate

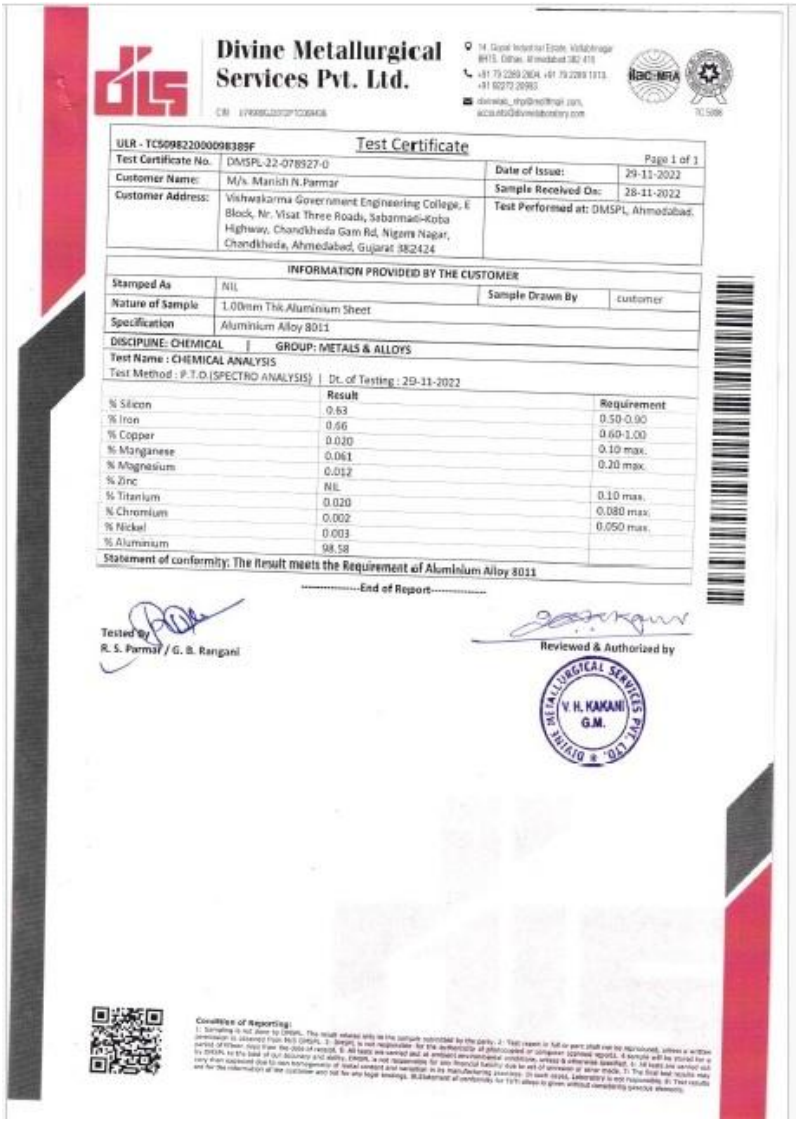

Divine Metallurgical Services Pvt. Ltd.

ULR - TC509822000098389F

Test Certificate

Page 1 of 1

Test Certificate No.	DMSPL-22-078927-0	Date of Issue:	29-11-2022
Customer Name:	M/s. Manish N.Parmar	Sample Received On:	28-11-2022
Customer Address:	Vishwakarma Government Engineering College, E Block, Nr. Visat Three Roads, Sabarmadi-Koba Highway, Chandkheda Gam Rd, Nigam Nagar, Chandkheda, Ahmedabad, Gujarat 382424	Test Performed at: DMSPL, Ahmedabad.	

INFORMATION PROVIDED BY THE CUSTOMER

Stamped As	NIL	Sample Drawn By	customer
Nature of Sample	1.00mm Thk.Aluminium Sheet		
Specification	Aluminium Alloy 8011		

DISCIPLINE: CHEMICAL | GROUP: METALS & ALLOYS

Test Name : CHEMICAL ANALYSIS

Test Method : P.T.D.(SPECTRO ANALYSIS) | Dt. of Testing : 29-11-2022

	Result	Requirement
% Silicon	0.63	0.50-0.90
% Iron	0.66	0.60-1.00
% Copper	0.020	0.10 max.
% Manganese	0.061	0.20 max.
% Magnesium	0.012	
% Zinc	NIL	0.10 max.
% Titanium	0.020	0.080 max.
% Chromium	0.002	0.050 max.
% Nickel	0.003	
% Aluminium	98.58	

Statement of conformity: The result meets the Requirement of Aluminium Alloy 8011

----------End of Report----------

Tested By
R. S. Parmar / G. B. Rangani

Reviewed & Authorized by

DIVINE METALLURGICAL SERVICES PVT. LTD. V. H. KAKANI G.M.

Condition of Reporting: